DIGITRANS

Co-funded by
the European Union

Electric Drive, Automotive Electronics and Energy-Saving Technologies for Modern Transport

Electric Drive, Automotive Electronics and Energy-Saving Technologies for Modern Transport

Editor: Andrii Hnatov

Andrii Hnatov
Oleksandr Dziubenko
Ruslan Bagach
Nadezhda Kunicina
Kristaps Vitols
Alexandr Ojegov
Robert Madalin Chivu
Ion Ion
Shchasiana Arhun
Olha Ulianets
Yuriy Borodenko
Anatolijs Zabasta
Pavlo Sokhin
Vadim Cazac
Michael Fratita

Riga 2026

This document has been prepared by the financial support of European Union. The authors from Kharkiv National Automobile and Highway University and Riga Technical University are responsible for the content of this document. This publication reflects the views only of the authors, and it cannot be regarded as the European Union's official position.

The book is developed in a frame of the project “ERASMUS+ Capacity-building in the Field of Higher Education 2023 Call for Proposals 101127683-DIGITRANS-ERASMUS-EDU-2023-CBHE.

The textbook is devised for students studying in the fields of electrical engineering, computer engineering, and automotive transport. The book comprehensively overviews key concepts, technologies, and applications related to modern electric drive systems, automotive electronics, and energy-efficient transportation solutions. It covers theoretical foundations, practical implementation, and recent advances in these fields, offering valuable information for students, researchers, and professionals in the automotive and electrical sectors.

Key Action: KA2 - Cooperation for innovation and the exchange of good practices

Action: Capacity Building in Higher Education

Action Type: Joint Projects

Deliverable: 2.2. Elaboration of text e-books for students and teachers.

Co-funded by the
Erasmus+ Programme
of the European Union

Project Coordinator: Anatolijs Zabasta

Project Scientific Manager: Nadezhda Kunicina

Editor: Andrii Hnatov

Institution: Riga Technical University

https://doi.org/10.7250/9789934371943

ISBN 978-9934-37-194-3

Contributors

Nadezhda Kunicina, professor, senior researcher of Institute of Industrial Electronics, Electrical Engineering and Energy, Faculty of Computer Science, Information Technology and Energy, Riga Technical University12/1 Azenes Str. - 503., Riga, LV 1048, Latvia, tel. +371 67089052, nadezda.kunicina@rtu.lv

Anatolijs Zabasta, senior researcher of Institute of Industrial Electronics, Electrical Engineering and Energy, Faculty of Computer Science, Information Technology and Energy, Riga Technical University 12/1 Azenes Str. - 503., Riga, LV 1048, Latvia, tel. +371 67089051, anatolijs.zabasta@rtu.lv

Kristaps Vitols, senior researcher of of Institute of Industrial Electronics, Electrical Engineering and Energy, Faculty of Computer Science, Information Technology and Energy, Riga Technical University 12/1 Azenes Str. - 501., Riga, LV 1048, Latvia, tel. +371 26407575, kristaps.vitols@rtu.lv

Andrii Hnatov, professor, Dr. of Science, Head of Vehicle Electronics Department, Kharkiv National Automobile and Highway University, 25, Yaroslav Mudry Str.street, Kharkiv, Ukraine, 61002, tel. +380 667430887, kalifus76@gmail.com

Shchasiana Arhun, professor, Dr. of Science, professor of Vehicle Electronics Department, Kharkiv National Automobile and Highway University, 25, Yaroslav Mudry Str.street, Kharkiv, Ukraine, 61002, tel. +380 993780451, shasyana@gmail.com

Oleksandr Dziubenko, Ph. D., assistant professor of Vehicle Electronics Department, Kharkiv National Automobile and Highway University, 25, Yaroslav Mudry Str.street, Kharkiv, Ukraine, 61002, tel. +380 667684116, dzyubenko.alan@gmail.com

Yuriy Borodenko, Ph. D., assistant professor of Vehicle Electronics Department, Kharkiv National Automobile and Highway University, 25, Yaroslav Mudry Str.street, Kharkiv, Ukraine, 61002, tel. +380 983629112, docentmaster@gmail.com

Olha Ulianets, assistant of Vehicle Electronics Department, Kharkiv National Automobile and Highway University, 25, Yaroslav Mudry Str.street, Kharkiv, Ukraine, 61002, tel. +380 957336312, olga.ulyanets@gmail.com

Ruslan Bagach, Ph. D., assistant professor of Vehicle Electronics Department, Kharkiv National Automobile and Highway University, 25, Yaroslav Mudry Str.street, Kharkiv, Ukraine, 61002, tel. +380 507255660, bagach.ruslan@gmail.com

Pavlo Sokhin, senior lecturer of Vehicle Electronics Department, Kharkiv National Automobile and Highway University, 25, Yaroslav Mudry Str.street, Kharkiv, Ukraine, 61002, tel. +380 633473433, paska1987@ukr.net

Vadim Cazac, Ph. D., associate professor of Electrical Engineering Department, Technical University of Moldova, 78, 31 August 1989 street, Chisinau, Republic of Moldova, MD-2012, tel. +373 79019692, vadimcazac@gmail.com

Alexandr Ojegov, Ph. D in Engineering, associate professor of Department of Physical and Engineering Sciences, Alecu Russo Balti State University, 38 Pushkin Str., Balti, Republic of Moldova, 3121, tel. +373 79215624, alexandr.ojegov@usarb.md

Chivu Robert-Mădălin, Ph. D., assistant professor of Department of Thermal Systems and Automotive Engineering, “Dunarea de Jos” University, 800001 Galati, Romania, tel 0040724874968, e-mail: robert.chivu@ugal.ro

Fratita Michael, Ph. D., Assistant Professor of Thermal Systems and Road Vehicles Department, "Dunarea de Jos" University of Galati, 25, 47 Domneasca street, Galati, Romania, 800008, tel. +40745553794, michael.fratita@ugal.ro

Ion Ion, professor, Dr. of Science, professor of Thermal Systems and Automotive, "Dunarea de Jos" University of Galati, 47 Domneasca St., 800008 Galati, Romania, tel. +40740566214, ion.ion@ugal.ro

Content

Introduction

The transformation of the global transportation sector is being driven by urgent environmental concerns, rapid technological advances, and the increasing demand for sustainable energy solutions. Against this backdrop, the development and integration of electric drive systems, automotive electronics, and energy-saving technologies have become critical priorities for the future of mobility.

This textbook, Electric Drive, Automotive Electronics, and Energy-Saving Technologies for Modern Transport, provides a comprehensive overview of key concepts, technologies, and methodologies shaping the next generation of transport systems. It is designed to equip students, researchers, and practitioners with the foundational knowledge and practical insights needed to understand, design, and optimize electric and hybrid vehicles.

The book is structured into six interrelated chapters:

Chapter 1 introduces the principles of electric drive systems, contrasting electric motors with internal combustion engines and analyzing the mechanical characteristics of various motor types, including induction, synchronous, and brushless DC motors.

Chapter 2 focuses on power supply systems and essential electronic devices used in modern transport, such as accumulator batteries, supercapacitors, inverters, and converters.

Chapter 3 addresses electric vehicle (EV) charging technologies, exploring the infrastructure, system types, power levels, economic factors, and emerging trends such as smart charging.

Chapter 4 examines the role of electric transport in climate change mitigation, highlighting transport energy consumption patterns, emission sources, and the environmental benefits of EV adoption.

Chapter 5 delves into advanced modeling and simulation techniques for electric and hybrid vehicle powertrains, including detailed modeling of batteries, inverters, electric motors, vehicle dynamics, auxiliary loads, and internal combustion engines.

Chapter 6 discusses the key characteristics of electric transport power sources, with emphasis on lithium-ion battery technologies, battery management systems, fuel cells, and supercapacitors.

Each chapter integrates theoretical background with applied perspectives, aiming to bridge the gap between engineering fundamentals and real-world technological challenges. Through a systematic exploration of modern transport innovations, this textbook seeks to foster a deeper understanding of sustainable vehicle technologies and prepare readers to contribute effectively to the evolving landscape of electric mobility.

Chapter 1: ELECTRIC DRIVE

1.1. Internal combustion engine vs Electric motor

The propulsion system is the heart of the electric vehicle, and the electric motor is located right in the center of the system. The electric motor converts electrical energy from the battery into mechanical energy, which allows the vehicle to move. It also works as a generator during regenerative braking, which sends energy back to the source, Figure. 1.1 [1-36].

Figure 1.1. Electric motor for electric car

The electric motor converts electrical energy from the battery into mechanical energy, which allows the vehicle to move. It also works as a generator during regenerative braking, which sends energy back to the source.

But not everything is as simple as it seems. Electric motor is extremely efficient, only 5% of the energy is lost. You should agree that this power must be curbed and you should be able to handle it, and for this you need to know some peculiarities of the work and the types of electric motors.

If we compare electric motors with internal combustion engines (ICE), we immediately need to note a number of their significant advantages:

1) The electric motor consists of much fewer parts, unlike ICE. This directly indicates the high reliability of electric motor in comparison with the internal combustion engine, Figure 1.2.

2) The engine torque reaches its maximum immediately when it is turned on, thus, electric cars do not require the presence of starters and gearboxes typical for ICE, Figure 1.3.

3) The operation of the electric motor at different speeds (from 0 to 18000 rpm) with high efficiency allows the electric car to do without a gearbox. To reverse the engine, i.e. to turn on the reverse, it is enough to change the polarity (for DC motors) or phase rotation (for AC motors), Figure 1.4.

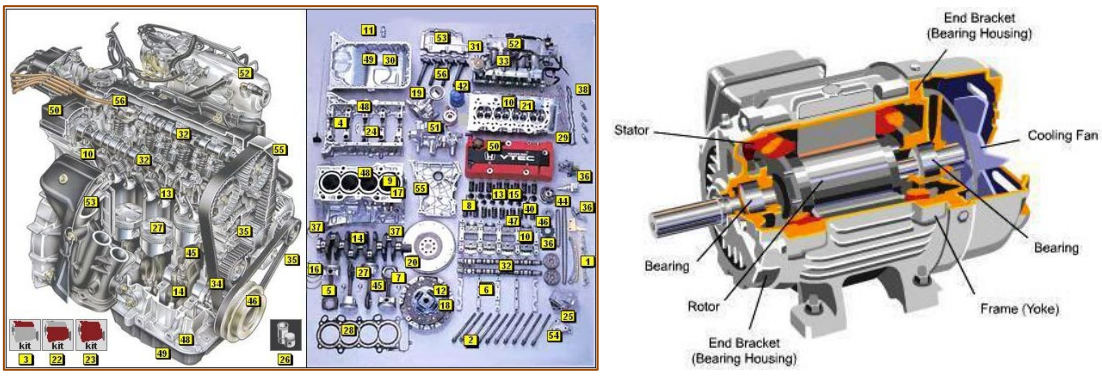

Figure. 1.2. Compare electric motors with internal combustion engines

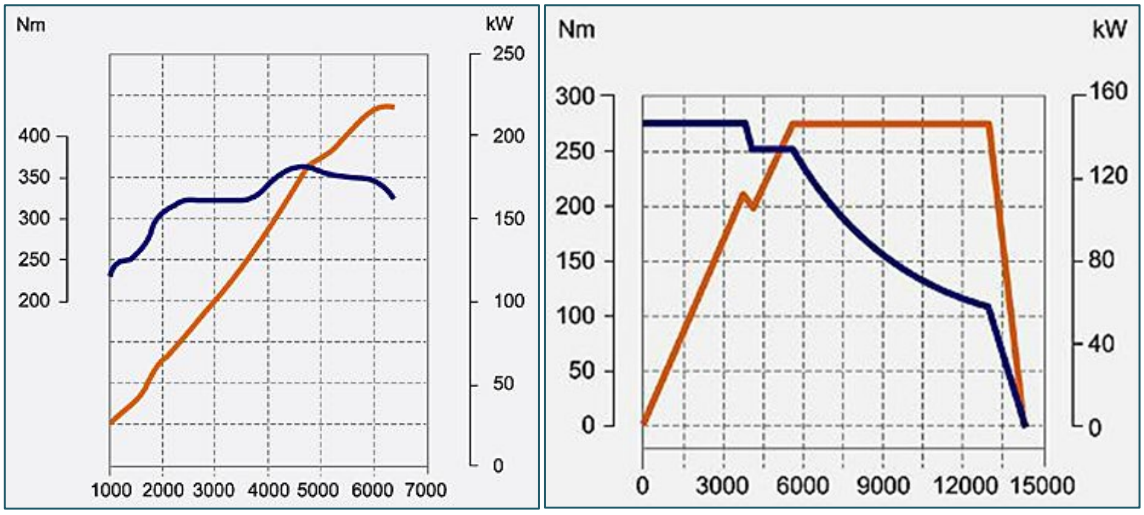

Figure1.3. ICE Vs Electric motor: torque and power

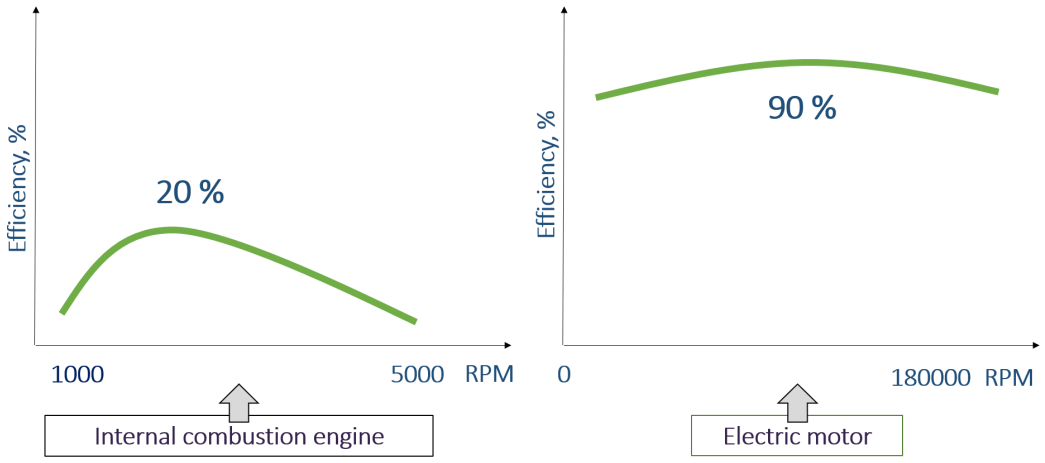

Figure1.4. ICE Vs Electric motor: speed range

4) The specific energy parameters of the electric motor are much higher than that of the internal combustion engine, Table 1.1.

Table 1.1 ICE vs Electric motor

Parameters	Typical ICE	Tesla – Induction motor
Weight	~180 kg	31.8kg
Power	~140 kW	270 kW
Weight/Power	~0.8 kW/kg	8.5 kW/kg

However, it is necessary to understand that it is not safe to start an electric vehicle from the entire potential of torque, which is much more powerful than many cars with internal combustion engines, and this causes inefficient battery consumption.

Electric motors can be classified by the type of current, Figure 1.5:

- AC motors;
- DC motors;
- Combined engines.

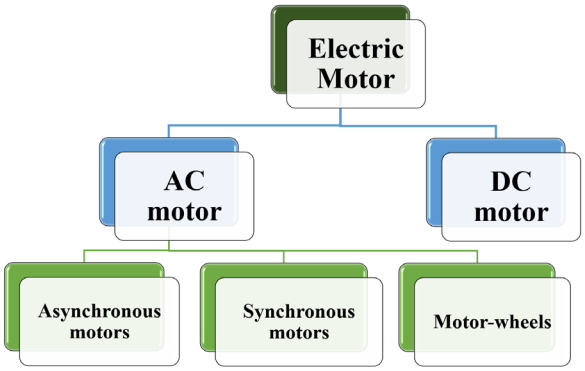

Figure 1.5. Classification of electric motors

1.2. Mechanical characteristic of an Induction motor

Induction motors (IM) have found widespread industrial applications due to several significant advantages over other types of motors. The induction motor is simple and reliable in operation, as it lacks a commutator. Induction motors are also cheaper and significantly lighter than DC motors.

A three-phase IM includes a stator winding connected to a three-phase IM network with voltage U1 and frequency f1, and a rotor winding, which can be implemented in two designs (Figure 1.6).

First Design: This involves a conventional three-phase winding made of conductors with terminals on three slip rings. Such a construction corresponds to an IM with a wound rotor (Figure 1.6,a) and allows for various electrical elements, such as resistors, to be included in the rotor circuit to regulate speed, current, and torque. Special connection schemes can also be implemented for the same purposes.

Second Design: The rotor winding is created by casting aluminum into the rotor slots, resulting in a structure known as a “squirrel cage”. The schematic of an IM with this winding, which has no terminals and is referred to as a squirrel-cage rotor, is shown in Figure 1.6,b.

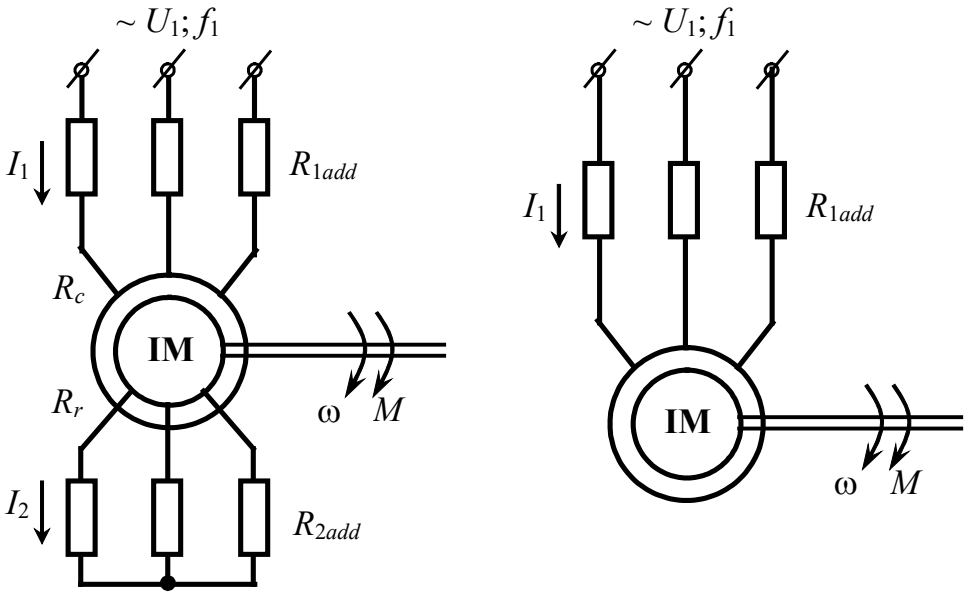

a b

Figure 1.6. IM switching diagram with a phase rotor (a) and a short-circuited rotor (b)

To derive expressions for the electromechanical and mechanical characteristics of an IM, its equivalent circuit is used, where the stator and rotor circuits are represented by their active and inductive resistances. A unique feature of the IM equivalent circuit is that the current, EMF, and rotor circuit parameters are converted (referred) to the stator circuit. This allows these two circuits to be depicted as electrically connected in the schematic, even though their actual connection is through the electromagnetic field.

Conversion is performed using the IM transformation coefficient for EMF

$$k = \frac{E_1}{E_2} \approx \frac{0,95U_{f.nom}}{E_{2k}}, \tag{1.1}$$

where E_1 and E_2 – are the phase EMFs of the stator and rotor at standstill;

$U_{f.nom}$ – is the phase nominal network voltage.

The calculation formulas for reduction have the following form

$$E_2' = E_2 k = E_1;\ I_2' = \frac{I_2}{k};\ R_2' = R_2 k^2 X_2' = X_2 k^2, \tag{1.2}$$

Where the dash indicates the reduced values.

In the theory of electrical machines, two main equivalent circuits of an induction motor are developed and applied: the more precise T-shaped and the simplified Π-shaped. Figure 1.7

presents the Π-shaped equivalent circuit, which is further used to derive formulas for the characteristics of an induction motor.

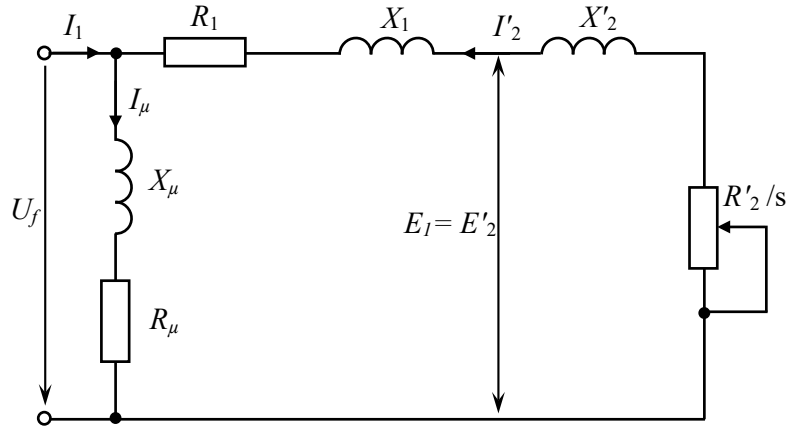

Figure 1.7. IM replacement diagram

In the diagrams (Figure 1.6 and 1.7), the following notations are adopted:

U_1, U_f are the effective values of the line and phase voltages of the network;

I_1, I_μ, I'_2 are the phase currents of the stator, magnetizing current, and the referred rotor current;

X_1, X'_2 iare the inductive reactances due to leakage fluxes of the stator winding phase and the referred rotor phase;

X_μ is the inductive resistance of the magnetizing circuit;

R_μ is the active resistance of the magnetizing circuit;

R_c, R_{1add}, $R_1 = R_c + R_{1add}$ are the active phase resistances of the stator winding, additional resistor and total stator resistance;

R'_r, R'_{2add}, $R'_2 = R'_r + R'_{2add}$ are the active phase resistances of the rotor winding, additional resistor and total rotor resistance reduced to the stator winding;

$s = \dfrac{\omega_0 - \omega}{\omega_0}$ – is the slip of the IM motor;

$\omega_0 = \dfrac{2\pi f_1}{p}$ –is the angular velocity of the IM magnetic field (synchronous speed);

f_1 – is the frequency of the supply voltage;

p – is the number of pairs of AC poles.

As can be seen from the diagram, the stator EMF is equal to the reduced rotor EMF, and the magnetizing current I_μ, which determines the magnetic flux IM, flows under the action of U_f along a certain circle consisting of the resistances of the magnetizing circuit X_μ and R_μ, and is the vector sum of the stator and reduced rotor currents, i.e. $I_\mu = I_1 + I'_2$.

According to the given equivalent circuit, we can obtain an expression for the secondary current

$$I_2' = \frac{U_f}{\sqrt{\left(R_1 + \frac{R_2'}{s}\right)^2 + \left(X_1 + X_2'\right)^2}}. \quad (1.3)$$

The torque of an induction motor can be determined from the loss expression, from which

$$M = \frac{3\left(I_2'\right)^2 R_2'}{\omega_0 s}. \quad (1.4)$$

Substituting the current value I_2' into (1.4), we obtain

$$M = \frac{3U_f^2 R_2'}{\omega_0 \left[\left(R_1 + \frac{R_2'}{s}\right)^2 + \left(X_1 + X_2'\right)^2\right] s}, \quad (1.5)$$

The torque curve $M = f(s)$ has two maxima: one in the generator mode, the other in the motor mode (with significant rotor resistances, the maximum torque may be in the anti-lock braking mode).

By equating, we determine the value of the critical slip scr at which the motor develops the maximum (critical) torque

$$s_{cr} = \pm \frac{R_2'}{\sqrt{R_1^2 + \left(X_1 + X_2'\right)^2}}. \quad (1.6)$$

Substituting the value of scr into (1.5), we find the expression for the maximum moment

$$M_{cr} = \frac{3U_f^2}{2\omega_0 \left[R_1 \pm \sqrt{R_1^2 + \left(X_1 + X_2'\right)^2}\right]}. \quad (1.7)$$

The "+" sign in equations (1.6) and (1.7) refers to the engine mode (or braking by counter-switching), the "–" sign to the generator mode of operation in parallel with the network (at $\omega > \omega_0$).

If expression (1.5) is divided into (1.7) and the corresponding transformations are performed, we can obtain

$$M = \frac{2M_{cr}\left(1 + as_{cr}\right)}{\frac{s}{s_{cr}} + \frac{s_{cr}}{s} + 2as_{cr}}, \quad (1.8)$$

where M_{cr} is the maximum engine torque;

s_{cr} is the critical slip corresponding to the maximum moment;

$$a = \frac{R_1}{R_2'}.$$

Here it is necessary to emphasize a very important circumstance for practice – the influence of changes in the mains voltage on the mechanical characteristics of the IM. As can be seen from (1.5), at a given slip, the motor torque is proportional to the square of the voltage, therefore, a motor of this type is sensitive to fluctuations in the mains voltage.

Mechanical characteristics of an Induction motor

The critical slip and angular velocity of ideal idling do not depend on voltage.

Figure 1.8 shows the mechanical characteristic of the IM.

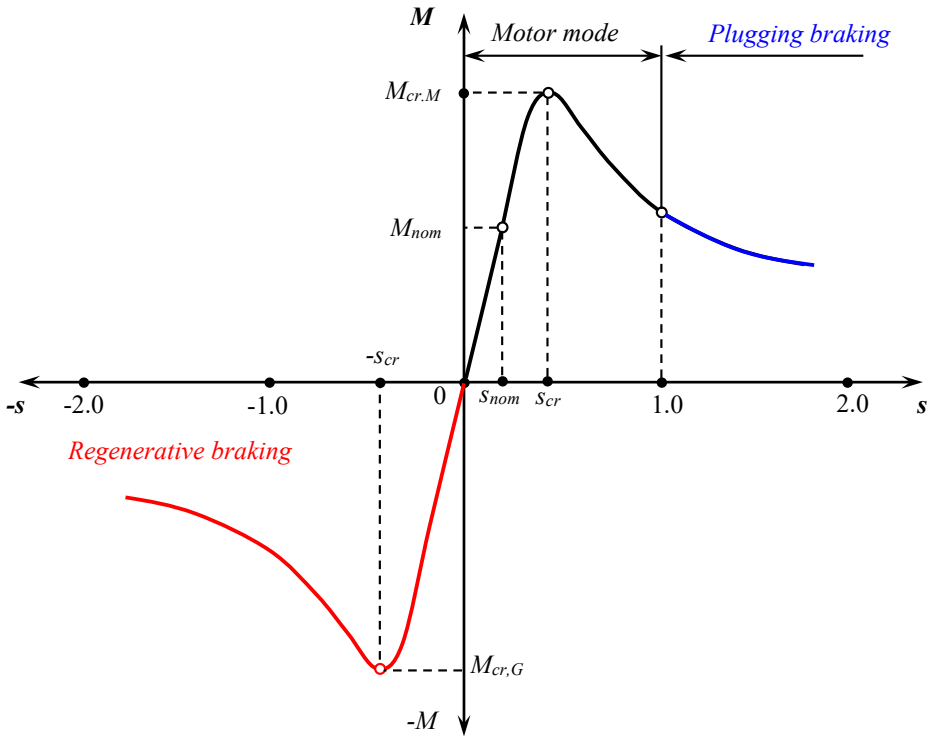

Figure 1.8. Mechanical characteristics of an induction motor

Its characteristic points:

1) $s = 0$; $M = 0$, while the engine speed is equal to the synchronous speed;

2) $s = s_{nom}$; $M = M_{nom}$, corresponding to the rated speed and rated torque;

3) $s = s_{cr}$; $M = M_{cr,M}$, maximum torque in motor mode;

4) $s = 1.0$; $M = M_{In.} = \dfrac{2M_{cr}\left(1+as_{cr}\right)s_{cr}}{1+s_{cr}^2\left(1+2a\right)}$ – the initial starting moment;

5) $s = -s_{cr}$; $M = M_{cr,G}$ – maximum torque in generator mode of operation in parallel with the network.

When $s > 1.0$, the motor operates in the braking mode by counter-switching, when $s < 0$, the generator mode of operation in parallel with the network (regenerative braking) takes place.

It should be emphasized that the absolute values in the motor mode and the generator mode in parallel with the network are the same.

However, it follows from (1.7) that the maximum torques in the motor mode and the generator mode are different. In the generator mode of operation in parallel with the network, the maximum torque in absolute value is greater, which follows from the relation:

$$M_{cr.G} = M_{cr.M} \frac{R_1 + \sqrt{R_1^2 + X_k^2}}{R_1 - \sqrt{R_1^2 + X_k^2}} \ , \tag{1.9}$$

where $X_k = X_1 + X_2'$.

If we neglect the active resistance of the stator in equation (1.8), we get a formula that is more convenient for calculations:

$$M = \frac{2M_{cr}}{\frac{s}{s_{cr}} + \frac{s_{cr}}{s}} \ , \tag{1.10}$$

where $s_{cr} = \pm \frac{R_2'}{X_k}$; $M_{cr} = \frac{3U_f^2}{2\omega_0 X_k}$

Substituting into expression (1.10) instead of the current values of M and s their nominal values and denoting the multiplicity of the maximum moment $\frac{M_{cr}}{M_{nom}}$ by λ – overload capacity, we obtain

$$s_{cr} = s_{nom}\left(\lambda + \sqrt{\lambda^2 - 1}\right). \tag{1.11}$$

Analysis of formula (1.10) shows that when $s > s_{cr}$ (non-working part of the characteristic), the equation of a hyperbola will be obtained if in this case the second term of the denominator in equation (1.10) is neglected, i.e.

$$M = 2M_{cr}\frac{s_{cr}}{s}, \tag{1.12}$$

or

$$\mathrm{M} = \mathrm{A/s}\,, \tag{1.13}$$

where $A = 2M_{cr}s_{cr}$.

This part of the characteristic practically corresponds only to the starting and braking modes.

For small values of slip ($s < s_{cr}$) for $M = f(s)$ the equation of the straight line will be obtained if the first term in the denominator (1.10) is neglected

$$M = 2M_{cr}\frac{s}{s_{cr}}, \tag{1.14}$$

or

$$M = B \cdot s, \tag{1.15}$$

where $B = \frac{2M_{cr}}{s_{cr}}$.

This linear segment of the characteristic represents its operational range, within which the motor operates in a steady state. On this segment, points corresponding to the motor's nominal parameters-nominal torque (M_{nom}), nominal current (I_{nom}), nominal speed (n_{nom}), and nominal slip (s_{nom}) are located. The static speed drop (Δn) in relative units on the natural mechanical characteristic of an induction motor at nominal torque is determined by its nominal slip.

The value of nominal slip depends on the rotor resistance. Induction motors with squirrel-cage rotors of standard design typically exhibit the lowest nominal slip for a given power and number of poles. Due to their design features, these motors have relatively low rotor resistance, leading to reduced values of critical slip (s_{cr}) and nominal slip (s_{nom}). For the same reasons, as the motor's power increases, its nominal slip decreases, and the stiffness of its inherent mechanical characteristic increases. This is illustrated by the curve in Figure 1.9, constructed based on average data for motors of various power ratings.

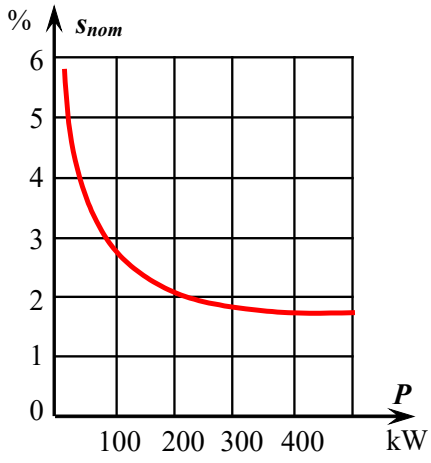

Figure 1.9. Nominal slip curve for IM of different capacities

The magnitude of the critical moment, as can be seen from (1.7), does not depend on the active resistance of the rotor, while the critical slip according to (1.6) increases as the rotor resistance increases. As a result, in motors with a phase rotor, when resistors are introduced into the rotor circuit, the maximum of the torque curve shifts towards large slips.

The value of the resistance required to construct the natural and rheostatic characteristics of a motor with a phase rotor is determined from the expression:

$$R_2 = \frac{s_{nom}E_{2k}}{\sqrt{3}I_{2nom}}, \tag{1.16}$$

where E_{2k}, I_{2nom} – is the linear voltage at a stationary rotor and the rated rotor current.

Figure 1.10 shows a family of rheostat characteristics in the engine mode in the coordinate axes M and ω for different values of the resistances of the rotor circuit. With a known approximation, the rheostat characteristics in their working part can be assumed to be linear. This makes it possible to use methods similar to those used to calculate the resistance of the armature circuit of a IM with independent excitation when calculating the resistance of the armature circuit of a DC motor. Some inaccuracy in determining the resistor resistance is introduced due to the fact that the characteristic of the IM in the section of the graph from $M = 0$ to the maximum torque at start-up is considered linear.

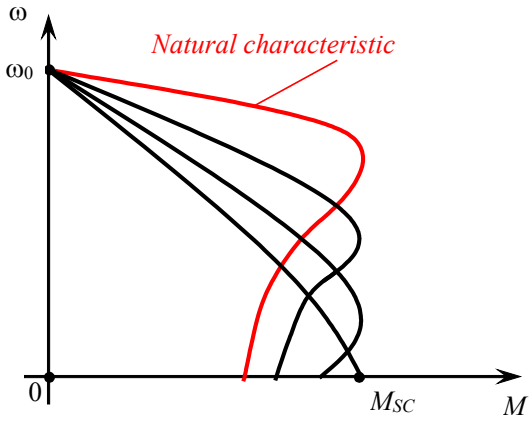

Figure 1.10. Intrinsic and rheostatic mechanical characteristics of an IM motor with a phase rotor

More accurate is the method when the characteristics are rectified over a smaller area. The maximum torque factor through $\lambda = \frac{M_{cr.M}}{M_{nom}}$ should be at least 1.8 for normal motors with a phase rotor, and at least 1.7 for motors with a squirrel-cage rotor. Crane motors are distinguished by a higher maximum torque factor. For example, for motors with a squirrel-cage rotor of the MTK series $\lambda = 2.3 \div 3.4$. Motors with a phase rotor of the mentioned series have approximately the same values of λ.

For motors with a squirrel-cage rotor, the factors of the initial starting torque and the initial starting current are of significant importance from the point of view of the electric drive.

1.3. Mechanical characteristic of a Synchronous motor

Synchronous motors, if they operate at a constant frequency with unchanged angular velocity, are used for drives that do not require speed regulation. Such drives include compressors, refrigeration machines, stone crushers, and others. The main advantage of a synchronous motor lies in its ability to operate with a high-power factor, leading to its increasingly wide application.

The angular velocity of a synchronous motor (Figure 1.11, b) during steady-state operation, as the load on the shaft increases up to a certain value not exceeding the maximum torque Mmax, remains constant and equal to the synchronous angular velocity

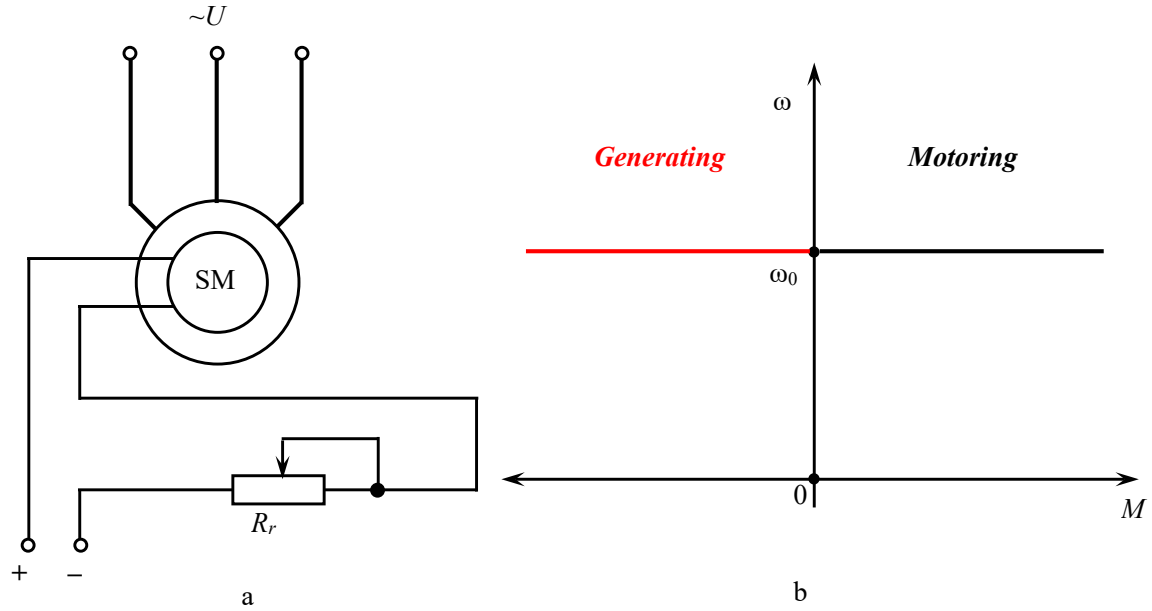

Figure 1.11. Connection scheme (a) and mechanical characteristic (b) of a synchronous motor

$$\omega_0 = \frac{2\pi f_1}{p}. \qquad (1.17)$$

Therefore, its mechanical characteristic is a straight line parallel to the horizontal axis. If the load torque exceeds Mmax, the motor may lose synchronism, disrupting the dependency shown in Figure 1.11, b.

Starting characteristics of a Synchronous motor

Modern synchronous motors have a special starting squirrel-cage winding in addition to the normal working winding, which is powered by direct current. This starting winding enables the motor to start as an induction motor, and thus, it possesses an induction characteristic during starting. Figure 1.12 shows two starting characteristics of a synchronous motor. One of them (curve 1) corresponds to a start with reduced initial starting torque Mst and a significant "entry torque" Men1, defined as the torque developed at a speed of approximately 0.95 of synchronous speed. At this speed, synchronization becomes possible after connecting direct current to the excitation winding

If the starting cage has increased active resistance, the initial starting torque Mst2 will be higher than in the previous case, while the entry torque M_{en2} will be lower (curve 2 in Figure 1.12). The choice between the two starting characteristics depends on the resistance torques of the industrial mechanisms.

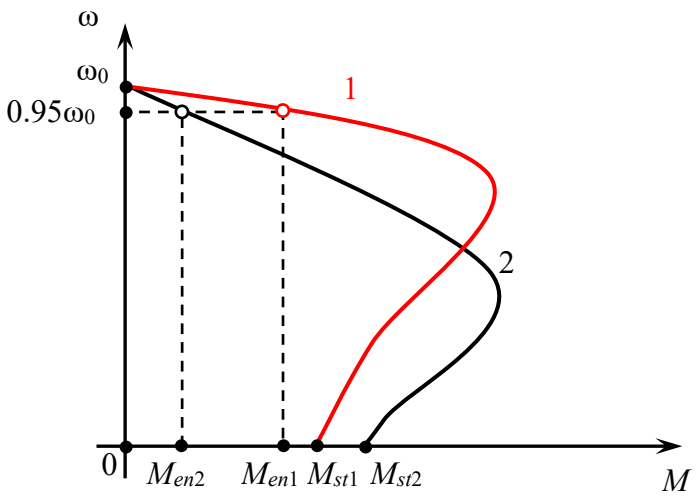

Figure 1.12. Starting characteristics of a synchronous motor

Angular Characteristic of a Synchronous motor

Under pulsating load conditions on the motor shaft during steady-state operation, the instantaneous speed fluctuates around its average value. These fluctuations occur due to changes in the angle between the voltage and the EMF of the synchronous machine. Speed fluctuations are significant when a synchronous motor is used with a pulsating load, such as a reciprocating compressor. To ensure stable motor operation in such cases, it is necessary to understand the relationship between torque M and the angle θ (in degrees) between the voltage and the EMF. This angle corresponds to the spatial displacement angle between the machine's resultant field axis and the pole axis (spatial angle θ is p times smaller than the electrical angle θ). The relationship between the torque of a synchronous machine and the angle θ is known as the angular characteristic

To find the angular characteristic, consider the simplified vector diagram of a non-salient pole machine, shown in Figure 1.13. Neglecting losses in the active resistance of the stator $R_c = 0$ (Figure 1.4), the power supplied to the synchronous motor can be assumed to be equal to the electromagnetic power, W

$$P = 3IU \cdot \cos\varphi, \text{ W} \qquad (1.18)$$

where I and U are the phase current and voltage of the stator.

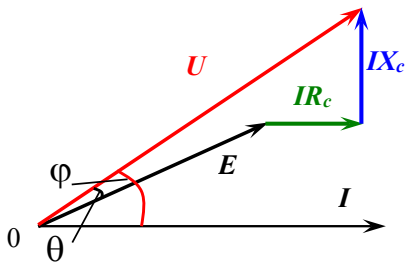

Figure 1.13. Simplified vector diagram of a synchronous motor

From the vector diagram (Figure 1.14), it follows that

$$U \cdot \cos\varphi = E\cos(\varphi - \theta). \tag{1.19}$$

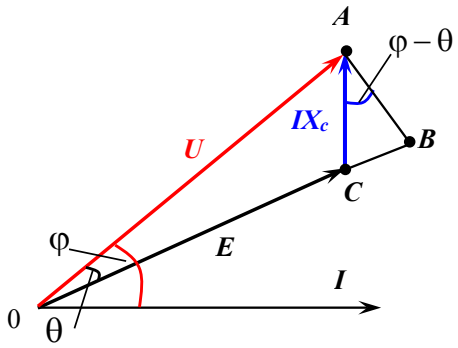

Figure 1.14. Simplified vector diagram of a synchronous motor, neglecting losses in the stator's active resistance

From the consideration of the auxiliary triangle ABC it is clear (Figure 1.14) that

$$\cos(\varphi - \theta) = \frac{AB}{AC} = \frac{U\sin\theta}{IX_c}.$$

Therefore

$$U \cdot \cos\varphi = EU\frac{\sin\theta}{IX_c}. \tag{1.20}$$

Now, substituting the obtained expression into equality (1.18) and replacing the angle φ with the angle θ, we obtain the equation of electromagnetic power:

$$P = 3EI_{sc}\sin\theta \tag{1.21}$$

where I_{sc} is the short circuit current

$$I_{sc} = \frac{U}{X_c}. \tag{1.22}$$

Then the electromagnetic moment:

$$M = \frac{P}{\omega_0} = \frac{3}{\omega_0}EI_{sc}\sin\theta. \tag{1.23}$$

In the case of a salient-pole machine, an additional reactive moment appears. However, for practical calculations, it can be neglected and formula (1.23) can be used.

When $\theta = 90^0$ the moment has a maximum value

$$M_{\max} = \frac{3}{\omega_0}EI_{sc}. \tag{1.24}$$

Therefore, the angular characteristic equation takes the following form:

$$M = M_{\max}\sin\theta. \tag{1.25}$$

As the load increases, the angle θ also increases. From equation (1.25), it is evident that, initially, as θ grows, the torque developed by the motor increases (Figure 1.15), which meets the conditions for stable motor operation. On the right side of the graph, when $\theta>90^0$, the condition for stable motor operation is violated because, with increasing load, θ continues to increase, while the developed torque decreases, causing the motor to lose synchronism. The left portion of the characteristic is the working part, while the right portion, where θ changes from 90^0 to 180^0, is the unstable part of the characteristic.

The nominal torque M_{nom} of the motor corresponds approximately to $\theta=30^0$. In this case, the ratio of the maximum torque to the nominal torque is

$$\lambda = \frac{M_{\max}}{M_{nom}} = 2 \div 2.5 .$$

However, in special cases, synchronous machines with a higher ratio of maximum to nominal torque, reaching 3.5–4, are sometimes selected.

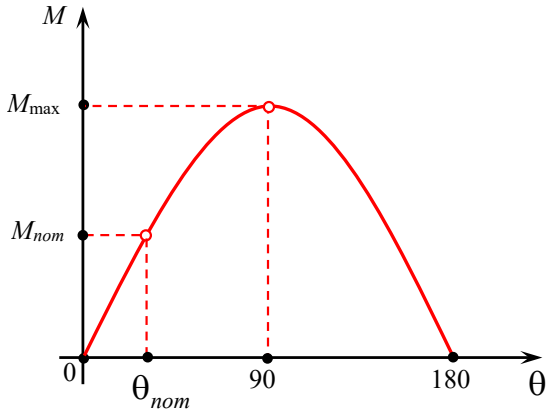

Figure 1.15. Angular characteristic of a synchronous motor

A synchronous motor can also operate in generator mode, delivering energy back to the grid at synchronous speed when the load torque on the shaft is negative. This corresponds to the left branch of the characteristic in Figure 1.11, b.

For braking purposes, this mode has little practical significance since it does not allow speed reduction. Dynamic braking of a synchronous motor is commonly used, during which the stator winding is disconnected from the grid and short-circuited through a resistor (Figure 1.16). The mechanical characteristics in this case resemble those of an induction motor during dynamic braking (Figure 1.17). The braking intensity depends on the resistance of the stator circuit and the magnetic flux created by the rotor winding current. The braking time, when the excitation circuits are powered by a self-excited generator located on the shaft of the synchronous motor, is longer than when powered by an independent DC source. This is because, as the rotation speed of the exciter decreases, its EMF also decreases, reducing the excitation current and the braking torque.

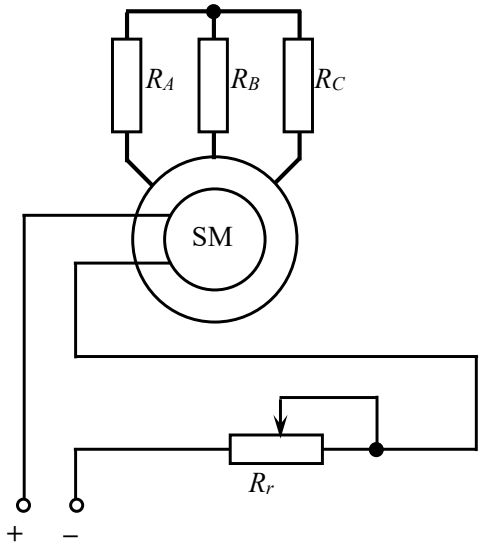

Figure 1.16. Schematic diagram of a synchronous motor during dynamic braking

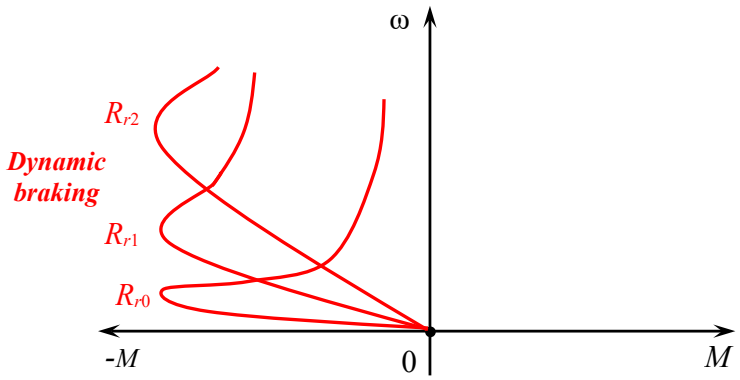

Figure 1.17. Mechanical characteristics of a synchronous motor in dynamic braking mode

Braking of a synchronous motor via counter-current is rarely used because it is accompanied by large current surges and complicates control apparatus due to the necessity of disconnecting the motor when approaching zero speed.

1.4. Brushless DC Motor

In order to improve the properties of DC motors, motors with a contactless commutator were created, which are called contactless DC motors (CDMS), Figure 1.18. The difference between CDMS and collector motors of traditional design is that in them the brush-collector assembly is replaced by a semiconductor commutator (inverter), controlled by signals coming from a contactless rotor position sensor. The working winding of the motor - the armature winding - is located on the stator core, and the permanent magnet - on the rotor.

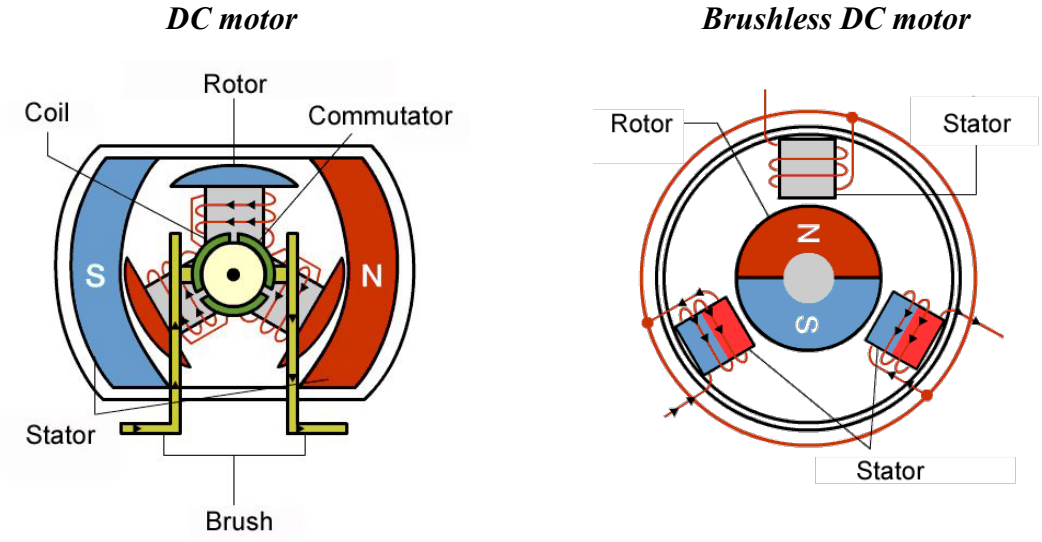

Figure 1.18. Circuit diagrams of DC electric motors

The motor shaft M (Figure 1.19, a) is mechanically connected to the rotor position sensor RPS, the signal from which is fed to the switch SB.

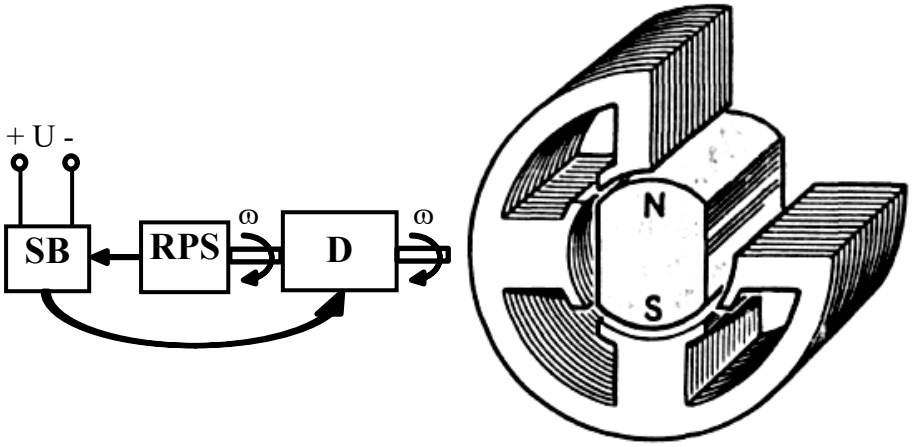

a b

Figure 1.19 - Block diagram (a) and magnetic system (b) of a four-phase brushless DC motor

The connection of the armature winding sections to the DC source occurs through the elements of the switch block SB. The purpose of the RPS is to issue a control signal to the switch block in accordance with the position of the permanent magnet poles relative to the armature winding sections.

As rotor position sensors, various sensitive non-contact elements with minimal dimensions and power consumption and a high multiplicity of minimum and maximum signals are used so as not to cause disturbances in the operation of the switch unit. Sensitive elements of the RPS must work reliably under external influences (temperature, humidity, vibrations, etc.) for which the engine is designed. Such features are inherent in a number of sensitive elements (sensors): inductive, transformer, magneto-diode, etc. It is most advisable to use Hall EMF sensors (Figure 1.20), which are a thin semiconductor plate with contact pads applied to it, to which pins 1-2

are soldered, which are connected to the voltage source U_1 and pins 3-4, from which the output signal U_2 is taken. If a current I flows in the circuit 1-2, and the sensor is in a magnetic field, the induction vector B of which is perpendicular to the plane of the sensor plate, then an EMF is induced in the sensor and a voltage U_2 appears at the terminals 3-4. The value of the EMF depends on the current I and the magnetic induction B, and the polarity depends on the direction of the current I in the circuit 1-2 and the direction of the magnetic induction vector B.

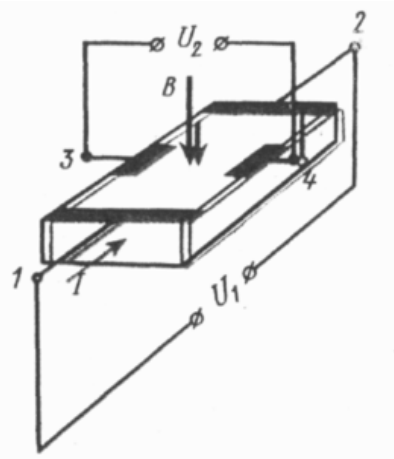

Figure 1.20. Hall EMF sensor

The Hall effect is the occurrence of an electric field in a conductor or semiconductor with a current when it is placed in a magnetic field.

The Hall effect is a consequence of the influence of the Lorentz force on the movement of current carriers. In a magnetic field, when a current flows through a conductor with a density, an electric field with a strength of

$$\vec{E} = R\left[\vec{B}, \vec{j}\right], \tag{1.26}$$

where R is the Hall constant.

Chapter 2: POWER SUPPLY AND ELECTRONIC DEVICES FOR MODERN TRANSPORT

Power supply systems play a vital role in the functioning of automobiles by providing the necessary energy to operate engines and other systems. There are a variety of power supply system technologies used in automobiles with traditional internal combustion engines, hybrid systems, and electric motors. In today's world, there is a drive to develop more efficient and environmentally friendly power supply systems, leading to the development of new technologies such as electric vehicles and alternative energy sources. Despite significant advances in vehicle power supply systems, challenges remain, such as: increasing energy efficiency, reducing emissions, and developing an infrastructure for alternative energy sources. However, with innovative developments and active technology development, there is ample opportunity to improve vehicle power supply systems in the future. Vehicle power supply systems have a significant impact on society and the environment. The transition to cleaner and more efficient energy sources can lead to reduced pollution and reduced dependence on volatile resources. Overall, vehicle power supply systems play a key role in today's transportation sector, and their development and improvement are essential to ensure a sustainable and efficient future.

This chapter is dedicated to the description, construction and operation mode of functioning of power supply electronic devices for modern transport [37-49].

2.1. Accumulator batteries

Accumulator batteries are devices designed to store electrical energy in chemical form and then use it as an electric current. The principle of operation of accumulators is based on reversible chemical reactions, which allow batteries to be charged and discharged repeatedly. A battery is composed of several cells connected together in series. A cell is an independent and complete unit that possesses all the electrochemical properties. The grouped cells are enclosed in a body to form a battery module. A battery pack is made up of battery modules connected in series and/or parallel to provide the voltage and energy required by the drive system.

The main components of a battery cell are [37]:

- Electrodes – anode (negative electrode) and cathode (positive electrode);
- Electrolyte – conducts ions between the anode and cathode;
- Separator – prevents contact between the electrodes but allows ions to pass.

The principle of operation of batteries is based on two main processes: charging and discharging. When charging, a current source is connected to the battery. In this case, electrons move to the anode, which causes oxidation reactions. Ions, such as lithium, move through the

electrolyte from the cathode to the anode and are built into the structure of the anode. The energy supplied during the charging process is stored in chemical form.

When the battery is discharged, it is connected to a load (such as an electronic device), electrons move from the anode to the cathode through an external circuit, creating an electric current. Ions move back to the cathode through the electrolyte, releasing the chemically stored energy as electrical energy.

Batteries are classified by the type of chemical element as [37-41]:

– Lithium-ion (Li-ion): the most popular type of battery with high energy density, long durability and minimal memory effect (Figure 2.1).

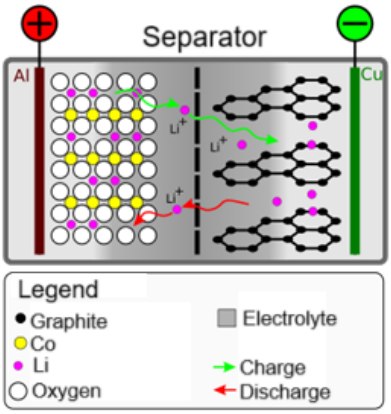

Figure 2.1. Scheme of a lithium-ion battery

– The nickel-cadmium battery (Ni-Cd) is a type of rechargeable battery using nickel oxide hydroxide and metallic cadmium as electrodes (Figure 2.2). Compared with other types of rechargeable cells they offer good cycle life and performance at low temperatures with a fair capacity but their significant advantage is the ability to deliver practically their full rated capacity at high discharge rates (discharging in one hour or less). However, the materials are costlier than that of the lead-acid battery, and the cells have high self-discharge rates.

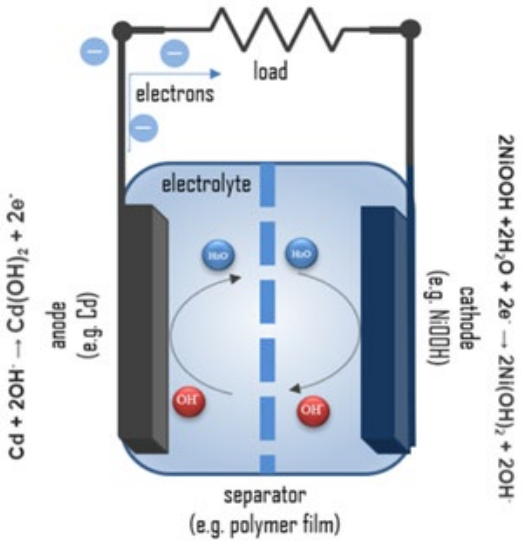

Figure 2.2. Scheme of a nickel-cadmium battery

– Nickel-metal hydride (Ni-MH): has a lower energy density compared to lithium-ion, but is more environmentally friendly (Figure 2.3).

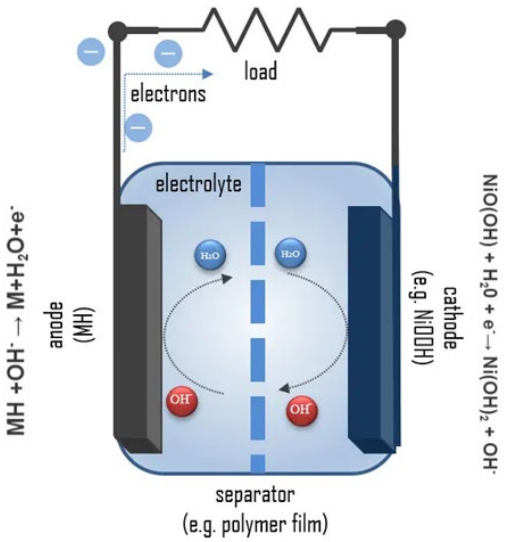

Figure 2.3. Scheme of a nickel-metal hydride battery

– Lead-acid (Pb-Acid): The oldest type of battery, used in car starters, uninterruptible power supply systems and for storing energy in power plants. They are distinguished by high reliability and low cost (Figure 2.4).

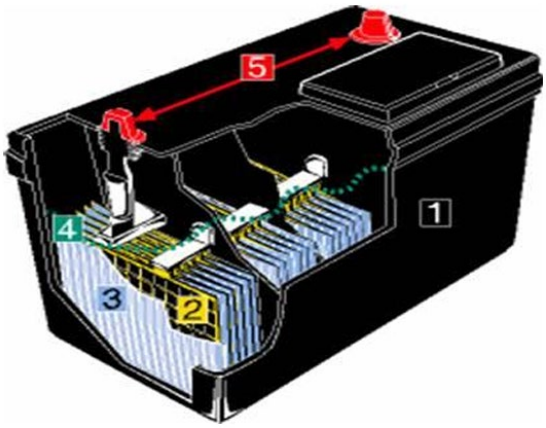

1 - Polyethylene body (monobloc); 2 - Internal positive and negative plates, made of lead; 3 - Plate separators made of porous synthetic material; 4 - Electrolyte, a dilute solution of sulfuric acid and water; 5 - Lead terminals, the connection between the battery and the device that needs energy

Figure 2.4. Construction of a lead-acid battery:

– Lithium Polymer (Li-Po): A variant of lithium-ion batteries with a polymer electrolyte that allows the development of battery with complex shapes and improved safety (Figure 2.5).

Battery capacity is the maximum amount of energy that can be extracted from the battery under certain conditions. This unit can be expressed in ampere hours (A·h) or watt hours (W·h), although the latter is more commonly used in electric vehicles.

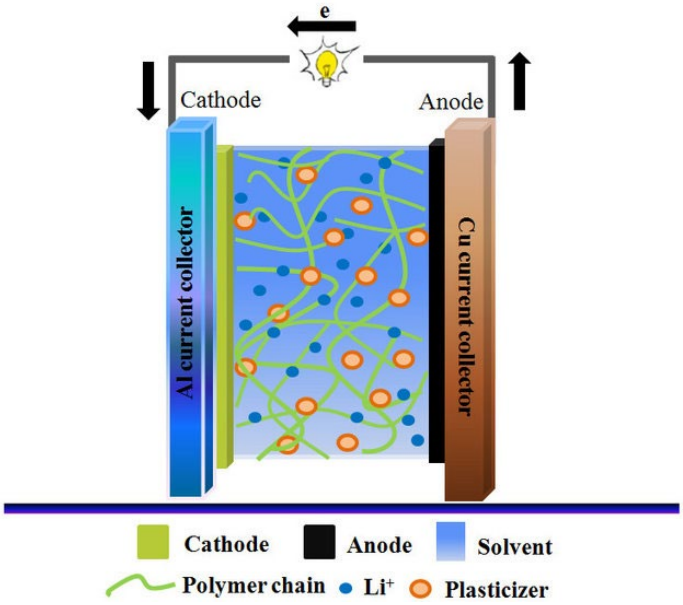

Figure 2.5. Scheme of a lithium polymer battery

The main types of batteries used in electric vehicles are nickel-metal hydride (Ni-MH) and lithium-ion (Li-ion) batteries. Nickel-metal hydride (Ni-MH) batteries are commonly used as secondary power sources in hybrid electric vehicles (HEVs), which work in tandem with an internal combustion engine (ICE). Li-ion batteries serve as the primary power source in battery electric vehicles (BEVs) due to their higher energy density compared to Ni-MH batteries, which means a greater capacity to store energy in a given mass and volume. In addition, they have improved efficiency, longer battery life, and faster rechargeability. However, Ni-MH batteries retain certain advantages over their Li-ion counterparts, such as being more cost-effective and exhibiting better tolerance to overcharging and overdischarging.

Table 2.1 provides an overview of the different types of batteries, along with their respective electrodes, electrolytes, and electrochemical reactions. These batteries encompass a range of chemical compositions, each with its own unique characteristics.

Lead-acid batteries are the oldest energy storage devices due to their advantages of high safety, high recycling rate and low cost. Lead-acid batteries have a specific energy of (30–50) Wh/kg, a specific power of (75–300) W/kg and a low self-discharge rate of (0.1–0.3)%, i.e., about 2% of the nominal capacity per month (at 25°C).

Nickel-based batteries can be divided into Ni-MH, Ni-Zn, Ni-Cd and Ni-Fe batteries according to the negative electrode material. Ni-MH batteries used in electric vehicles can have higher discharge rates and higher energy densities, while also producing large amounts of heat through the production of hydrogen. Compared with other nickel-based batteries, Ni-Zn batteries have a shorter cycle life and are not generally used as a power source, and Ni-Zn batteries do not cause environmental pollution problems.

The Ni-Cd battery can achieve fast charging, but it is gradually being phased out of the market because it produces toxic substances that pollute the environment and even endanger human

health. The Ni-Fe battery has a longer cycle life than other nickel-based batteries, but it has a larger mass, a higher cost, and a higher self-discharge rate.

Table 2.1. Different types of batteries and their chemical reactions [37]

Battery type	Electrodes	Electrolyte	Electrochemical reactions
Lead-Acid (Pb-Acid)	Anode: Lead Dioxide (PbO_2) Cathode: Lead (Pb)	Dilute sulfuric acid (H_2SO_4)	Anode: $PbO_2 + SO_4^{2-} + 4\ H^+ + 2\ e^- \leftrightarrow PbSO_4 + 2\ H_2O$ Cathode: $Pb + SO_4^{2-} \leftrightarrow PbSO_4 + 2\ e^-$ General: $PbO_2 + Pb + 2\ H_2SO_4 \leftrightarrow 2\ PbSO_4 + 2\ H_2O$
Nickel-Cadmium (Ni – Cd)	Anode: nickel oxide hydroxide (NiOOH) Cathode: Cadmium (Cd)	Potassium hydroxide (KOH)	Anode: $NiOOH + H_2O + e^- \leftrightarrow Ni(OH)_2 + OH^-$ Cathode: $Cd + 2OH^- \leftrightarrow Cd(OH)_2 + 2e^-$ General: $2NiOOH + Cd + 2H_2O \leftrightarrow 2Ni(OH)_2 + Cd(OH)_2$
Nickel-Metal hydride (Ni-MH)	Anode: nickel oxide (NiO) Cathode: hydrogen absorbing alloy	Potassium hydroxide (KOH)	Anode: $NiOOH + H_2O + e^- \leftrightarrow Ni(OH)_2 + OH^-$ Cathode: $MH + OH^- \leftrightarrow M + H_2O + e^-$ General: $NiOOH + MH \leftrightarrow Ni(OH)_2 + M$
Lithium-ion (Li-ion)	Anode: graphite Cathode: lithium cobalt oxide ($LiCoO_2$)	Lithium salt in an organic carbonate solvent	Anode: $LiC_6 \leftrightarrow C_6 + Li^+ + e^-$ Cathode: $CoO_2 + Li^+ + e^- \leftrightarrow LiCoO_2$ General: $LiC_6 + CoO_2 \leftrightarrow C_6 + LiCoO_2$
Lithium-polymer (Li – Po)	Anode: lithium carbide Cathode: lithium cobalt oxide ($LiCoO_2$)	Polymer	Anode: $C_6H_4Li + 6Li^+ + 6e^- \rightarrow 6C + 7Li$ Cathode: $LiCoO_2 + Li^+ + e^- \rightarrow LiCoO_2(Li_{1-x}CoO_2)$ General: $C_6H_4Li + Li_{1-x}CoO_2 \rightarrow 6C + 7Li + LiCoO_2$

In the past, batteries for electric vehicles (EVs) were the traditional ones mentioned above, but in recent years, most electric vehicles use lithium batteries as energy storage devices and power sources. As a result, researchers have begun to experiment with different materials to improve the performance of lithium batteries, such as: lithium-ion monomer batteries, lithium-ion polymer batteries (Li-Po), lithium iron phosphate ($LiFePO_4$) batteries, etc. The high energy density of lithium iron phosphate batteries allows them to be manufactured in smaller capsules, reducing the space required for placement. Lithium iron phosphate batteries efficiently discharge energy into the moving vehicle, resulting in a long service life. Lithium-ion polymer batteries have increased reliability and robustness compared to lithium iron phosphate batteries, but their power density and conductivity are poorer. Lithium iron phosphate batteries can easily cause environmental pollution during production. During use, they can overheat and cause burns or even explosions. They are also characterized by high energy density, low self-discharge rate and stable performance, but their usefulness decreases when subjected to extreme temperature conditions, which limits their widespread application in BEVs.

The appearance of rechargeable all-solid-state batteries (ASSB) is another development of electrochemical energy storage devices. They have an energy density of (250-400) Wh/L, a

power density of (1500-6000) W/L, and a cycle life of (2000-3000). For them, the electrolyte is very important in energy storage. When halides are used in ASSB, they have high ionic conductivity, high energy density, high stability, and excellent mechanical deformability. This can effectively alleviate concerns about autonomy and safety.

Li-ion batteries have higher energy densities, meaning they can store more energy in a smaller, lighter cell, and they also have a reduced memory effect.

An important aspect when comparing different types of batteries is their operating temperature, as this can limit their adoption. Lead-acid and lithium batteries are the best in this regard, withstanding temperatures as low as -20°C, although in the case of Li-ion batteries, low temperatures severely affect their capacity, causing them to self-discharge. In fact, this type of battery has an optimal operating temperature of +40°C. Lithium-ion batteries must operate within a safe and reliable operating range, which is restricted by temperature and voltage. Exceeding the restrictions will lead to a rapid decrease in battery performance and even lead to a safety hazard (it may catch fire or even explode), because above 150°C, the electrolytes begin to self-destruct. In terms of life cycles, the batteries that offer worse results are Ni-MH and lead-acid, while lithium batteries are capable of withstanding up to 3000 cycles, and Na-S batteries are the ones that offer better results, withstanding up to 4500 cycles.

There are many battery production companies in the market. Some of them are world-famous and have long been established as industry leaders. Here are a few such companies:

- *Panasonic*: A Japanese company known for its high-quality lithium-ion batteries used in a wide range of devices, from portable electronics to electric vehicles.
- *Samsung SDI*: A division of Samsung Corporation that specializes in battery manufacturing. They produce batteries for mobile devices, electric vehicles, power systems, and other applications.
- *LG Chem*: Another large corporation from South Korea that produces lithium-ion batteries. Their batteries are widely used in mobile devices, electric vehicles, and energy storage.
- *BYD Company*: A Chinese company that has become known for its innovative solutions in the field of electric vehicles and batteries, including lithium iron phosphate batteries.
- *Tesla*: A company that produces electric vehicles, energy storage systems, and solar panels. Their Powerwall and Powerpack lithium-ion batteries have received wide recognition.
- *CATL* (Contemporary Amperex Technology Co. Limited): A Chinese company, one of the largest lithium-ion battery manufacturers in the world, supplying its products to various industries including automotive, energy, and portable electronics.
- *EnerSys*: A world leader in the production of lead-acid batteries for various industrial and commercial applications such as telecommunications, transportation, defense, etc.

Research into current challenges such as increasing capacity, reducing production costs, improving safety and environmental friendliness helps to anticipate future directions of battery technology development.

2.2. Supercondencers

In today's world, where the demands for energy storage and use are becoming increasingly high, supercondencers are a promising technology that can solve many energy-related problems. Unlike traditional chemical batteries, supercondencers offer high energy density, fast charging and discharging, long service life, and are environmentally friendly. These devices are becoming increasingly important in various fields such as the automotive industry, energy-saving technologies, and medical devices.

Today, in the era of rapid technological development and increasing energy demand, supercondencers appear before us as a promising research direction that promises to revolutionize the way we store and use energy. Unlike traditional chemical batteries, supercondencers have unique characteristics, including high energy density, fast charging and discharging speed, long service life, and environmental safety. These features make them attractive for a wide range of applications, including electric vehicles, portable devices, renewable energy, medical devices, and more. Supercondencers, sometimes also called ultracondencers or supercondencer batteries, are devices that can store and release energy electrostatically, using an electric field instead of the chemical reactions that are typical of conventional batteries. This difference allows them to provide higher energy density and faster recharge, making them an ideal choice for applications that require high energy performance and fast charging times, such as electric vehicles.

A supercondencer is an electrochemical device used to store energy, a capacitor with an organic or inorganic electrolyte, in which the "plates" are an electric double layer at the interface between the electrode and the electrolyte. In terms of characteristics, it occupies an intermediate position between a capacitor and a chemical power source [42].

Unlike batteries, supercondencers store energy in the form of an electric field generated between two electrodes separated by an electrolyte. This mechanism enables supercondencers to provide high energy density, fast charging and discharging, long service life, and high operational stability. As a result, they are widely used in various fields, including electronics, automotive, and renewable energy.

A general view of supercondencers Maxwell 1200F, 2.7V is presented in Figure 2.6.

The main characteristics of a supercondencer include [42]:

1. Energy density. This is a parameter that determines the amount of energy that can be stored in a supercondencer per unit volume or mass.

2. Power. This is the ability of a supercondencer to charge and discharge quickly. Due to this characteristic, supercondencers can provide more power than traditional batteries, making them ideal for applications that require a quick start or short-term power peaks.

3. Service life (durability). Supercondencers tend to have a long service life because they do not involve chemical reactions that can lead to wear of the electrodes, as occurs in batteries.

4. Cycle stability. Supercondencers can withstand a significant number of charge and discharge cycles without degrading their performance. This makes them a good choice for applications that require frequent recharging.

5. Working voltage. This is the maximum voltage that the supercondencer can withstand without damage.

6. Internal resistance. Supercondencers typically have low internal resistance, which allows for efficient energy transfer during charging and discharging.

7. Temperature range. The ability of the supercondencer to operate at different temperatures. Some supercondencers are capable of operating in extreme conditions, making them suitable for use in a wide range of climates.

Figure 2.6. General view of supercondencers Maxwell 1200F, 2.7V

Supercondencers can be classified based on various criteria, including electrode materials, design, electrolyte type, and operating principle. Here are some of the main classifications:

– by electrolyte type:

  - Organic electrolyte supercondencers: the electrolyte consists of organic compounds, such as a salt in an organic solvent.
  - Polymer electrolyte supercondencers: the electrolyte is a polymer material that provides good conductivity and stability.

– by electrode type:

  - Active carbon supercondencers: the electrodes are made of active carbon materials, such as carbon nanotubes, graphene, or activated carbon.
  - Pseudocapacitive supercondencers: the electrodes contain materials with high ion adsorption and desorption capacity, such as metal oxides and polymer composites.

– by operating principle:

  - Double layer supercondencers (EDLC): energy is stored by forming a double electrical layer at the interface between the electrode and electrolyte (Figure 2.7).

- Pseudocapacitive supercondencers: energy is stored by fast chemical reactions on the surface of the electrodes, allowing for higher energy density than EDLC.

– by design:

- Flat supercondencers: have a flat design with electrodes separated by an electrolyte, assembled into a flat stack.
- Cylindrical supercondencers: have a cylindrical shape and are used in applications where compactness is important.

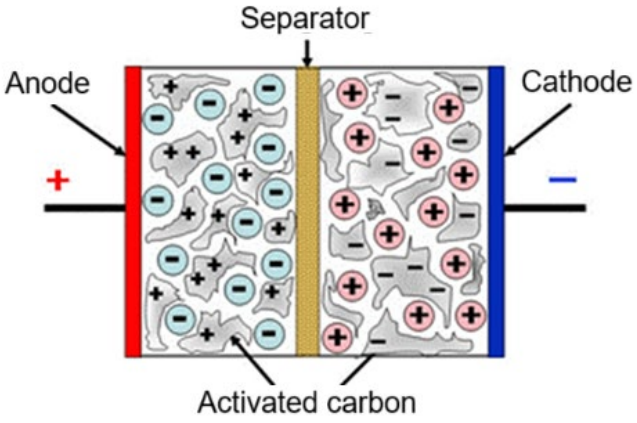

Figure 2.7. Double layer supercondencer

Supercondencers, sometimes called capactors or ultracondencers, are electrical devices that are capable of storing and releasing energy in significant quantities in very short time intervals. This is due to a special operating principle that distinguishes them from conventional capacitors and batteries.

Principle of energy storage is the next: the basic idea behind supercondencers is to use two main energy storage mechanisms: the electrical double layer (EDL) and pseudocapactivity. These mechanisms allow supercondencers to achieve high energy density at a relatively low cost and with a long service life.

The mechanism of the electrical double layer is based on the formation of a double layer of charged ions on the surface of the electrode and electrolyte. When the supercondencer is charged, positive ions are attracted to the negatively charged electrode, and negative ions are attracted to the positively charged electrode. This creates an electrical double layer, which provides high capacity and fast charging/discharging of the device.

Pseudocapactivity is based on fast and reversible oxidation-reduction reactions at the electrode surface. This allows supercondencers to release large amounts of energy in short time intervals. However, unlike the electrical double layer, pseudocapactivity typically has a lower capacitance but a higher energy density [42].

Supercondencers differ from conventional electrolytic capacitors and batteries in the following ways:

– Fast charging and discharging: Supercondencers are able to accept and release energy much faster than batteries, making them an ideal choice for applications that require high power.

– Long cycle life: Unlike batteries, supercondencers typically have a long cycle life because they do not involve chemical processes that degrade the electrodes.

– Low Maintenance Costs: Since there is no chemical degradation process, supercondencers require minimal maintenance and do not require component replacement for a long time.

A supercondencer stores energy due to electrostatic charges that are created on opposite surfaces of electrodes that belong to a double electric layer. This layer is created between the electrolyte and the electrodes. During the charging process, randomly distributed electrolyte ions move towards the surface of the electrode that has the opposite polarity (Figure 2.8). This process is of physical, not of chemical nature. In addition, it is completely reversible. This is largely what determines the high power of supercondencers, their long service life, long storage time and ease of maintenance.

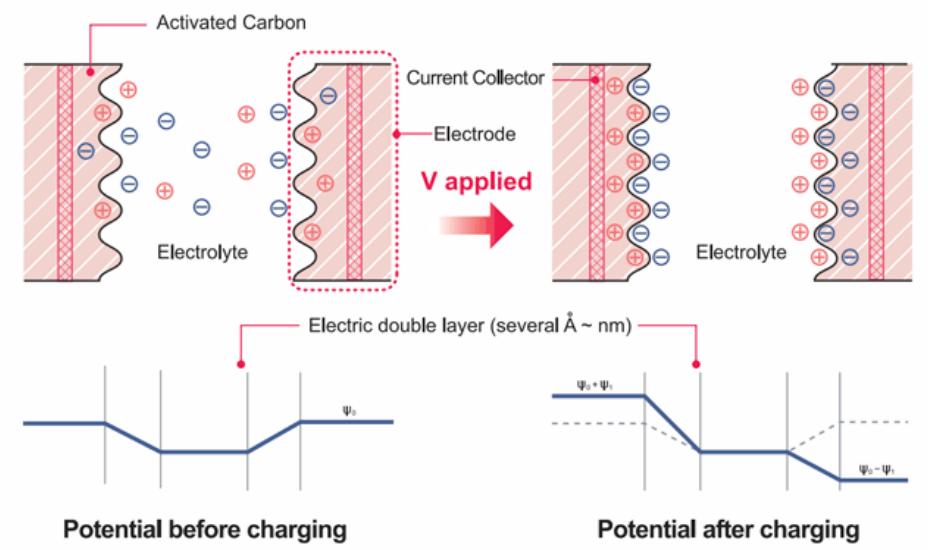

Figure 2.8. Operating principle of a supercondencer

The operating principle of supercondencers makes them a key element in many technologies that require high power, fast charging/discharging and durability, such as automotive electronics, renewable energy storage and industrial energy conservation systems.

Supercondencers are a key element in various applications due to their unique characteristics such as high power, fast charging and discharging, and long life without loss of capacity. The main areas where supercondencers are widely used are discussed below [42]:

1. Automotive industry. Supercondencers play an important role in automotive electronics, especially in energy recovery and engine starting systems. They are able to quickly store and release energy, making them an ideal choice for providing high power during engine starting and improving the energy efficiency of cars.

2. Energy sector. In the energy sector, supercondencers are used to store energy from renewable sources such as solar and wind energy. They help smooth out fluctuations in energy production and ensure stability in power grids.

3. Electronics and portable devices. In mobile devices, smartwatches, tablets, and other portable devices, supercondencers can be used to quickly charge and maintain long operating times without recharging. They can also serve as an auxiliary power source in the event of interruptions in the main power source.

4. Processing industry and industrial applications. In industry, supercondencers can be used for energy-saving systems, such as regenerative brakes in elevators and escalators, control of electric drives and stabilization of power grids. They can also be used in energy saving and voltage regulation systems.

5. Medical technology. In medical technology, supercondencers can be used to store energy in implantable devices such as pacemakers and defibrillators. Their fast charging and reliability make them the preferred choice for such medical applications.

The use of supercondencers in various fields continues to expand with the development of manufacturing technologies and improvement of their characteristics. Their high performance, reliability and environmental safety make them an important element of modern technology and innovation.

Supercondencers are the subject of active research and development in the energy and electronics industries, and their development prospects promise significant benefits for various industries and technologies. The main directions and prospects for the development of supercondencers are presented below:

1. Increasing the capacitance and energy density. One of the main directions of supercondencer development is to increase their capacitance and energy density. This includes the development of new materials for electrodes with a larger surface area and improving electrolytes to increase the efficiency of energy storage.

2. Improving the electrochemical properties. Research in the field of electrochemical properties of supercondencers is aimed at increasing their stability, reducing internal resistance and increasing the operating temperature ranges. This will expand the scope of application of supercondencers in various operating conditions.

3. Nanotechnology and new materials. The use of nanotechnology and the development of new materials, such as carbon nanoparticles, metal oxides and polymers, have the potential to improve the performance of supercondencers. This includes increasing the energy density, reducing the size of the devices and increasing their efficiency.

4. Integration into energy storage systems. Supercondencers are increasingly being integrated with other energy storage systems, such as lithium-ion batteries or solid-state batteries. This allows for the creation of hybrid systems that combine the benefits of both types of devices, such as high power and long life.

5. Development of new manufacturing methods. With the development of new manufacturing methods, such as nanotechnology, 3D printing and thin-film technologies, supercondencers are becoming more accessible and cost-effective. This facilitates their widespread adoption in various industries and applications.

6. Environmental and economic sustainability. The prospects for the development of supercondencers are also related to their environmental and economic sustainability. They do not contain toxic materials, can be recycled and have a long service life, making them an attractive choice from a sustainability perspective.

Eaton Corporation PLC, Skeleton Technologies Inc., Cap-XX Limited, Maxwell Technologies Inc. (Tesla Inc.), Kyocera Corporation are the main companies operating in the supercondencer market.

Supercondencers are electronic devices with unique characteristics that make them an important element of modern technology. Their main advantages include high power, which allows them to store and release energy quickly and efficiently. Due to this feature, supercondencers are widely used in the automotive industry for engine starting, in regenerative systems for collecting energy during braking, and in other areas where high power and fast response are required.

2.3. Invertor

An invertor (inverter, or power inverter) is a device for converting direct current into alternating current with a possible change in voltage. It is usually a generator of periodic voltage, close to a sinusoid in shape, or a discrete signal. The main switching elements are silicon controlled rectifiers or power transistors. They are arranged in a bridge circuit and are switched on (and off in the case of transistors) in such a way that an oscillatory signal is obtained. Some inverters work together with other devices that set the system frequency. They are called linear commutated. Other inverters have the ability to set the frequency independently. They are called self-commutated. Larger uninterruptible power supply devices use more powerful inverters with batteries of significant capacity, capable of autonomously powering consumers for hours, regardless of the network, and when the network returns to normal, the UPS will automatically switch consumers directly to the network, and the batteries will begin to charge. Requirements for inverters, as well as for other power devices, include: high efficiency, reliability, as small as possible dimensions and weight. It is also necessary for the inverter to withstand the permissible level of higher harmonics in the input voltage, and not to create unacceptably strong impulse interference for consumers.

Conventionally, the following inverter elements can be distinguished [43-49]:

– Input circuit, provides control and protection of input circuits, generates voltage for power supply: inverter components, cooling system, LCD backlight and other devices;

– PWM (pulse-width modulation) controller, generates signals of a given frequency and duty cycle, creates a reference voltage, and also contains feedback signal processing circuits: amplifier, comparator and protection unit;

– MOSFET unit, controlled by the PWM controller setting the initial shape of the output signal;

– DC-AC converter, generating the final shape of the output signal;

– LC amplifier, increases the output signal voltage to the required value.

– Feedback unit, provides output voltage stabilization.

The main elements of a car inverter are:

– a body made of aluminum alloy with increased thermal conductivity, which prevents the device from overheating;

– semiconductors that provide the conversion of direct current from a 12 V source to alternating current;

– a fan for additional cooling (in power inverters);

– protective systems that prevent the device from failing.

Externally, a portable DC/AC inverter presents a compact device that can be connected directly to the battery or to the cigarette lighter socket - in addition, high-quality models usually have a USB port for charging gadgets and a socket for connecting 12 volt devices. An example of a such inverter can be seen in Figure 2.9.

Figure 2.9. General view of a portable power inverter Radio Shack, 12 VDC to 115 VAC

An inverter for electrical and hybrid vehicles shows like a module with necessary connectors (Figure 2.10).

The inverter is designed to convert electric current from direct (from the battery) to alternating current, which the engine runs on. The inverter also allows you to control the acceleration or deceleration of the electric vehicle, depending on the position of the accelerator pedal. The principle of operation is that, using a certain circuit, the inverter converts the input signal, for

example, 220 volts of single-phase voltage with a frequency of 50 Hz, into a signal with a high frequency of 10 kHz and even higher.

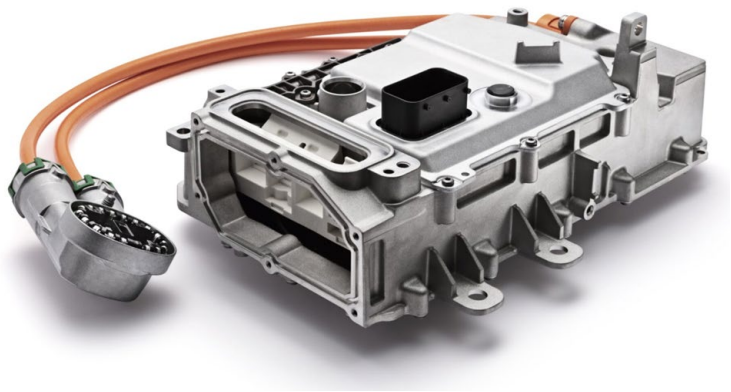

Figure 2.10. General view of an internal inverter for electric and hybrid vehicles

Then, using its components or even under the control of an external control device, it re-forms an output signal from this signal. For example, in the case of a frequency converter, an output voltage for an electric motor is formed with a quasi-sinusoid of a certain frequency.

At the inverter output, the voltage is not alternating. The inverter, by partially opening its keys in each unit of time, forms a voltage of a certain magnitude and polarity. But since the signal has a high frequency, then for the devices powered, the signal will strongly resemble a normal alternating voltage.

The higher the frequency of the signal, the smoother the output sine wave will be, although its correct name would be quasi-sinusoid.

Thus, the inverter has the ability to produce a signal in a very wide range of frequencies and voltages with the same power supply.

There are many variants of constructing inverter circuits. Historically, the first were mechanical inverters, which in the era of development of semiconductor technologies were replaced by more technologically advanced inverters based on semiconductor elements, and digital voltage inverters. But still, as a rule, three main circuits of voltage inverters are distinguished [43-49]:

1) Bridge inverter without transformer (Figure 2.11). Application area: uninterruptible power supply devices with a capacity of more than 500 VA, installations with a high voltage value (220...360 V).

2) inverter with zero transformer pin (Figure 2.12). Application area: uninterruptible power supply devices for computers with a power of (250...500 VA), at low voltage (12...24 V), voltage converters for mobile radio communication systems.

3) Bridge circuit with transformer (Figure 2.13). Application area: uninterruptible power supply devices for important consumers with a wide range of power: units ÷ tens of kVA.

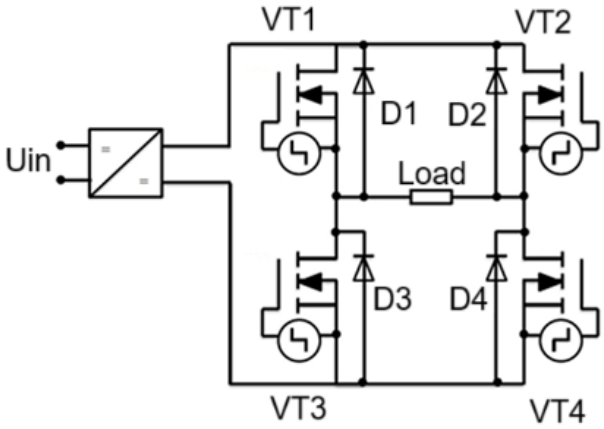

Figure 2.11. Bridge inverter without transformer

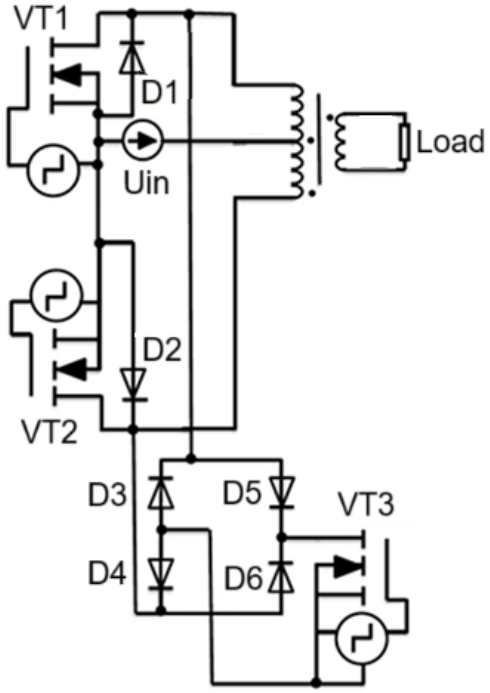

Figure 2.12. Inverter with zero transformer pin

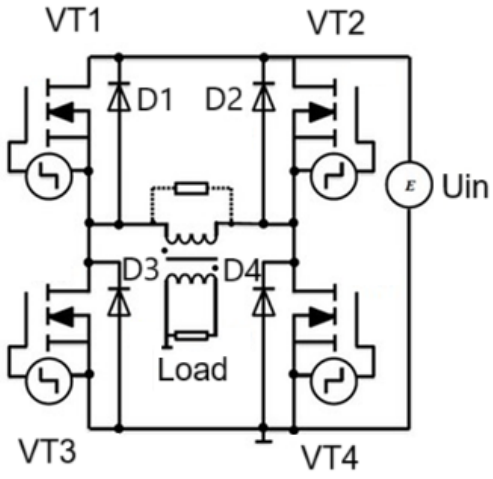

Figure 2.13. Bridge circuit of invertor with transformer

GTO and IGBT inverter circuits (Figure 2.14 and 2.15) allow the use of electrical energy either directly from a battery or from a power supply to produce a three-phase power source that can be connected to an electric motor.

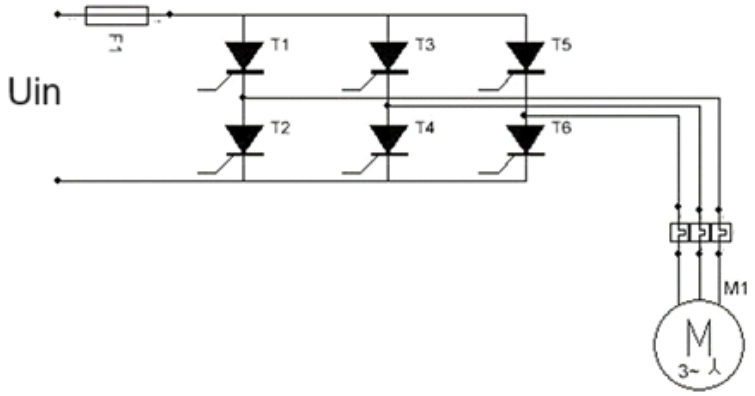

Figure 2.14. GTO (Gate Turn Off) scheme of invertor

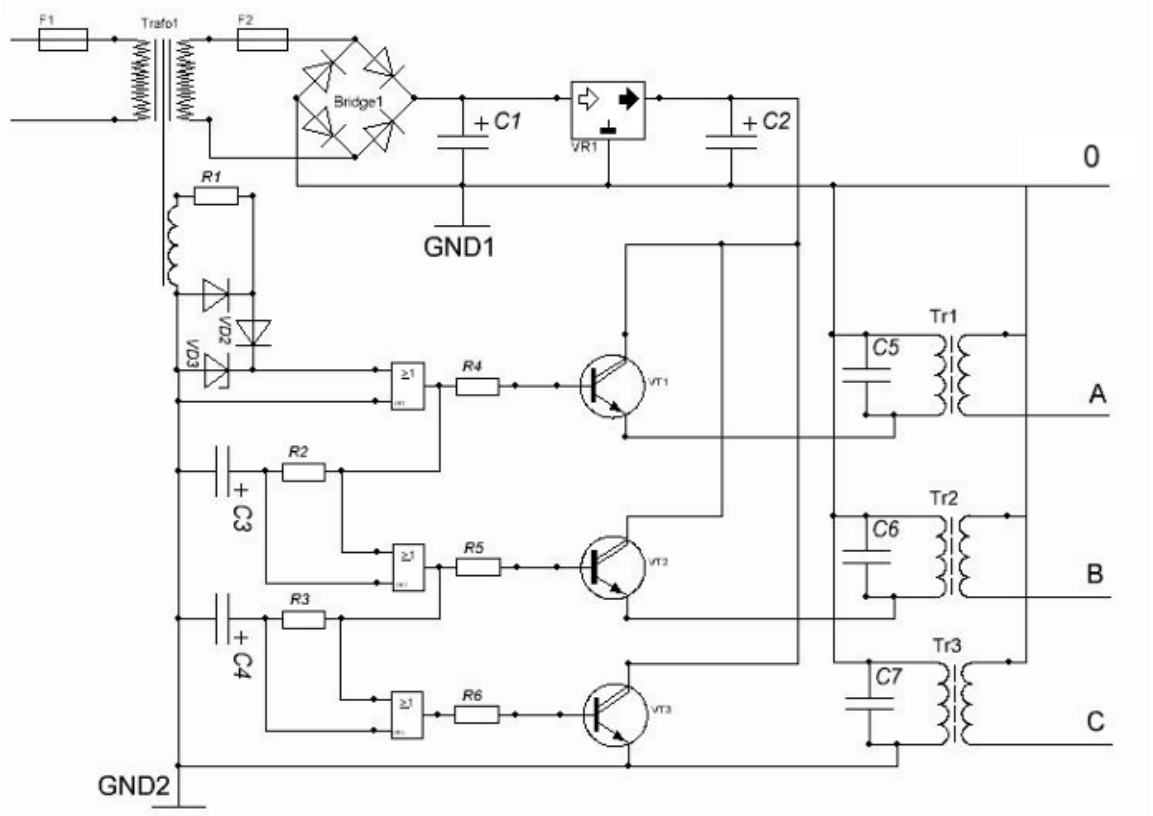

Figure 2.15. IGBT (Insulated Gate Bipolar Transistor) scheme of invertor

There are single-phase and three-phase inverters.

Single-phase voltage inverters are divided into two groups: with a pure sine wave at the output and with a modified sine wave. Most modern devices allow a simplified form of the network signal (modified sine wave). A pure sine wave is important for devices that have an electric motor or transformer at the input, or if it is a special device that works only with a **pure** sine wave at the input.

Three-phase inverters are usually used to create three-phase current for electric motors, for example, to power a three-phase asynchronous motor. In this case, the motor windings are directly connected to the inverter output. The inverter power is selected based on the peak value for the consumer.

There are three inverter operating modes: starting, continuous, and overload mode. In starting mode (charging a tank, starting a refrigerator), the power can exceed the inverter's nominal value twice for a split second, which is acceptable for most models. Continuous mode – corresponding to the inverter's nominal value. Overload mode – when the consumer's power is 1.3 times higher than the nominal value – in this mode, an average inverter can operate for about half an hour.

According to the operating principle, inverters are divided into:

– autonomous:
  - voltage inverters (AVI);
  - current inverters (ACI),
  - resonant inverters (ARI);
– dependent inverters, driven by the power supply.

The main companies that produce inverters for vehicles are:

– TBS (Netherlands);
– Victron (Netherlands);
– Sibkontakt (Russia);
– Acme Power (China-Taiwan);
– EPSolar (EPEVER) (China).

Thus, based on the above, the inverter is designed to convert electric current from direct (from the battery) to alternating current, on which the engine operates. The inverter also allows you to control the acceleration or deceleration of the electric vehicle, depending on the position of the accelerator pedal.

2.4. Converter

The converter is an electronic device that modifies the electrical parameters (amplitude, shape, type, etc.) of the input signal for conjugation with the power supply system of the load electrical circuit. DC/DC converters (supply transformers) and AC/DC converters (rectifiers) are used in modern vehicles [43-49].

DC/DC converters (Figure 2.16) are electronic circuits or electromechanical equipment that convert a direct current source from one voltage level to another voltage level. The need for a voltage-current converter is given by the wide range of equipment with various supply voltages - thus, these converters are necessary to provide the voltage required for each equipment.

Characteristics for voltage-current converters are the input voltage, in fact, the voltage of the power supply, and the output voltage, respectively the voltage required for the various equipment that needs to be powered. Another important characteristic for these equipment is the mode of regulation of the supply voltage and the output voltage.

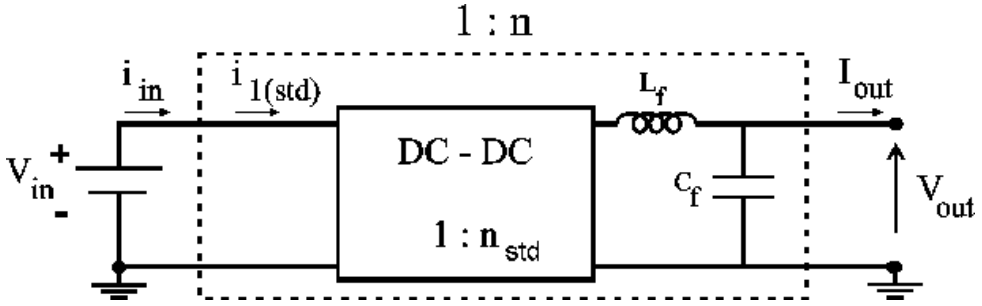

Figure 2.16. Block scheme of a DC/DC convertor

From a functional point of view, we have two types of DC - DC converters:

Step up DC/DC (Buck) converters (Figure 2.17) - voltage increase takes place, where the output voltage is higher than the input (supply) voltage. Among the most current models in this range are the DC/DC 12V/24V converter (Figure 2.18) or the DC/DC 5V/12V converter.

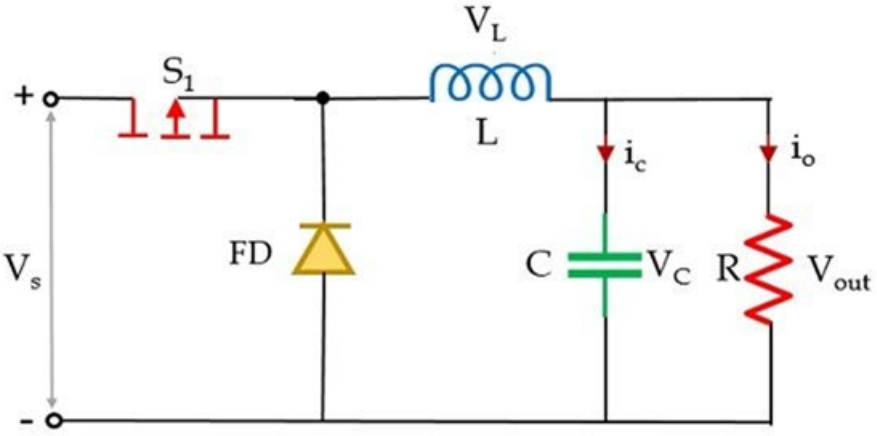

Figure 2.17. Electrical scheme of a buck converter

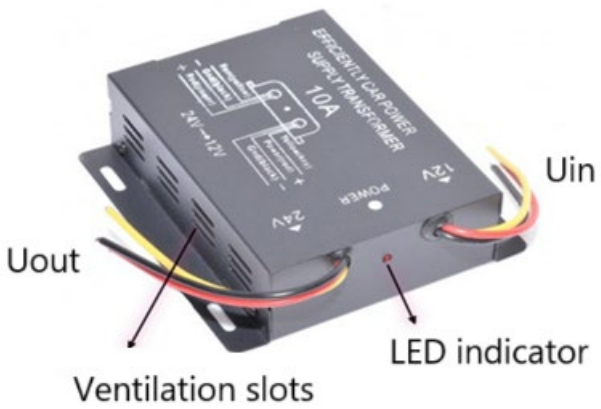

Figure 2.18. General view of a 12V/24V DC/DC converter for electric and hybrid vehicles

Step down DC/DC (Boost) converters (Figure 2.19) – voltage reduction takes place, where the output voltage is lower than the input (supply) voltage.

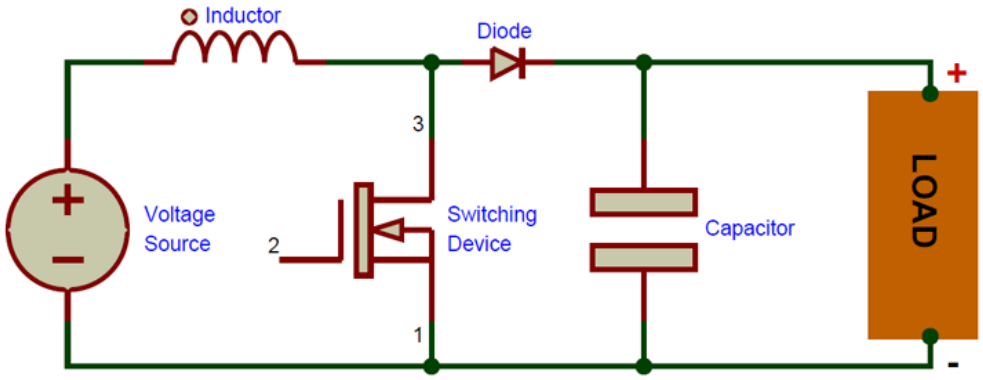

Figure 2.19. Electrical scheme of a boost converter

The use of DC/DC converters has the following advantages:

DC/DC converters help regulate the voltage from a higher voltage to a lower one or vice versa, providing the power needed to operate the working equipment and isolating the primary and secondary circuits.

DC/DC converters offer high efficiency and adaptability in converting one voltage level to another voltage level, compensating for voltage drops in the cable and providing protection against overvoltage, undervoltage or short circuit, forming the direct current in voltages higher or lower than the input.

An AC/DC converter (rectifier) is an electrical device that serves to convert alternating current into direct current.

Three-phase rectifiers from the vehicle generator are used in modern automobiles to power batteries or supercondencers. The three-phase half-wave rectifier (Figure 2.20) and the three-phase full-wave rectifier (Figure 2.21) can be distinguished.

In the case of the use of three-phase half-wave rectifier the rectified voltage on the load is:

$$V_{DC} = 1.17 \cdot V_{phase} = 0.827 \cdot V_{peak} \quad (2.1)$$

where V_{phase} is the effective value of the phase voltage and V_{peak} is the peak value of the phase voltage ($V_{phase} = 0.707 \cdot V_{peak}$).

While using the three-phase full-wave rectifier the rectified voltage on the load is:

$$V_{DC} = 1.35 \cdot V_{phase} = 0.954 \cdot V_{peak} \quad (2.2)$$

Thus, converters are essential components in electric vehicles, playing a crucial role in transforming, managing and controlling the flow of electrical energy to various components of the vehicle. They enable efficient energy conversion between the battery, electric motor and other auxiliary devices, thus contributing to the optimal operation and performance of the vehicle.

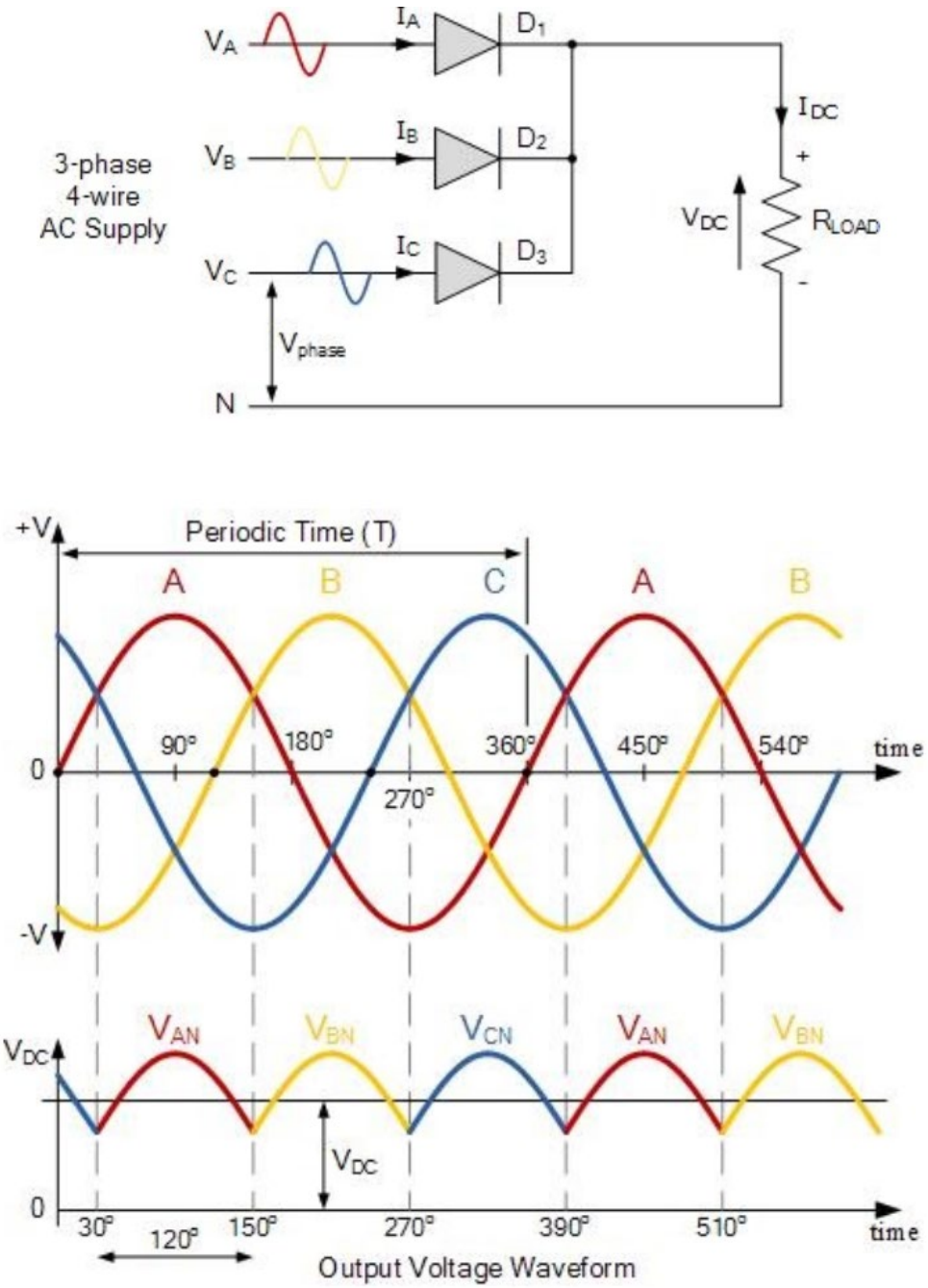

Figure 2.20. Scheme of the three-phase half-wave rectifier and its input/output diagram

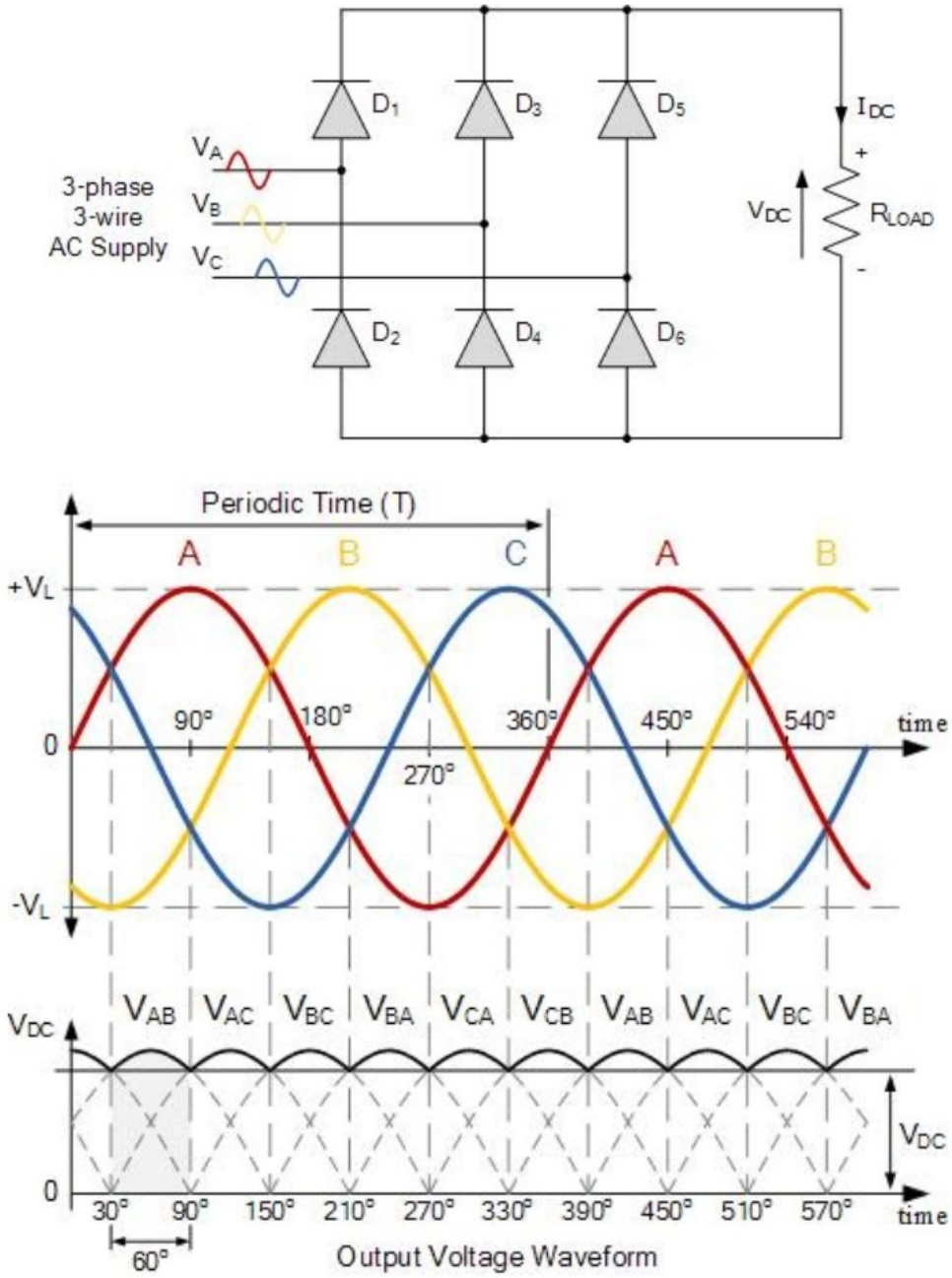

Figure 2.21. Scheme of the three-phase full-wave rectifier and its input/output diagram

Chapter 3: ELECTRIC VEHICLE CHARGING TECHNOLOGIES

The current issues with electric vehicles are closely linked to the range provided by batteries, the time required for charging, and their estimated lifespan. These aspects are deeply interconnected, being influenced by the technical characteristics of the batteries and their usage patterns. Specifically, the maximum charging power of a station is limited by the battery's ability to handle current, which is defined by parameters such as the charge and discharge rates.

Lithium-ion (Li-Ion) batteries, the most commonly used in electric vehicles, operate optimally at a charging rate between 1C and, in special cases, 3C, where “C” represents the battery's capacity expressed in ampere-hours (Ah). For example, a battery with a capacity of 10 Ah charged at 1C would require a current of 10 A, while at 3C, it would require 30 A.

However, fast charging (at high C values) can accelerate the battery degradation process. Slow charging (below 1C) is preferable for extending battery life as it reduces thermal and chemical stress on the active materials. This is an essential strategy for users who prioritize sustainability and long-term cost efficiency.

In recent years, lithium iron phosphate (LiFePO4) batteries have become increasingly common in electric vehicles due to their significant advantages. They offer a much longer lifespan than Li-Ion batteries, theoretically 5 to 10 times greater, thanks to their chemical stability and superior resistance to charge-discharge cycles.

However, LiFePO4 batteries have notable disadvantages, such as:

- Lower energy density: Their energy storage capacity per unit of mass is lower, leading to increased overall vehicle weight. This is a challenge, particularly in transportation, where weight directly impacts performance and autonomy;
- Lower charge rate: Charging is recommended at 0.5C to 1C, making the process slower compared to Li-Ion batteries. Charging beyond these limits reduces the lifespan of the batteries, even though they are more durable by design.

Another essential factor influencing battery lifespan is the Depth of Discharge (DoD). Deep discharging, using a large proportion of the battery’s total capacity to extend vehicle range, leads to faster cell degradation. This phenomenon affects all types of batteries, including Li-Ion and LiFePO4. Frequent discharges beyond 80-90% of total capacity cause irreversible changes to the internal chemical structure, reducing usable capacity and, consequently, lifespan. To maximize longevity, it is recommended to maintain a charge level between 20% and 80% whenever possible.

To address these limitations and optimize battery performance, the following strategies are essential:

- Adaptive Charging: Implementation of intelligent charging systems that adjust the charging rate based on the battery type and its current condition;

- Use of IoT Technology: Integration of connected devices for real-time monitoring of battery status to prevent overcharging or excessive discharging;
- User Education: Informing consumers about best practices, such as avoiding deep discharges and opting for slow charging whenever possible.

As new solutions such as solid-state batteries are developed, significant improvements are anticipated in terms of range, charging times, and battery lifespan.

3.1. Charging infrastructure

The electric vehicle charging infrastructure is undergoing continuous expansion and transformation, significantly supported by funding from various European Union initiatives. These funds aim to extend charging networks and integrate advanced technologies to support the transition to sustainable mobility. Compared to conventional refueling stations, charging stations for electric vehicles have both specific advantages and challenges. One of their distinctive features is the high level of automation, which exclude the need for constant on-site staff. This reduces operational costs and facilitates large-scale station management. However, a major disadvantage is the longer time required to fully charge an electric vehicle compared to refueling an internal combustion engine vehicle. To mitigate this limitation, it is essential to have a greater number of charging stations distributed strategically. Fortunately, their placement is flexible and space-efficient. Charging stations require minimal space and can be easily integrated into public or residential parking areas, or even installed at users' homes, thus enhancing charging accessibility.

From a technical perspective, these stations connect directly to the power grid and do not impose special location requirements, apart from ensuring a stable power supply and complying with electrical safety standards. In the long term, integrating these stations with smart grids and renewable energy sources can optimize energy consumption and reduce the impact on the national power grid. Charging stations for electric vehicles may lead to grid overloading, necessitating the development and adaptation of existing infrastructure to accommodate the new consumption patterns generated by electric vehicles. Establishing appropriate interconnections and strengthening grid capacity are essential to ensure stability and energy supply efficiency.

In residential areas, alternating current (AC) charging at Level 1 and Level 2 is generally sufficient. These systems, delivering power up to 22 kW, are suitable for long-term charging, such as overnight, when vehicles remain stationary for extended periods. Instead, in public spaces, it is preferable to install Level 2 AC charging stations, which enable faster recharging for users who require increased range within a shorter time frame.

On highways, at road junctions, or in other high-traffic areas, it is essential to deploy fast direct current (DC) charging stations equipped with the CCS 2 standard. These stations are capable of providing both three-phase alternating current (AC) charging and fast DC charging with power outputs of up to 350 kW, significantly reducing waiting times for users.

Optimizing residential area charging is crucial for the sustainable development of zero-emission vehicle (ZEV) traffic. Promoting overnight charging, when overall energy demand is lower, is vital. This approach can help prevent overloading the electrical infrastructure during peak hours and make more efficient use of surplus energy generated by renewable sources. Nighttime charging offers the advantage of smoothing out electricity consumption and reduces the need for costly investments in expanding energy transmission and distribution infrastructure.

The integration of smart devices based on Internet of Things (IoT) technology into charging stations can play a key role in achieving this goal. These devices enable real-time monitoring of consumption and dynamic adjustment of energy flow based on grid conditions. For instance, charging can be automatically delayed or accelerated to avoid peak consumption periods or to utilize surplus energy from renewable sources such as solar or wind power.

An effective mechanism for managing consumption could involve implementing a differentiated electricity tariff system. This system can be calibrated based on grid load levels and the availability of renewable energy. During periods of low demand and surplus green energy, lower tariffs could encourage consumers to charge electric vehicles, optimizing resource use.

Such a tariff model could be supported by smart applications that inform users of real-time charging costs and allow them to schedule charging during the most advantageous times. This mechanism not only helps reduce costs for users but also contributes to balancing the power grid and increasing sustainability.

Developing charging infrastructure requires careful planning that integrates modern technologies, meets the diverse needs of users, and promotes optimal energy resource usage. By adapting infrastructure, leveraging IoT technology, and implementing differentiated tariffs, an efficient transition to sustainable electric mobility can be ensured.

At the European Union (EU) level, the transition to sustainable mobility continues to accelerate. By early 2024, the number of battery electric vehicles (BEVs) in circulation exceeded 4.5 million units. Of these, 1.5 million BEVs were registered in 2023 alone, highlighting a significant year-over-year increase in the adoption of fully electric vehicles. This trend reflects both the growing accessibility of BEVs and the EU’s policy focus on reducing greenhouse gas emissions in the transportation sector [50].

In addition to BEVs, plug-in hybrid electric vehicles (PHEVs) play a complementary role in the transition to greener transport solutions. Since 2021, PHEV registrations have stabilized at approximately 900,000 units annually, emphasizing the demand for electric vehicles that offer the range of conventional internal combustion engine vehicles [50].

To support and sustain this growth pace, the European Union has implemented financial mechanisms and initiatives aimed at expanding the charging infrastructure for electric vehicles. Significant emphasis has been placed on installing public charging stations to reduce range anxiety among consumers and address the anticipated increase in demand for charging services.

By early 2024, over 630,000 public charging stations had been installed across EU member states.

However, the current infrastructure remains insufficient to meet the EU's ambitious objectives. According to projections, the European Union aims to install 3.5 million public charging stations by 2030 to align with the estimated growth in electric vehicle adoption. Achieving this goal will require a consistent installation rate of approximately 34,100 new stations per month over the next seven years. This level of infrastructure expansion will demand coordinated efforts among member states, including simplified regulatory frameworks, incentives for private investment, and integration of renewable energy sources into the grid. Moreover, innovative technologies such as ultra-fast charging and smart grid systems will be essential for enhancing the efficiency and accessibility of the charging network, ensuring it meets the needs of both urban and rural areas.

According to data from the European Alternative Fuels Observatory (EAFO) [51], the distribution of electric vehicle charging stations across the EU is heavily concentrated in just a few member states. Approximately 61% of the total number of public charging stations in the Union are located in three countries: the Netherlands, France, and Germany. This high concentration underscores both the leadership role of these countries in the early adoption and promotion of electric vehicles and the significant regional disparities in charging infrastructure. Figure 3.1 provides a detailed illustration of this distribution, highlighting the discrepancies among EU member states.

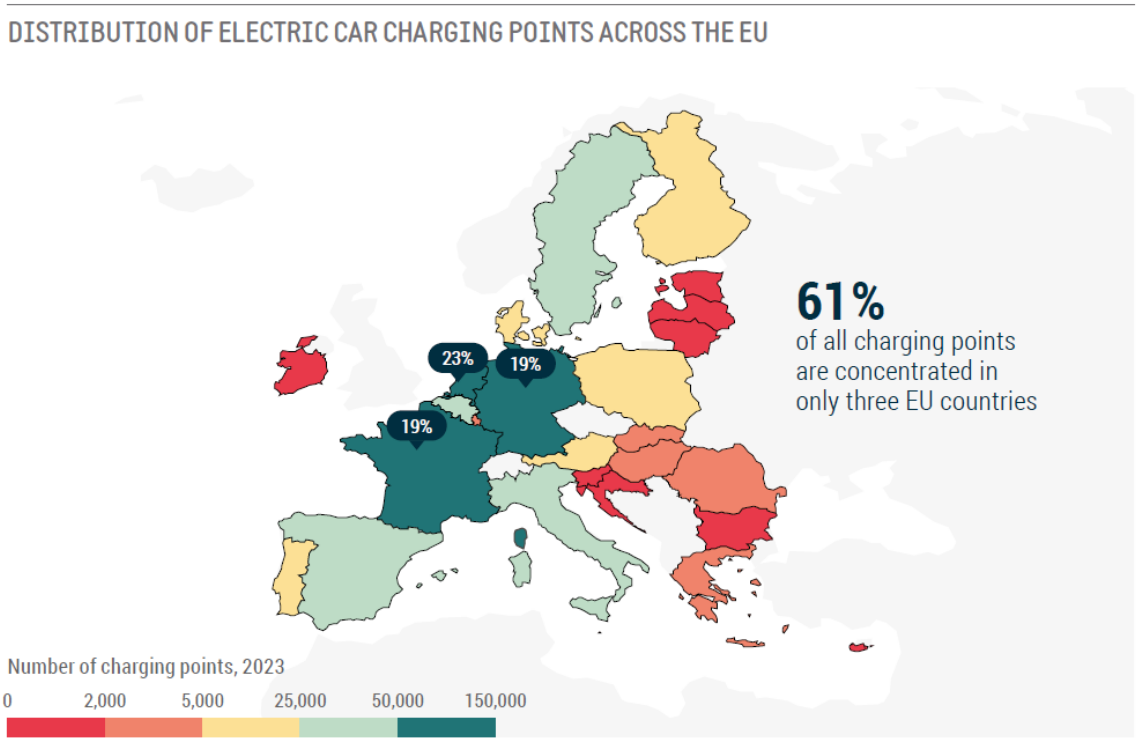

Figure 3.1. Distribution of electric car charging point across the UE [52]

These regional imbalances can be attributed to a combination of factors, including varying levels of public and private funding, the degree of electric vehicle adoption, national support

policies, and existing technological infrastructure. The Netherlands, France, and Germany have made substantial investments in developing dense charging networks to support the transition to electric mobility, allowing them to emerge as leaders in this sector. This situation may negatively impact the uniform adoption of electric vehicles across all member states, emphasizing the importance of cohesion policies and support strategies for less developed regions in terms of charging infrastructure.

Considering the strategy for locating charging stations for electric vehicles, there is a significant deficit of high-power fast-charging stations, which are essential for supporting the widespread use of electric vehicles, particularly for long-distance travel and in areas with high traffic volumes. Of the total electric charging stations installed in the European Union, only 13.5% are fast-charging stations. This modest proportion underscores a critical imbalance in infrastructure development, potentially hindering the pace of electric vehicle adoption, especially among users who depend on fast charging for efficient travel.

Fast-charging stations, operating at high power levels such as 50 kW and above, are vital for reducing charging times and enhancing the appeal of electric vehicles compared to conventional vehicles. The absence of a sufficiently dense network of such stations can create logistical and psychological barriers for potential users, including range anxiety and the inconvenience of long charging times. Although there are numerous European projects providing funding for the development of fast-charging networks, progress is frequently impeded by factors such as regulatory complexities, differing national and local priorities, and the high costs associated with installing high-power stations.

In this context, it is imperative to establish closer collaboration between national governments and European Union institutions to create a coordinated and effective approach. This collaboration should focus on harmonizing technical standards for charging stations, simplifying authorization processes for installations, ensuring consistent funding, and establishing a regulatory framework to encourage private investments. Moreover, member states must develop integrated national plans that prioritize the strategic placement of fast-charging stations in critical transport hubs, including highways, urban centers, and cross-border areas.

In the long term, addressing the shortage of fast-charging stations will be crucial for developing a robust infrastructure capable of supporting the rapid growth of the electric vehicle fleet. This will facilitate the transition to a sustainable and energy-efficient transportation system.

According to the data presented in the graph in Figure 3.2, the electric vehicle charging infrastructure in Europe varies significantly between countries, depending on factors such as the maturity of the charging network, the level of urban development, and national strategies for implementing electric mobility. Among the analyzed countries, Norway stands out with the most robust infrastructure, characterized by an average power of fast-charging stations of approximately 60 kW. This performance reflects Norway’s commitment to promoting the use of electric vehicles, supported by favorable fiscal policies and a modernized infrastructure.

Eastern European countries have managed to integrate high-power charging stations, benefiting from the delayed development of their networks, which coincided with recent urban infrastructure upgrades. This timing allowed for the adoption of the latest charging technologies. The relatively low number of electric vehicles in these regions enabled a focus on quality, with networks including a higher proportion of high-power stations rather than lower-power ones. This strategic approach was facilitated by local conditions, such as the low density of electric vehicles and the need for synchronized modernization of urban infrastructure [50].

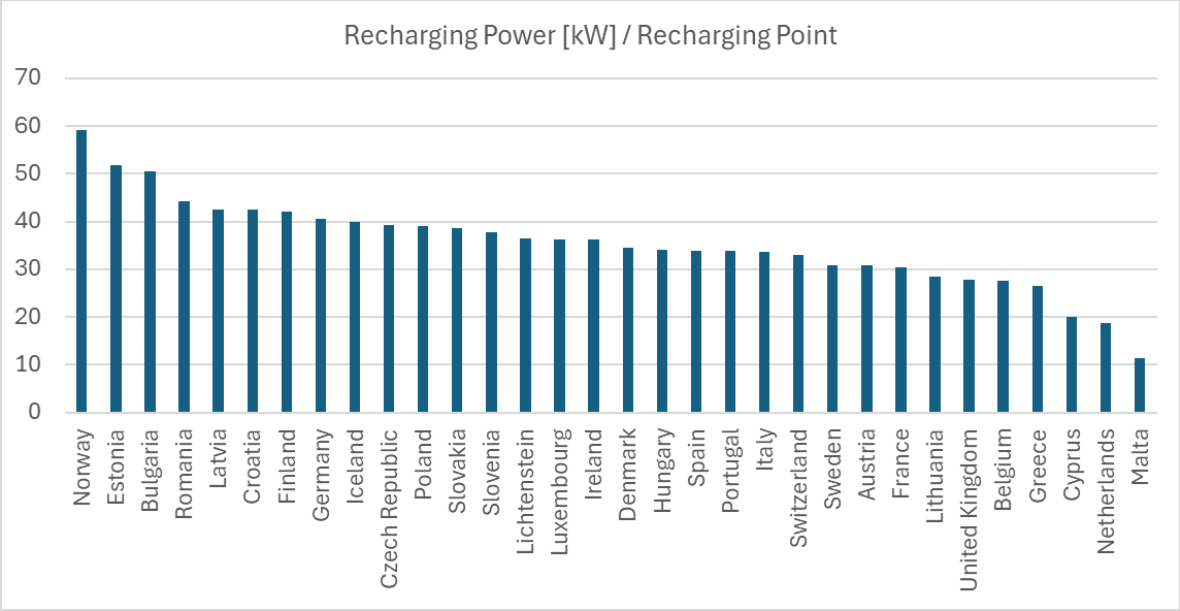

Figure 3.2. Rechargin Power/Rechargin Point [51]

At the European level, 87% of electric vehicles were registered between 2020 and 2023. This rapid growth can be attributed to ambitious political initiatives such as the European Green Deal, the *Fit for 55* plan promoting a 55% reduction in emissions by 2030, driving the transition to electric mobility, and the Alternative Fuels Infrastructure Regulation (AFIR), which provides funding and support for the development of alternative fuel infrastructure networks, including fast-charging stations.

3.2. Types of charging systems

To ensure high compatibility between charging stations and electric vehicles, international standards have been implemented for electric vehicle (EV) charging technology. The technology for charging electric vehicles is regulated by several standards and rules that vary depending on the regions where they are applied. These standards were developed to ensure interoperability between different models and brands of electric vehicles, as well as to facilitate the global transition to electric mobility.

The first fast charging standard for direct current (DC) was CHAdeMO. This DC fast-charging system was developed by an association formed by Tokyo Electric Power Company (TEPCO) and several top manufacturers from the automotive and electronics industries, including Toyota,

Nissan, Mitsubishi, Subaru, Hitachi, Honda, and Panasonic. The name CHAdeMO comes from the expression “CHArge de Move”, reflecting its goal of facilitating the rapid charging of electric vehicles regardless of their brand or model. This standard has been widely adopted globally due to its reliability and interoperability, and is used for fast DC charging [53].

In the European Union, the predominant standard for electric vehicle charging is the Combined Charging System (CCS), officially introduced in 2014. CCS offers flexibility through its compatibility with both alternating current (AC) and direct current (DC) charging, using standardized connectors. The CCS Combo 2 variant was adopted as the official standard in Europe, according to regulations set by the European Committee for Electrotechnical Standardization (CENELEC). In 2019, the European Committee for Electrotechnical Standardization officially adopted the CHAdeMO standard, stipulating that public charging stations must also include CCS Combo 2 connectors. The integration of these standards was carried out under the IEC-62196 framework, an international standard that regulates the plugs, sockets, and connectors used in electric vehicles. This standard is complementary to IEC 61851, which establishes the technical specifications for electric vehicle power supply equipment.

The adoption of common standards, such as IEC-62196 and CCS, ensures uniformity in the charging infrastructure and facilitates the expansion of the electric vehicle market globally. Moreover, interoperability between different charging systems helps reduce costs and increase accessibility for users. These efforts highlight the importance of standardized regulations in accelerating the transition to electric mobility and reducing global carbon emissions.

The establishment of a charging station with multiple charging nodes is of interest because EV chargers are intended to serve a function similar to that of a traditional refueling station. In this regard, EV charging stations can be classified as either AC or DC charging stations. Electric vehicles can charge from both types of stations, as they are equipped with an AC/DC converter that allows battery charging at home through the use of traditional outlets (e.g., Schuko in Europe). However, when faster charging is required, EV charging stations must be used, as they can directly supply DC to the batteries.

Charging stations can supply electricity through various connectors, depending on the desired standard. However, electric charging stations must include several safety systems such as:

- Water and humidity resistance, to ensure vehicle charging regardless of weather conditions;
- A locking system for the charger during the charging process;
- Communication with the vehicle to limit the charging power in case of an overloaded network;
- No electricity is supplied if the locking system is not activated or the cable is not properly connected;
- Immobilization of the vehicle while the locking system is activated / the vehicle is charging, so that the vehicle cannot leave and damage the charging station.

The most common connectors for electric vehicle charging are shown in Figure 3.3. These connectors are regulated by the standards mentioned earlier.

Figure 3.3. Types of connectors used for EV charging [54]

Modern electrical connectors used in electric vehicle charging systems are equipped with several pins that serve different essential functions, as illustrated in Figure 3.4. The widely used Type 2 alternating current standard in Europe includes a total of 7 pins. Of these, three pins (L1, L2, L3) are for three-phase alternating current power supply, one is for neutral (N), and one represents the reserve neutral (which ensures grounding protection). Additionally, two extra pins are dedicated to communication functions: CP (Control Pilot) regulates the energy flow between the charging station and the vehicle, while PP (Proximity Pilot) detects the presence and compatibility of the connected cable.

Figure 3.4. Pinout Type 2 and CCS2 connector

In the case of low-power charging stations (Pmax < 7 kW), the charging process can be carried out in single-phase mode, using only the L1 and N pins, while L2 and L3 are not used. This flexibility allows the Type 2 standard to be adapted to various charging scenarios, from residential infrastructure to public stations. Another advanced European standard is CCS2 (Combined Charging System), which combines the functionality of the Type 2 alternating current connector with a specialized connector for high-power direct current. This hybrid design allows users to use the same charging station for both slow charging and fast charging, providing a practical and efficient solution for modern electric vehicles.

The same communication protocol is used for Type 1 connectors, CCS1, and the dedicated Tesla connector, which rely on the two additional communication pins: CP (Control Pilot) and PP (Proximity Pilot) to detect the presence and compatibility of the connected cable. On the other hand, GB/T connectors, primarily used in China, and the Japanese CHAdeMO standard implement distinct communication protocols, Figure 3.5. These standards require access to the vehicle's CAN Bus (Controller Area Network) communication protocol. The connection via CAN Bus allows for bidirectional exchange of detailed information between the charging station and the vehicle, including real-time diagnostics of components, temperature monitoring, and adjustment of the charging current to ensure the safety of the charging process.

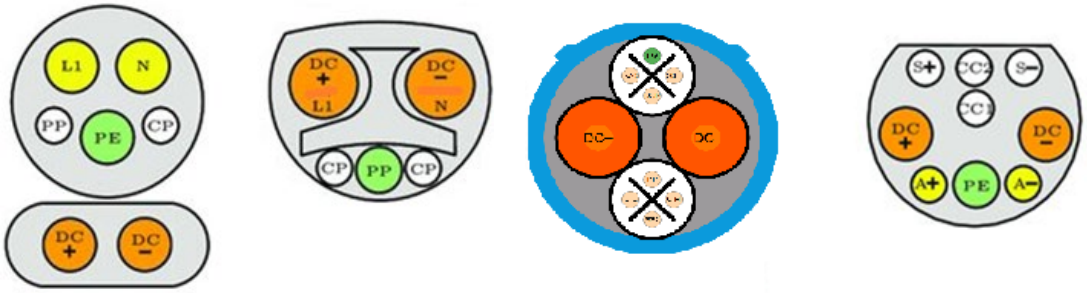

Figure 3.5. Charger Type 1, Tesla, CHAdeMO, GB/T

If battery discharge is determined by the required power, its charging can be controlled using optimal charging strategies. Monitoring and estimating the State of Charge (SOC) and State of Health (SOH) play a significant role in battery charging methods. Optimal charging strategies should be as fast as possible, while keeping the temperature and SOH of the battery within the desired range. The component responsible for optimal battery charging is the Battery Management System (BMS), which analyzes and monitors all information gathered from the EV battery. It works in collaboration with the battery charging circuit by exchanging data to control the intensity and voltage of the battery cells.

3.3. Charging power levels

The main difference between these three standards analyzed is that while the first two classify the charging modes based on the type of power (DC or AC power), the latter classifies the charging modes by the charging power involved. To describe the nominal power, the term “Level” is used in SAE standards, and the term “Mode” is used in IEC standards.

The SAE-J1772 standard, supported by SAE International (a global professional association and standards organization), establishes the following charging modes (Table 3.1):

- AC Level 1: A standard electrical outlet providing a 120 V AC voltage with a maximum current of 16 A, enabling charging at a maximum power of 1.9 kW.
- AC Level 2: A standard electrical outlet with a 240 V AC voltage and a maximum current of 80 A, thus providing a maximum power of 19.2 kW.
- DC Level 1: An external charger providing a maximum voltage of 500 V DC with a maximum current of 80 A, offering a maximum charging power of 40 kW.
- DC Level 2: An external charger providing a maximum voltage of 500 V DC with a maximum current of 200 A, offering a maximum charging power of 100 kW.

Table 3.1. The SAE-J1772 Standard with EV Charging Modes [55]

Charge Method	Volts [V]	Maximum Current [A]	Maximum Power [kW]
AC Level 1	120	16	1.9
AC Level 2	240	80	19.2
DC Level 1	200-500	80	40
DC Level 2	200-500	200	100

The international standard IEC-62196, created by the International Electrotechnical Commission (IEC) in 2001, establishes the general characteristics of the charging process, as well as how the energy is supplied. This standard is derived from IEC-61851 and provides an initial classification of the type of charging based on its nominal power and, therefore, the charging time (Table 3.2 and Figure 3.1). In Table 3.2, four charging modes for electric vehicles can be identified.

Mode 1 represents the slowest form of charging an electric vehicle's battery. This solution is often used in residential areas because the maximum current of 16A is supported by most residential electrical connections. Despite its convenience, this mode is best suited for overnight charging or situations where charging speed is not a priority, as it can take several hours to fully charge a vehicle.

Mode 2 is a solution that can also be implemented in residential areas with the approval of the electricity distributor. This mode supplies the vehicle with up to 32A, either on a single-phase or three-phase connection. Compared to Mode 1, Mode 2 offers a moderate charging speed, making it ideal for daily usage in environments with limited charging infrastructure but where faster charging is desired.

Mode 3 refers to fast charging in alternating current (AC). This solution can deliver power levels of up to 120 kW; however, the most common installations offer 22 kW. This is because the majority of vehicles on the market can charge in AC with power outputs ranging between 11 kW and 18 kW. Mode 3 is typically found in public and commercial spaces, such as parking lots, shopping centers, and office complexes, providing a balance between speed and accessibility.

Mode 4 charging represents the only ultra-fast charging solution. It is characterized by direct current (DC) charging, which is significantly faster than AC methods. Most electric vehicles can charge at rates of 1C to 3C in this mode, where "C" is the battery capacity. For instance, a 50 kWh battery charged at 2C would receive 100 kW of power. This mode is predominantly used in dedicated fast-charging stations along highways or in urban hubs, enabling vehicles to gain substantial range in just minutes, making it essential for long-distance travel and reducing downtime.

Table 3.2. IEC-62196 Standard with EV Charging Modes [56]

Charge Mode	Phase used	Current (max) [A]	Voltage (max) [V]	Maximum Power [kW]
Mode 1	AC single-phase AC three-phase	16	230-240	3,8 7,6
Mode 2	AC single-phase AC three-phase	32	230-240 480	7,6 15,3
Mode 3	AC single-phase AC three-phase	32 - 250	230 – 240 480	60 120
Mode 4	DC	250 - 400	600 – 1000	400

Guobiao Standards (GB) created the GB/T-20234 standard for EV charging infrastructures in China. Although China initially adopted the European standard IEC-62196, it preferred to use its own standard. This standard classifies charging modes between AC and DC, as shown in Tabule 3.3.

Table 3.3. The GB/T-20234 standard with EV charging modes [57]

Mode	Standard	Voltage [V]	Current [A]	Max Power [kW]
AC Charging	GB/T-20234.2-2015	250	10	27,7
			16	
			32	
		440	16	
			32	
			63	
DC Charging	GB/T-20234.3-2015	750 - 1000	80	250
			125	
			200	
			250	

The SAE-J1772 standard is the only one that includes a 120 V charging mode. The other standards, even in their lowest charging modes, operate at higher voltages. In terms of the most powerful modes, SAE-J1772 is also the standard that provides a lower voltage, 500 V, compared to 1000 V offered by both IEC-62196 and GB/T-20234.

Regarding amperage, the standard that offers a lower current intensity is GB/T-20234, with 10 A, compared to the 16 A offered by the other two standards. However, in their strongest modes, SAE-J1772 supports a maximum current intensity of 200 A, compared to 250 A in GB/T-20234 and 400 A in IEC-62196.

When it comes to AC-based charging modes, the standard offering the lower power is SAE-J1772, with 1.9 kW, compared to 2.5 kW in GB/T-20234 and 3.8 kW in IEC-62196. The standard offering the higher power is IEC-62196, with 120 kW, compared to 27.7 kW in GB/T-20234 and 19.2 kW in SAE-J1772.

A similar trend is seen in DC-based charging modes, where IEC-62196 is the standard offering higher power, 400 kW, compared to 250 kW in GB/T-20234 and 100 kW in SAE-J1772.

Tesla has its own fast-charging points, called Supercharger Stations. These work on DC and use their own system. While they have a maximum charging power of 145 kW, it is currently limited to 120 kW, allowing half-charging in just 20 minutes, or 80% in half an hour. Although Tesla claims that its Superchargers are ultra-fast charging points, considering the IEC-62196 criteria, these charging points would be similar to Mode 3 (fast charging). In addition, Tesla users have 400 kWh of free charging in the Tesla network, which is enough to drive approximately 1600 km, a strategy designed to encourage users to purchase Tesla vehicles.

3.4. Charging economics

Electric vehicles (EVs) offer significant financial savings compared to fossil fuel-powered vehicles. The cost of charging an electric vehicle is considerably lower than refueling with gasoline or diesel, even in countries with higher electricity tariffs. For example, with an energy consumption of 15 kWh/100 km, the cost of electricity can range from €2.25 (in Sweden) to €9.90 (in Italy), depending on the local price of electricity. By comparison, fueling an internal combustion engine vehicle with a fuel consumption of 7 liters/100 km typically costs between €11 and €13, depending on fuel prices, making EVs significantly more economical in the long run.

The sustainability of electric vehicles is strongly influenced by electricity costs relative to fluctuations in gasoline and diesel prices, which are driven by global markets and additional taxes. For instance, during energy or geopolitical crises, fossil fuel prices can rise dramatically, whereas electricity prices are often mitigated by the increasing share of renewable energy sources. This allows EV owners to rely on predictable transportation costs, facilitating more stable financial planning.

In many countries, electric vehicles (EVs) benefit from tax exemptions, free parking, preferential electricity rates, and government subsidies. At the same time, internal combustion engine vehicles are subject to additional taxes related to CO_2 emissions, which increase the cost of fossil fuels. These policies encourage the transition to electric mobility and make the cost advantage of EVs even more pronounced. Moreover, home charging, especially when energy is sourced from private systems such as solar panels, can nearly eliminate operating costs. In addition to direct savings and financial stability, EVs provide further benefits in the context of the future of transportation. As renewable energy becomes increasingly accessible, electricity prices are expected to decline further, whereas fossil fuels will remain subject to additional taxes and resource shortages. Over the long term, the savings achieved by using electric vehicles

are likely to increase, reinforcing their position as an economical and sustainable solution for transportation.

Electric vehicles (EVs) have significantly lower maintenance costs due to their simplified architecture compared to internal combustion engine (ICE) vehicles. One of the primary reasons for this is the absence of complex components associated with combustion engines and their transmissions. EVs are equipped with one or two electric motors, a reducer, and a differential unit integrated directly into the drive axle.

Additionally, regenerative braking not only recovers and stores energy in the battery but also reduces wear on the conventional braking system, resulting in a braking system that can be optimally dimensioned for reduced stress and wear. Moreover, EVs do not require periodic oil changes, or the replacement of essential fluids typically needed in combustion engines, thereby eliminating the costs associated with these routine services.

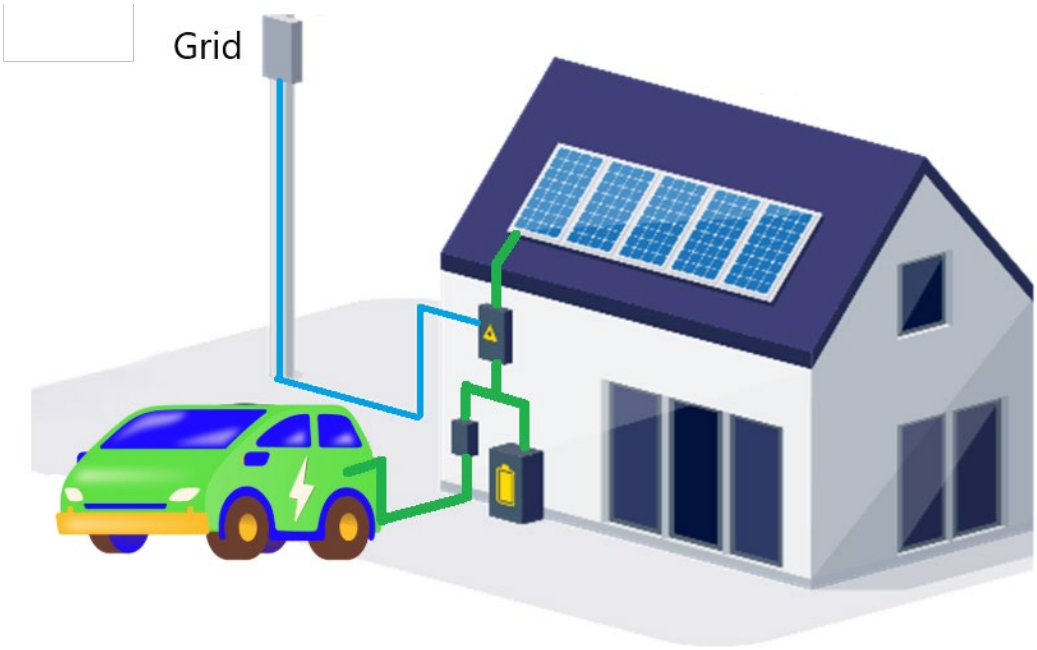

Figure 3.6. Charging the electric vehicle using photovoltaic panels

For individual households, an effective method of generating electricity for electric vehicle charging is the implementation of a photovoltaic system. Solar panels convert solar energy into electrical power at grid-compatible parameters. The generated energy can be used directly for the electric vehicle's charging or stored in a battery system for later use.

This approach reduces dependence on the electrical grid and helps lower charging costs, particularly in regions with a high number of sunny days. Appropriately sized photovoltaic systems can cover a substantial portion of an electric vehicle's energy demand, and when combined with an energy storage system, such as LiIon, LiFePo4 batteries, they can provide complete energy autonomy.

Furthermore, the integration of photovoltaic systems with energy storage solutions enables optimized energy management, ensuring that excess energy is stored for periods of low solar

generation. This enhances both the sustainability and cost-efficiency of the charging process, reducing overall energy expenses over time.

3.5. Smart charging

Electric vehicles (EVs) require high charging power, which involves significant electricity consumption over a short period. If the charging of EVs were to occur unchecked during peak consumption hours, the energy system would be subjected to an overload, potentially destabilizing the grid. This issue would not only affect the grid's ability to supply power to other consumers, but could also lead to increased costs, additional carbon emissions (due to the activation of fossil-fuel-based energy sources to meet peak demand), and the risk of power outages. To address this challenge, the concept of smart charging was introduced. This technology integrates electric vehicles, charging stations, and grid operators within an advanced communication network. Through this integration, charging stations can monitor, manage, and regulate the EV charging process to optimize energy usage and reduce the impact on the grid. Depending on how the charging process is managed, smart charging can be divided into two main categories:

– User-Managed Charging (UMC)

– Supplier-Managed Charging (SMC)

The Vehicle-to-Grid (V2G) technology enables bidirectional energy transfer between the electric vehicle and the electrical grid, providing the ability to supply energy during peak consumption periods or when grid balancing is required. This technology transforms the electric vehicle into a mobile energy storage unit, contributing to grid stabilization and enhancing the quality of energy supply services by reducing voltage and frequency fluctuations. In this context, the energy stored in the vehicle can be used to power the household, supporting energy independence and reducing reliance on conventional energy sources.

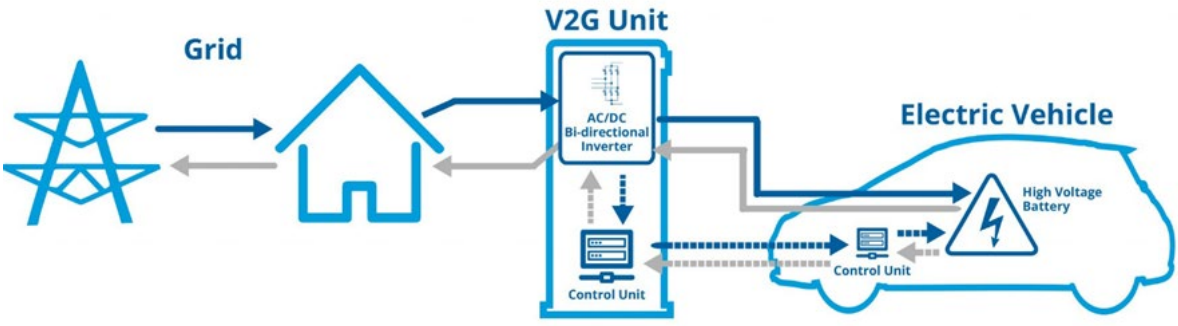

Figure 3.7. Vehicle-to-Grid diagram [58]

In contrast to V2G, the user-managed charging (UMC) system allows for direct control by the user over the timing and duration of electric vehicle charging, based on dynamic electricity rates. Users can schedule their charging outside of peak hours to benefit from lower prices, but without directly interacting with the electrical grid to support its stability. UMC helps

redistribute energy demand, avoiding grid overload during peak hours; however, it cannot contribute to the active balancing of the grid, as V2G technology does.

Within the UMC system, users have direct control over the timing and duration of electric vehicle charging, benefiting from dynamic Time-of-Use (TOU) rates. This method encourages users to schedule their charging outside of peak hours, when energy prices are lower, thereby helping to reduce pressure on the electrical grid. User behavior in this system is influenced by fluctuating rates, which leads to an increased demand immediately after the reduction in energy prices, as shown in Figure 3.8.

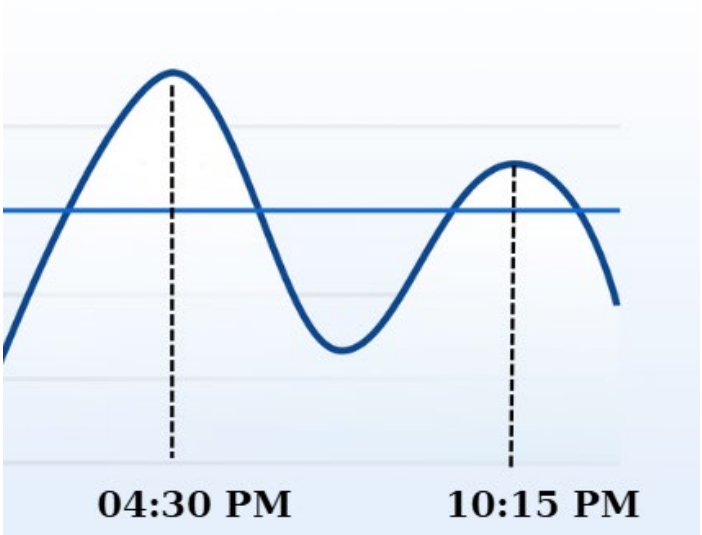

Figure 3.8. Grid consumption with user managed charging (UMC)

The charging profile specific to the UMC system often leads to a delay in the formation of consumption peaks, shifting them to less congested time intervals, typically between 9:00 PM and 11:00 PM, depending on local regulations. However, while demand redistribution helps to avoid overload during critical hours, it may generate new consumption peaks during periods previously considered more stable. This dynamic highlights the importance of continuous planning and optimization to efficiently manage electric vehicle charging within the context of the grid.

Supplier-Managed Charging (SMC), also known as Vehicle-to-Grid (V2G), refers to a technology where energy transfer occurs bidirectionally, from the grid to the battery and from the battery to the grid. This concept represents an advanced technology in which electric vehicles directly interact with the electrical grid to optimize energy consumption and storage. In this scenario, the charging and discharging processes are managed automatically by the grid operator, who makes decisions based on a range of factors, such as energy demand and supply, real-time pricing, weather conditions, and the state of charge of the connected vehicle batteries. This approach not only enables more efficient use of energy resources but also stabilizes the electrical grid by supplying energy during peak demand periods and absorbing surplus energy during low consumption periods. As such, SMC contributes to the transition towards a more sustainable and flexible energy system, promoting the integration of electric vehicles as active elements within the energy infrastructure.

Given the variability of electricity production from renewable sources, particularly wind and solar, it becomes necessary to optimize the electric vehicle charging process to avoid overloading the grid during peak hours (between 06:30–09:30 and 15:30–19:30). Scheduling charging outside of these intervals helps reduce imbalances in the energy system, facilitating the integration of a higher proportion of renewable energy into the grid.

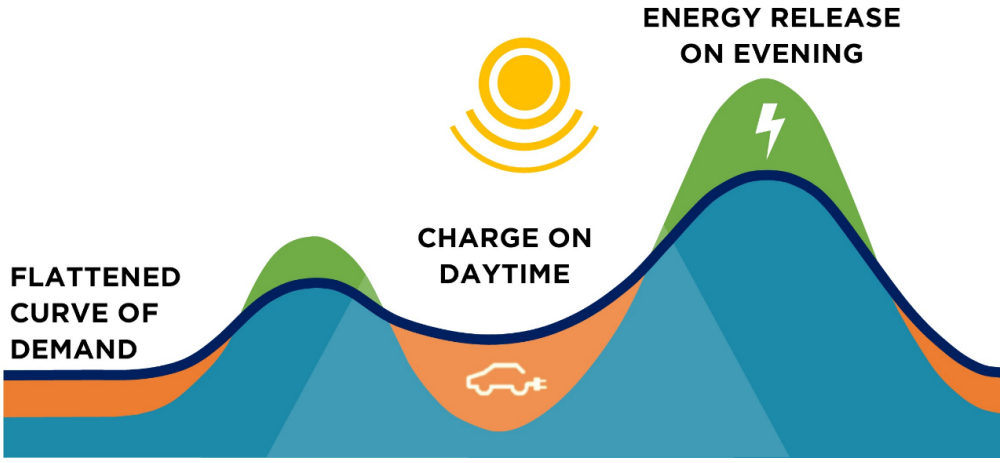

Figure 3.9. Grid load management when using V2G [59]

Supplier-managed charging, integrated within the Vehicle-to-Grid (V2G) concept, facilitates a new paradigm in the integration of electric vehicles into the modern energy ecosystem. This technology transforms electric vehicles from passive energy consumers into active participants, capable of supplying energy to the grid and contributing to its balancing.

Grid operators implement advanced algorithms and intelligent management systems to coordinate energy transfers, optimizing the correlation between renewable energy production and dynamic consumption requirements. Within supplier-managed charging (SMC), operators can adjust the electric vehicle charging processes, for instance, by gradually distributing charging or by regionally unlocking charging stations, thus helping to reduce consumption peaks and stabilize the electrical grid. Otherwise, after work users arrive home, and connect their vehicles to the grid to charge the battery and overload the grid as in Figure 3.10.

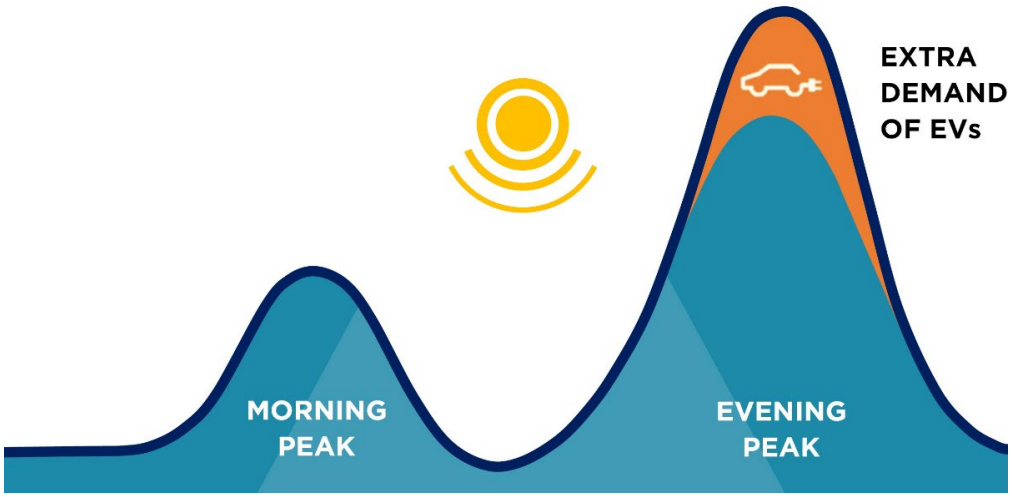

Figure 3.10. Grid without load management [59]

Smart charging of electric vehicles represents an advanced solution for optimizing the use of renewable energy, particularly photovoltaic energy. Photovoltaic systems installed on residential properties allow for the capture of solar energy and its conversion into a valuable resource for the entire household, including for the charging of electric vehicles. Thus, smart inverters can dynamically control the electric vehicle charging station based on the excess electricity produced by the photovoltaic system. This adaptability is crucial for maximizing the use of electricity generated by solar panels, as it ensures the exclusive use of green energy when it is available in surplus.

An important aspect of smart charging is the management of energy flow between the household, vehicle, and grid. Advanced algorithms allow for the adjustment of charging based on solar production, and during surplus periods, the energy is stored in the vehicle's battery. During peak consumption times or at night, this stored energy can be redirected to the household to supplement the energy demand, thereby reducing dependence on the conventional electrical grid. The Vehicle-to-Grid (V2G) technology plays a crucial role in this process, as it enables bidirectional interaction between the vehicle and the grid, facilitating energy redistribution.

Another significant factor in the implementation of smart charging is the ability to set a minimum battery charge level for the vehicle. This ensures the continuous availability of the vehicle for use, even when the charging process cannot reach full capacity. Thus, users can benefit from solar energy advantages without compromising the vehicle's range. This flexibility is essential for the optimal integration of the charging system into users' daily routines.

The use of solar energy through photovoltaic systems significantly contributes to the energy independence of the household. By storing energy in the vehicle's batteries and redistributing it when necessary, households can reduce costs associated with grid energy. This practice supports the development of an autonomous local energy system, one that does not rely on external energy sources, providing both financial savings and a reduction in carbon footprint.

At the same time, the integration of smart charging with photovoltaic sources and V2G contributes to the promotion of a sustainable economy, characterized by a reduction in dependence on conventional energy resources and optimization of renewable energy use. Thus, electric vehicles become not only an eco-friendly mode of transportation but also an efficient energy management tool, supporting the transition to a cleaner and more sustainable energy system.

For efficient distribution of electric energy to charging stations, the concept of Load Balancing is employed. This system ensures the management of simultaneous energy demands across multiple charging stations within a given area, utilizing either a centralized system or a communication protocol between the charging stations and the grid. The primary objective of this mechanism is to monitor and regulate the flow of energy, preventing the overloading of the available network capacity or the individual charging stations. The load balancing system can be either centralized, with control handled by a local server, or decentralized. This system provides high availability for electric charging stations, even in the context of a congested energy system.

For instance, if the maximum available capacity in a specific area is 66 kW, a common solution would involve the installation of three Type 2 charging stations, each with a nominal power of 22 kW. While this method offers a basic implementation, it limits the maximum number of vehicles that can be charged simultaneously. By utilizing Load Management/Load Balancing technology, it becomes possible to increase the number of installed stations while optimizing the distribution of available energy. For example, six charging stations can be installed, and energy management can be carried out according to well-defined operational scenarios.

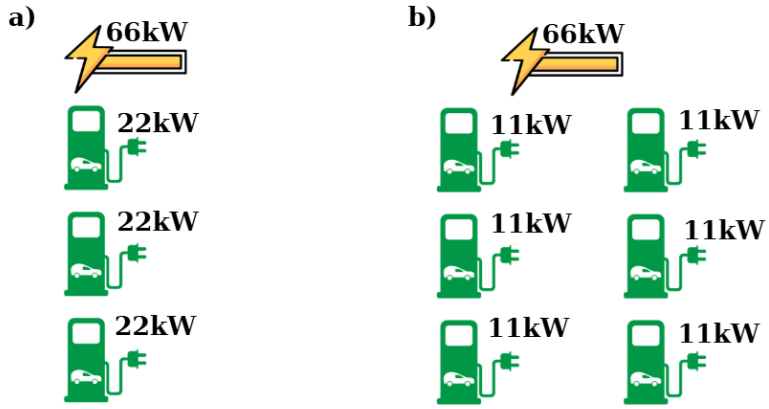

Figure 3.11. Power distribution at classic charging stations

One frequently used scenario is the Fixed Power Allocation, where the available energy is equally distributed among all charging stations. In the presented example, each of the six stations receives a fixed allocation of 11 kW, thus adhering to the total 66 kW limit imposed by the grid. However, this method has some limitations that may affect the service quality. Considering the profile of vehicles on the market and the behavior of electric vehicle users, the following observations can be made:

– Not all stations are used simultaneously;

– Electric vehicles have different charging requirements depending on the model and battery state;

– After reaching 80% of the battery capacity, the charging regime switches from constant current (CC) to constant voltage (CV), resulting in a reduction in absorbed power.

Given these premises, more flexible energy management methods are needed.

Static Load Management optimizes the distribution of electrical energy, allowing charging stations to supply connected vehicles with the necessary power without exceeding the grid's maximum limit. The system monitors each vehicle's requirements and allocates energy based on instantaneous consumption, ensuring efficient resource use and grid stability.

For example, if two stations are used by plug-in hybrid vehicles, each requiring 5 kW, and another two stations are used by city electric vehicles, consuming between 7 and 9 kW, the remaining available power for the other two stations will be 19 kW. In this scenario, four

vehicles can be charged simultaneously without exceeding the grid's maximum limit, while the other two stations will remain available with 86% of their maximum capacity (19 kW out of 22 kW).

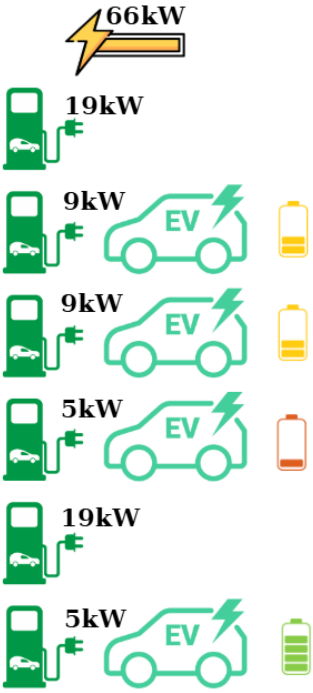

Figure 3.12. Static Load Management

For electric vehicles capable of charging at higher power levels (e.g., 22 kW), energy distribution is adjusted using algorithms such as:

– Prioritization based on order ("first-come, first-served");

– Equal distribution among connected vehicles;

– Weighted allocation, which optimizes charging based on the instantaneous consumption of each vehicle.

A higher level of optimization is represented by Dynamic Load Management (DLM), which involves dynamically adjusting the available power based on the conditions of the electric grid. This system allows:

– Real-time adjustment of the charging power based on network availability and overall consumption;

– Cost reduction by charging vehicles during periods with lower energy tariffs;

– Load balancing at the grid level, reducing the risk of overloading the system.

Implementing DLM requires integration with smart grids and the use of advanced algorithms capable of analyzing and responding quickly to consumption fluctuations. This helps avoid overloading the grid.

In summary, energy management technologies such as Static Load Management and Dynamic Load Management allow for more efficient use of electric vehicle charging infrastructure. They contribute to increasing the operational capacity of the network, reducing associated costs, and ensuring optimal access for users, without exceeding the technical limits of the system. By adopting these solutions, the integration of electric vehicles into a sustainable ecosystem is facilitated, capable of meeting the mobility demands of the future.

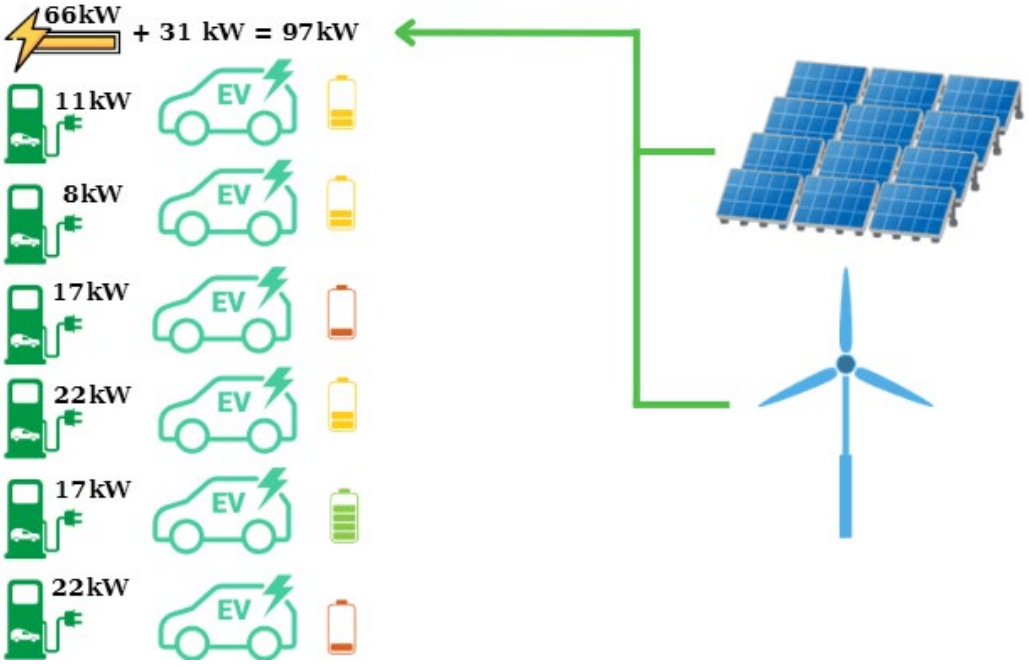

Figure 3.13. Dynamic Load Management (DLM)

Chapter 4: CLIMATE MITIGATION AND ELECTRIC VEHICLES

Against the backdrop of a steady rise in global temperatures and an increase in extreme weather events, efforts to combat climate change have become a top priority worldwide. Although climate change is influenced by a wide range of factors, a major sector of interest is transport, which is responsible for a significant proportion of global greenhouse gas emissions. Road transport, in particular, is a massive source of pollution, with high emissions of carbon dioxide (CO_2) and other polluting particles resulting from the burning of fossil fuels. In this context, electric vehicles stand out as a promising alternative, offering great potential for reducing carbon emissions. Electric vehicles work by converting electricity stored in batteries into kinetic energy, which eliminates the need to burn fossil fuels and, implicitly, direct CO_2 emissions. The major advantage of this technology is the elimination of exhaust emissions, which are among the main air pollutants in cities. In addition, electric vehicles generate a low level of noise compared to vehicles with internal combustion engines, which contributes to the reduction of noise pollution in the urban environment. The environmental benefits of electric vehicles are even more pronounced when the energy used to charge them comes from renewable sources, such as solar, wind or hydropower. This is important to understand the real impact of electric vehicles on the environment, as the carbon emissions associated with electricity generation can vary significantly depending on the energy mix used. Recent studies show that in countries where renewables have a large share in the energy mix, electric vehicles can reduce greenhouse gas emissions by up to 60% compared to conventional vehicles. However, in addition to the multiple benefits, electric vehicles also come with significant technical and economic challenges. One of these challenges is related to battery technology, the central element of electric vehicle operation. Currently, lithium-ion batteries are the dominant technology due to their high energy density and relatively long lifespan, but their production is associated with environmental and supply issues. The extraction of lithium and other metals needed for batteries, such as cobalt and nickel, can cause major environmental damage and require high water consumption, especially in arid areas. Recycling batteries is another challenge, as the process is complex and requires advanced technologies to recover critical materials into a form that can be effectively reused. Despite these challenges, global research efforts are focused on developing sustainable recycling solutions, as well as discovering greener energy storage technologies that will gradually replace reliance on rare metals and other hard-to-reach materials. The infrastructure required for the use of electric vehicles is another critical element. Charging stations must be strategically located and accessible to support the transition to electrified transport without negatively affecting the user experience. The lack of adequate charging infrastructure can be a major impediment to the widespread adoption of electric vehicles, which is why many governments and private sector companies are investing in expanding and upgrading charging station networks. New fast charging methods and technologies that allow direct charging from renewable sources are also analyzed, thus ensuring a more efficient and sustainable use of energy. Public policies and economic incentives play a

decisive role in the adoption of electric vehicles. Subsidies for the purchase of electric vehicles, tax exemptions and infrastructure financing programs are some of the measures adopted globally to accelerate the transition to green transport. These initiatives have begun to demonstrate positive effects, generating notable increases in the number of electric vehicles sold annually and contributing to public awareness of the benefits of this technology. By analysing these aspects, this chapter examines the impact of electric vehicles on climate change, providing insight into how their adoption can reshape the transport landscape and reduce harmful emissions.

4.1. Transport energy consumption

The transport sector is one of the largest consumers of energy globally, having a significant impact on the increase in demand for fossil fuels and, implicitly, on the generation of greenhouse gases. Land transport, which includes personal vehicles, public transport and road freight transport, is the dominant segment from the perspective of energy consumption. This sub-chapter analyses the structure of energy consumption specific to this sector, highlighting the role of different types of fuels, the energy efficiency levels of transport systems and the challenges that accompany the transition to sustainable solutions. Currently, land transport depends mostly on fossil fuels, mainly gasoline and diesel, used in internal combustion engines. These fuels offer the advantage of high energy density, making them practical for large-scale use. However, this dependence comes with significant environmental costs, given that the burning of fossil fuels generates substantial emissions of carbon dioxide (CO_2), nitrogen oxides (NO_x) and fine particulate matter, which contribute to both climate change and the degradation of air quality. In this sense, land transport is considered one of the main polluting factors, especially in urban agglomerations, where the density of vehicles is high. In addition to the environmental impact, the energy efficiency of land transport raises additional issues. Personal vehicles, for example, are often used to transport a small number of passengers, which makes the ratio between the energy consumed and the utility obtained low. This inefficiency becomes even more evident in the context of the constant increase in the number of vehicles on the road, which accentuates both energy consumption and congestion of the road infrastructure. Unlike personal vehicles, public transportation systems such as buses, trains, and subways are significantly more energy-efficient. They can carry a large number of passengers simultaneously, thus reducing energy consumption per individual. In particular, electric trains, when powered by renewable energy, are an optimal example of energy efficiency and sustainability. However, the adoption of public transport as the main means of mobility is limited by the availability and quality of infrastructure, as well as socio-cultural factors influencing user preferences. Apart from land transport, maritime and air transport also contribute to overall energy consumption, albeit in a different manner. Shipping is relatively energy efficient when it relates energy consumption to the volume and weight of the goods being transported. However, the use of heavy fuels, such as fuel oil, has a negative environmental impact, generating significant emissions of sulphur and other pollutants. Air transport, on the other hand, although fast and indispensable for long distances, has one of the

highest levels of energy consumption per kilometer and per passenger. The heavy use of aviation gasoline, a petroleum-derived fuel, amplifies the carbon footprint of this mode of transport, especially at high altitudes, where emissions have a disproportionate climate impact. Transition to sustainable solutions In the context of climate change and the urgent need to reduce greenhouse gas emissions, the transition to more efficient and less polluting technologies and transport systems becomes imperative. In land transport, electric and hybrid vehicles represent promising alternatives, with the potential to significantly reduce the consumption of fossil fuels. They run on electricity, and their impact on the environment is directly influenced by the energy source used to charge the batteries. In addition, the development of new energy storage technologies and the improvement of charging infrastructure are key factors for accelerating the widespread adoption of electric vehicles. Also, the expansion and modernization of public transport networks is another essential pillar of the transition to sustainable energy consumption. Promoting the use of electric trains and other energy-efficient means contributes to reducing total energy consumption in the transport sector and reducing associated emissions. In this regard, public policies and investments in infrastructure play a fundamental role, providing the necessary framework for the adoption of sustainable solutions. The analysis of energy consumption in transport reveals the complexity of this sector and the importance of developing integrated strategies that meet both the mobility requirements of society and the objectives of reducing environmental impact. An effective method of estimating energy consumption in transport is simulation. In the paper [60], the authors perform simulations for energy consumption in the field of public passenger transport. The simulation model was implemented using the SUMO (Simulation of Urban Mobility [61]) platform, an established software tool in the modeling and analysis of urban transport systems. The simulation targets a typical public transport route, capturing the complexity of vehicle-infrastructure-environment interactions. SUMO allows the integration of a wide range of factors that significantly influence the energy consumption and pollutant emissions of vehicles, such as the elevation profile of the route, driving style, traffic light cycles, unpredictable traffic events and specific characteristics of the vehicle. The model also incorporates modules for estimating energy consumption and emissions, based on the principles of physics of motion. Energy consumption and emissions modelling equations take into account the multiple contributions of different powertrain components and vehicle-environment interactions. Thus, the model includes terms that represent the energy required to overcome rolling resistance forces, aerodynamic forces and gravitational forces associated with altitude variations. Energy losses in the transmission system and auxiliary components of the vehicle are also considered. The analysis carried out showed an inversely proportional correlation between the average distance between public transport vehicle stops and the specific energy consumption. Thus, in the simulated scenario, longer stopping distances (250m, 350m, 500m and 1000m Figure 4.1) led to a significant reduction in energy consumption compared to shorter distances (100m). This trend can be attributed to the increased frequency of accelerations and decelerations over short distances, processes involving significant energy losses associated with overcoming inertial forces and rolling resistance. However, optimizing the distance between stops is not a problem with a one-size-fits-all solution, as this parameter influences both the energy efficiency of the

system and the quality of service offered to users. Thus, an excessive increase in the distance between stops can lead to a decrease in the frequency of the service and an increase in waiting times, negatively affecting the comfort and attractiveness of public transport. In conclusion, the results obtained underline the need to adopt a multidisciplinary approach in the optimization of public transport networks, which takes into account both energy aspects and those related to transport demand and user comfort. Advanced simulation models, capable of integrating a wide range of variables, such as the route elevation profile, traffic conditions, vehicle type and user behavior, can be valuable tools in this endeavor [60].

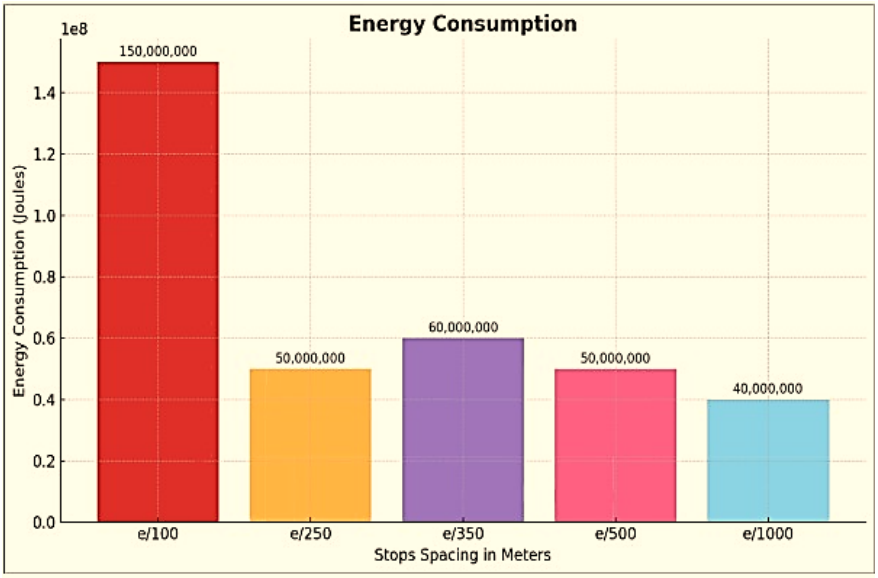

Figure 4.1 Energy consumption for urban passenger transport [60], [61]

Another type of passenger transport is the high-speed rail transport. Maglev reindeer (magnetic levitation) is a leading innovation in rail transportation, using electromagnetic fields to levitate, propel and guide vehicles over a dedicated rail without physical contact. This operating principle completely eliminates mechanical friction between wheels and rails, which significantly reduces energy losses, ensures a high level of comfort and allows outstanding speeds of up to 600 km/h to be achieved, as seen in the case of the Shanghai Maglev train [62-64]. The levitation system is ensured by the use of strong magnets. In the case of EMS (Electromagnetic Suspension) technology, the train is attracted to the rail by means of active electromagnets that provide stable levitation at a distance of 10-15 mm from the rail. On the other hand, EDS (Electrodynamic Suspension) technology uses superconducting magnets, which create a repulsive magnetic field, raising the train to a height of 100-200 mm and providing a high degree of stability and energy efficiency. The propulsion of Maglev trains is based on a Linear Synchronous Motor (LSM), which uses coils placed along the rail to generate variable magnetic fields. They interact with the magnets mounted on the train, resulting in a propulsive force capable of accelerating the vehicle to very high speeds, without vibrations or disturbing noises. In addition, this technology allows precise control of speed and direction, including fast and safe braking. The lateral stability of the train is also maintained through magnetic interactions, eliminating the need for additional mechanical components, such as wheels, which are characteristic of conventional trains. From a technical point of view, Maglev

trains offer a number of impressive performances. They are capable of carrying between 200 and 1,200 passengers, depending on the vehicle configuration, and have an energy consumption of only 0.08-0.10 kWh/passenger-km, making them considerably more efficient than airplanes. Also, the maximum acceleration of a Maglev train can reach 4 m/s², and the durability of the infrastructure is extended to over 50 years, thanks to the elimination of mechanical wear. However, the construction of the infrastructure necessary for their operation involves high costs, estimated at more than 30-50 million USD/km, which limits their large-scale implementation. Despite the costs, Maglev trains bring significant benefits, such as high speed, reduced travel time, superior comfort due to the absence of vibrations, as well as quiet operation. They also help reduce noise pollution and carbon emissions, making them an environmentally friendly solution for medium and long-distance transport. Thus, Maglev technology not only redefines modern transport, but also has the potential to transform urban and interurban mobility in a sustainable and efficient way. This represents a promising direction for the future of high-speed transport, combining cutting-edge technological performance with a sustainable vision of global mobility. Energy consumption in high-speed trains has evolved significantly over time as rail technologies and infrastructures have been improved. The first high-speed trains, such as the Japanese Shinkansen launched in 1964, used conventional technologies based on electric traction powered by dedicated rail networks. Although these represented a significant leap in terms of rail transport efficiency, the energy consumption compared to high speeds was relatively high, mainly due to the mechanical friction between the wheels and the rails and the increased aerodynamic resistance at high speeds. As technology advanced, engineers focused on reducing energy consumption by optimizing vehicle design and improving infrastructure. The use of lightweight materials for the construction of trains, such as aluminum and composite alloys, has contributed to reducing their weight, thus decreasing the energy required for propulsion. In addition, advanced aerodynamic designs were developed, which minimized drag. For example, the TGV trains in France and the ICE in Germany have adopted elongated and elegant shapes, considerably reducing energy consumption at speeds above 300 km/h. Another key factor in reducing energy consumption was the shift to more efficient electrical systems, such as synchronous motors and braking (regenerative) energy recovery systems. These technologies allow trains to recover some of the energy lost during braking and return it to the power grid, thus increasing overall efficiency. For example, modern trains, such as the Eurostar and the N700 Shinkansen series, recover up to 20-30% of the energy used, which helps to reduce operational costs and environmental impact. In recent years, the introduction of Maglev trains (magnetic levitation) has radically changed the paradigm of energy consumption in the field of high-speed transport. Although the infrastructure required for their operation involves a high initial energy consumption during construction, Maglev trains are extremely efficient in operation, due to the elimination of mechanical friction between the train and the rail. With an average consumption of 0.08-0.10 kWh/passenger-km, Maglev outperforms both conventional trains and other forms of high-speed transport, such as airplanes, in efficiency. In the long term, the energy sustainability of high-speed trains is a priority, and the integration of renewable energy sources into electrified rail networks is becoming increasingly common. Many rail networks now use solar, wind, or hydroelectric power to power

trains, significantly reducing their carbon footprint [65]. For example, trains in the Netherlands run 100% on wind power, a model that could be replicated in other countries. Thus, the evolution of high-speed trains reflects a constant technological progress aimed at increasing energy efficiency and reducing environmental impact. From its beginnings based on conventional technology, to the implementation of Maglev trains and renewable energy, high-speed rail transport is proving to be a modern, sustainable and efficient solution for the mobility needs of the 21st century [66]. In the context of increasing greenhouse gas emissions from the transport sector, which account for around 25% of global CO_2 emissions, high-speed trains offer a sustainable alternative to air and road transport, which are responsible for the bulk of these emissions. High-speed trains mainly use electricity for propulsion, eliminating dependence on fossil fuels. In addition, modern rail systems have integrated energy-efficient technologies, such as optimised electric motors, regenerative braking systems and aerodynamic designs, which reduce energy consumption per passenger. For example, the average consumption of high-speed trains, such as the French TGV or the Japanese Shinkansen, varies between 0.05 and 0.15 kWh/passenger-km, significantly lower compared to airplanes, which consume an average of 0.2-0.3 kWh/passenger-km, or passenger cars, with 0.4-0.6 kWh/passenger-km [67]. Another important contribution to reducing the climate impact of rail transport is the integration of renewable energy sources into the power supply of electricity grids. In many regions, high-speed trains are already running on solar, wind or hydroelectric power. For example, the railway network in the Netherlands is powered entirely by wind energy, and other countries, such as Germany and Japan, are expanding their infrastructure to incorporate renewable sources. This transition reduces indirect emissions associated with energy production, contributing to the decarbonisation of transport. High-speed trains not only emit less CO_2, but also contribute to reducing noise pollution and other harmful emissions, such as nitrogen oxides and fine particulate matter, which are commonly associated with road and air transport. They also have the ability to reduce traffic congestion by replacing many short-haul flights and personal car travel. In the European Union, the widespread adoption of high-speed rail transport could reduce emissions from the transport sector by up to 10%, according to estimates by the European Environment Agency [68]. A notable example of the success of high-speed trains in combating climate change is the Madrid-Barcelona line in Spain [69] . After the opening of this line, air traffic between the two cities decreased by more than 50%, which led to a significant reduction in CO_2 emissions. Similarly, the Paris-Lyon line has demonstrated that high-speed trains can take over 90% of the transport market share over distances of up to 500 km, providing a sustainable and affordable solution. In the long term, the expansion of high-speed rail networks and the modernisation of existing ones is a key strategy for reducing emissions from the transport sector. Combining them with integrated urban mobility plans, such as green public transport and the use of green energy, can amplify the positive impact on the environment. Thus, high-speed rail transport becomes a central pillar in the transition to a cleaner, more efficient and more sustainable mobility system, contributing significantly to the global goals of limiting global warming to below 1.5°C, according to the Paris Agreement [65], [68], [70] . The use of nuclear energy in high-speed rail transport is an innovative idea that could fundamentally transform this sector, providing a stable, efficient and low-carbon source. In the

context of accelerating the energy transition and the need to reduce global greenhouse gas emissions, nuclear energy is emerging as a viable option for powering high-speed rail networks, due to its ability to produce large amounts of electricity with a low environmental impact. The main attraction of nuclear energy in this area lies in its potential to provide reliable, continuous and fluctuation-free energy, regardless of weather conditions or the availability of other renewable sources. Modern nuclear power plants, based on advanced reactors, can provide electricity needed to operate high-speed rail networks, reducing dependence on fossil energy sources. For example, a medium-sized nuclear reactor with a capacity of 1 GW could simultaneously power several high-speed train lines, including extensive long-distance networks. In the long term, Small Modular Reactors (SMRs) could become ideal solutions for the integration of nuclear energy into rail transport. These compact reactors are designed to be installed close to consumption areas, reducing energy losses associated with long-distance transmission. For example, an SMR with a capacity of 300 MW could provide the necessary energy for an entire regional high-speed rail network. In addition, these reactors are much safer than traditional models, being equipped with passive protection systems that minimize the risk of accidents. Another advantage of nuclear energy is its low environmental impact. Over the entire life cycle, nuclear energy produces much less CO_2 emissions compared to fossil fuels and even some renewable sources, such as solar energy, if the production of materials for photovoltaic panels is taken into account. Thus, the integration of nuclear power plants or SMRs into rail networks could significantly contribute to the decarbonisation of high-speed transport, aligning with the objectives set by the Paris Agreement. However, the deployment of nuclear energy in this area also involves challenges. The high upfront costs for the construction of nuclear power plants and the necessary infrastructure are a significant obstacle, and public acceptance of this technology is often influenced by fears about the safety and management of radioactive waste. However, recent advances in advanced reactors, which produce less waste and are more efficient, could help overcome these barriers. Nuclear energy could also play a complementary role in the energy mix of high-speed rail transport. In combination with renewables, such as wind and solar, nuclear could act as a backbone, ensuring a steady flow of energy during periods of high demand or in the absence of optimal conditions for renewables. Thus, the use of nuclear energy in high-speed rail transport could represent a revolutionary solution to simultaneously meet the needs of rapid mobility and environmental protection objectives. With strategic investments in research, infrastructure and appropriate regulations, nuclear energy has the potential to contribute to creating a more sustainable, efficient and safe transport system for the future. This approach could become a key element of global strategies to combat climate change and develop a low-carbon economy [64].

Maritime transport is one of the essential pillars of the global economy, accounting for about 90% of international trade. However, this sector is also a major consumer of energy, having a significant impact on the environment through greenhouse gas emissions. Analysing energy consumption in maritime freight and passenger transport is essential to identify solutions that reduce the carbon footprint and ensure sustainable transport. Maritime freight transport, especially that carried out by means of high-capacity ships such as container ships, oil tankers and bulk carriers, is one of the most energy-efficient in relation to the tonne of cargo transported

[71]. Their specific energy consumption varies between 3 and 10 g CO_2/tonne-km, considerably lower than that of road or air transport [72]. However, the large volume of cargo transported and the high number of ships in operation contribute to the annual emission of around 1 billion tonnes of CO_2, equivalent to 3% of global emissions. The main source of energy used in shipping remains fuel oil, a fossil fuel with a high sulfur content, which contributes to air pollution through SO_2 emissions and fine particulate matter [73]. In maritime passenger transport, such as cruise ships and ferries, energy consumption is significantly higher per passenger-km, due to the additional requirements for comfort, facilities and on-board services. Cruise ships, for example, can consume between 150 and 250 kWh/passenger per day, including the energy needed for propulsion, air conditioning, restaurants, entertainment and other activities [72], [74]. Although it represents only a small part of the global maritime sector, this type of transport has a disproportionately large ecological footprint, contributing to both CO_2 emissions and local marine pollution. In recent years, efforts to reduce energy consumption and emissions in the maritime sector have led to the adoption of more efficient technologies and alternative fuels. Efficient diesel engines, the use of liquefied natural gas as an alternative to fuel oil and the implementation of hybrid propulsion systems have helped to reduce fuel consumption and associated emissions. For example, ships powered by liquefied natural gas emit up to 20% less CO_2 and almost eliminate sulfur emissions [75] . Another important aspect is the use of performance optimization technologies, such as improved hydrodynamic hull designs, special coatings to reduce friction and the use of advanced thrusters [76], [77]. These measures can reduce fuel consumption by up to 15-20%, without affecting operating speed. Also, digitalization and the use of on-board energy management systems allow for continuous monitoring and optimization of fuel consumption, thus reducing costs and environmental impact. To increase the sustainability of maritime transport, renewable energy sources and innovative technologies are becoming increasingly relevant. Ships equipped with modern sails, kites or solar panels have demonstrated that renewable energy can be integrated into maritime transport, reducing dependence on fossil fuels. For example, hybrid ships Figure 4.2 that combine electric propulsion and solar energy can reduce emissions by up to 30% compared to traditional ships [78], [79].

In the long term, the transition to alternative fuels, such as ammonia, green hydrogen or marine biofuels, could completely transform the maritime sector, significantly reducing carbon emissions and helping to achieve global decarbonisation goals. However, the adoption of these solutions depends on the development of adequate infrastructure, high costs and regulatory requirements. Thus, energy consumption in maritime freight and passenger transport is a key factor in the transition to a more sustainable global transport system. Electric vehicles are powered exclusively by batteries that store electricity, used to power electric motors, thus eliminating the need for fossil fuels. These batteries, mainly lithium-ion batteries, are designed to offer high energy density, durability and the ability to be recharged thousands of times over the life of the vehicle. The energy efficiency of electric vehicles is significantly higher compared to vehicles with internal combustion engines, due to the fact that electric motors convert about 85-90% of the stored energy into movement, unlike internal combustion engines, which have an efficiency of only 20-30%, with the rest of the energy being lost in the form of heat.

Figure 4.2 Ship with hybrid propulsion [78]

On average, an electric vehicle (EV) consumes between 15 and 20 kWh/100 km, depending on factors such as vehicle size, weight, powertrain efficiency, traffic conditions and driving style. Smaller vehicles, designed for urban use, have a lower consumption, around 12-15 kWh/100 km, while larger models, such as electric SUVs, can consume between 20 and 25 kWh/100 km [80, 81]. In addition to the intrinsic efficiency of electric motors, other technologies, such as regenerative braking, help reduce energy consumption by recovering some of the vehicle's kinetic energy during deceleration and storing it in the battery. For comparison, a car powered by gasoline or diesel has an equivalent energy efficiency of about 50-70 kWh/100 km, 3-4 times higher than the consumption of an electric vehicle [80, 82, 83]. This major difference reflects the energy losses in internal combustion engines and demonstrates the clear advantage of electric propulsion. For example, in the case of a gasoline-powered vehicle, much of the energy is lost through the heat generated by the engine, friction, and exhaust emissions, resulting in only a fraction of the fuel's energy being converted into useful motion. In addition to low energy consumption, electric vehicles also offer other benefits. They do not produce direct emissions of CO_2 or other polluting particles, helping to improve air quality, especially in urban environments. Additionally, the energy needed to power them can come from renewable sources such as solar or wind power, allowing them to be completely carbon neutral over their entire lifetime. However, the efficiency and consumption of electric vehicles are influenced by factors such as travel speed and the use of on-board accessories. At high speeds, energy consumption increases significantly due to aerodynamic resistance, and the use of air conditioning or heating systems can increase total consumption by 10-20%. In contrast, in urban environments, where regenerative braking is frequently used, the energy efficiency of electric vehicles is optimal. Thus, electric vehicles are not only a more energy-efficient solution, but also offer opportunities for reducing environmental impact, especially when integrated into a renewable energy system. This combination of efficiency and sustainability makes them a viable and necessary alternative for the future of global mobility.

Hybrid vehicles combine an internal combustion engine with one or more electric motors, with the ability to reduce fuel consumption and CO_2 emissions. There are two main types: Classic hybrids (HEV): Use electricity to support the heat engine and recover energy through regenerative braking. The average consumption of an HEV is 20-30% lower than that of a conventional vehicle, being between 4 and 6 liters/100 km [84]. Plug-in hybrids (PHEVs): These have a larger battery that can be charged externally, allowing between 40 and 100 km to be covered in pure electric mode. The energy consumption of a PHEV in electric mode is similar to that of an EV, between 15 and 20 kWh/100 km, but when using the combustion engine, consumption can reach 5-8 liters/100 km, depending on the conditions. PHEVs offer flexibility in use, reducing dependence on charging infrastructure [85] , but their contribution to reducing emissions depends on the frequency of electric mode use. Studies show that many users predominantly use the combustion engine, which reduces the environmental benefits of these vehicles. The development of charging infrastructure is essential for expanding the use of EVs and PHEVs. Currently, global charging station networks include more than 3 million points, but this figure needs to grow exponentially to support the growing demand. Charging time ranges from 30 minutes to 12 hours, depending on battery capacity and station type (from 7 kW AC to 350 kW DC) [86, 87].

4.2. Emissions from the transportation sector

The transport sector is a fundamental pillar in the functioning of modern economies, playing an important role in facilitating trade, the mobility of people and the global integration of markets. However, despite its economic importance, transport is responsible for a significant proportion of global greenhouse gas emissions, contributing considerably to climate change and air pollution. Transport emissions vary significantly depending on the type of vehicle, the energy source used, powertrain technologies and existing infrastructure. Also, user behaviour and operational practices have a significant impact on the emission levels generated by this sector. As economic and social demands increase, and urbanization continues to accelerate, road, air, sea and rail transport are becoming major sources of pollution, with direct effects on air quality, public health and, implicitly, on global ecosystems. In this sub-chapter, a detailed analysis of the sources of CO_2, NOx, SOx and fine particulate emissions from the different transport subsectors will be carried out, assessing the impact of these emissions on global warming and human health. In addition, this sub-chapter will examine emerging trends in international and national regulations aimed at reducing transport emissions, including measures to promote sustainable transport, the transition to electric and hybrid vehicles, the development of efficient charging infrastructure, and the promotion of alternative fuels such as hydrogen and biofuels. In the context of an increasingly interconnected global system, it will also look at technological developments and innovations that promise to make the transport sector more energy efficient and less polluting. Finally, this paper will address the need for integrated global emission reduction policies that support the transition to a sustainable transport system without compromising the economic and social needs of different regions of the world. Thus, understanding the complexity and interdependence of greenhouse gas emissions from the

transport sector is fundamental for the development of effective strategies to mitigate climate change and protect the environment.

Pollutant emissions from the transport sector The transport sector is an essential element of modern economies, facilitating the mobility of people and goods globally. However, the sector is also one of the biggest contributors to greenhouse gas emissions, air pollution and other forms of environmental degradation [88]. Emissions from transport have a direct impact on climate change, air quality and public health, thus being an area of interest for regulatory policies and sustainable technological solutions [89]. Pollutant emissions from transport come mainly from the use of fossil fuels (petrol, diesel and natural gas) in the various modes of transport: road, rail, sea and air. Each mode of transport contributes differently to emissions of CO_2 and other pollutants, such as nitrogen oxides (NOx), volatile organic compounds (VOCs), sulfur dioxide (SO_2) and fine particulate matter (PM) [90-93].

Currently, road transport is the main source of emissions in the transport sector, having a major impact on the environment and human health. Petrol and diesel vehicles emit significant amounts of CO_2, NOx and fine particulate matter, especially in urban areas where traffic density is high. According to estimates, road transport accounts for around 70-75% of CO_2 emissions from the transport sector. NOx emissions from diesel vehicles are a major problem, being associated with health problems such as respiratory and cardiovascular diseases. Internal combustion engine vehicles also generate fine particulate matter (PM) emissions, which have harmful effects on the respiratory system [91, 92]. Given its impact on climate change, public health and air quality, it is imperative to adopt effective measures to reduce these emissions. The proposed solutions include the transition to cleaner technologies, the optimization of transport infrastructure and the promotion of effective public policies. A fundamental measure for reducing emissions is the gradual replacement of internal combustion engine vehicles with electric vehicles (EVs) and hybrids. Electric vehicles are powered exclusively by batteries and do not emit pollutants during operation, making them an ideal solution for reducing CO_2 and NOx emissions. In the long term, the energy efficiency of EVs, which consume an average of between 15 and 20 kWh/100 km, gives them a considerable advantage over fossil fuel vehicles, which have an equivalent efficiency of 50-70 kWh/100 km. Hydrogen is another promising technology, used in fuel cell vehicles, which emit only water vapor. However, the success of these technologies depends on the source of hydrogen production and the electricity used [92]. For example, an electricity grid powered predominantly by renewable sources, such as solar or wind energy, contributes significantly to reducing emissions throughout the life cycle of vehicles. In addition to electrification, the use of advanced biofuels, such as second- and third-generation biofuels, can provide a transitional solution for conventional vehicles. These fuels have a significantly lower carbon footprint and are produced from waste or non-food materials, thus reducing their environmental impact [94]. Infrastructure plays a crucial role in optimising road transport and reducing emissions. The development of an extensive network of EV charging stations, including fast chargers, is essential to support EV adoption. In addition, the implementation of intelligent transport systems, which monitor and manage traffic flows, can reduce congestion and, implicitly, the emissions generated by the stationary or slow movement

of vehicles. Building accessible bike lanes and sidewalks in urban areas can encourage active mobility, thereby reducing the use of personal vehicles over short distances. Also, promoting efficient and environmentally friendly public transport, such as electric or hybrid buses, can lessen dependence on private cars, reducing the total number of vehicles on the road [95]. According to the International Energy Agency [97] , the land transport sector is responsible for about 20-25% of global greenhouse gas emissions. Of this proportion, more than 70% are generated by road transport, while rail transport contributes to a much lesser extent, accounting for only 1-2% of total emissions. Road vehicles, including cars, trucks and buses, emit more than 7.3 gigatons of CO_2 annually, underlining their dominant role in air pollution. At regional level, pollutant emissions from transport vary significantly. For example, countries in the European Union have reported a steady increase in CO_2 emissions from transport, despite the overall reduction in emissions from other sectors. In 2021, transport accounted for around 30% of the EU's total CO_2 emissions, and 72% of this came from road transport. In the United States, ground transportation is the largest contributor to CO_2 emissions, even surpassing the energy sector, with a contribution of about 29% to total national emissions. A worrying aspect is the distribution of vehicle types and their contribution to pollution. Passenger cars are responsible for around 45-50% of global transport emissions, while heavy-duty vehicles such as trucks and buses contribute around 35%. This is due not only to the large number of personal vehicles, but also to the high fuel consumption and distances travelled by commercial vehicles. In terms of air pollutant emissions, nitrogen oxides and fine particles have a significant impact on public health, especially in densely populated urban areas [96]. According to the World Health Organization, NOx emissions from transportation are responsible for about 40% of total concentrations in the atmosphere, and diesel vehicles are the main source. Also, the fine particles emitted by diesel engines contribute to the appearance of respiratory and cardiovascular diseases, being classified as carcinogens. In terms of fuels used, petrol and diesel vehicles generate the most CO_2 and NOx emissions. The average fuel consumption for a petrol-powered car is around 7-9 litres/100 km, which corresponds to an emission of 2.3-2.6 kg of CO_2 per litre of fuel burned. Diesel vehicles, although more fuel-efficient, produce higher concentrations of NOx and fine particulate matter. In contrast, electric vehicles have zero emissions during operation, but the electricity production required to charge them can generate indirect emissions, depending on the energy source used. An analysis of global trends suggests that the adoption of electric and hybrid vehicles has started to positively influence emissions reductions. In 2022, more than 10 million electric vehicles were sold globally, accounting for about 14% of total light-duty vehicle sales. However, this progress is insufficient to counter the continued growth in the total number of registered vehicles, which exceeded 1.4 billion in 2023. In conclusion, land transport remains a major source of polluting emissions, with serious implications for the environment and human health. The statistics highlight the urgency of adopting stricter policies, innovative technologies and a more sustainable transport system to reduce the impact of this sector on climate change and air quality [96-98]. Compared to road transport, rail transport is much greener, generating only 1-2% of global CO_2 emissions. Due to the extensive electrification of rail networks in many regions, rail transport has a low energy consumption of around 0.6-1.0 MJ/passenger-km for passengers and 0.1-0.3 MJ/t-km for

freight. In countries that use renewables for electricity generation, the carbon footprint of rail transport is even smaller [99, 100]. In the case of shipping, it plays a key role in international trade, handling about 80% of the total volume of trade, but contributes only 2.5-3% to global CO_2 emissions. The energy efficiency of shipping is remarkable, with a consumption of 0.02-0.05 MJ/t-km, but the use of heavy marine fuels causes significant emissions of sulfur oxides (SOx) and NOx, which contribute to acid rain and affect air quality in port areas [101, 102]. Air transport, although it accounts for only 2-3% of global CO_2 emissions, has a disproportionate climate impact, as emissions are released at high altitudes, amplifying the radiative effects by 2-4 times those of ground-level emissions. The average fuel consumption for passenger aircraft is 3-4 liters/100 km per passenger, which corresponds to an emission of 9-12 kg CO_2 per passenger/100 km, thus being less efficient than rail or road transport at full capacity [103-105]. The comparative analysis highlights that land transport is the largest polluter in terms of total emissions and public health impact, followed by air transport, which, although it generates lower emissions in absolute terms, has an intense climate impact. Shipping and rail transport, on the other hand, are much more energy efficient and contribute significantly less to global pollution. This data highlights the need for continued investment in cleaner technologies, electrification and the transition to renewable energy sources for all modes of transport, thus helping to reduce their impact on climate change and achieve global sustainability goals.

Factors influencing transport emissions

Emissions from the transport sector are influenced by a multitude of interrelated factors that contribute to air pollution levels and the climate impact associated with this sector. Understanding these factors is essential to develop effective solutions to reduce emissions and support the transition to a more sustainable transport system. Among the most important factors influencing transport emissions are the type of fuel used, the technological characteristics of vehicles, transport infrastructure, user behaviour and public policy. A first influencing factor is the type of fuel used. Fossil fuels such as petrol, diesel and kerosene are the main sources of energy for transport globally, but their combustion generates significant emissions of carbon dioxide (CO_2), nitrogen oxides (NOx), sulphur oxides (SOx) and fine particulate matter (PM10 and PM2.5). Diesel, for example, is more energy efficient than gasoline, but produces higher amounts of fine particulate matter and NOx, contributing to air pollution and public health problems. On the other hand, alternative fuels such as compressed natural gas (CNG), liquefied petroleum gas and biofuels have a lower environmental impact, but the infrastructure required to use them is often underdeveloped. Electric vehicles (EVs) and hydrogen-powered vehicles offer promising solutions for reducing direct emissions, but their impact depends on the energy sources used to produce electricity or hydrogen. Another critical factor is vehicle technology. Technological advances have led to improved energy efficiency of vehicles, thus helping to reduce fuel consumption and associated emissions. Vehicles equipped with more efficient engines, advanced fuel management systems, and exhaust aftertreatment technologies, such as particulate filters and catalytic converters, emit fewer pollutants. Hybrid and plug-in hybrid vehicles also combine internal combustion engines with electric motors, thus reducing emissions in urban or short-distance environments. In the case of electric vehicles, the lack of

direct emissions is a significant advantage, but indirect emissions related to battery production and electricity generation must be taken into account. Transport infrastructure also plays a key role. The quality and expansion of road, rail, port and airport networks influence both fuel consumption and emissions. For example, poorly maintained or congested roads can lead to increased fuel consumption due to frequent stops, accelerations, and decelerations. Instead, well-designed infrastructure, such as modern motorways or electrified railways, can help reduce energy consumption and emissions. In urban areas, the development of efficient public transport networks, such as metros and trams, can significantly reduce the use of personal vehicles and, implicitly, the associated emissions. User behaviour is another factor influencing transport emissions. Driving style, transport preferences and mobility habits play an important role in determining energy consumption and pollution levels. For example, aggressive driving, sudden acceleration, and excessive speed increase fuel consumption and emissions. At the same time, choosing less polluting means of transport, such as bicycles, public transport or car-sharing, can significantly reduce users' carbon footprint. Public awareness of the environmental and health impacts of transport can encourage behaviour change and the adoption of more sustainable practices. In addition, public policies and regulations have a considerable impact on transport emissions. The implementation of strict emission standards, such as Euro norms for vehicles in the European Union, has led to reductions in air pollutant emissions over time. Subsidies for the purchase of electric vehicles and investments in charging infrastructure also help accelerate the transition to green mobility. At the same time, emission taxes, low emission zones and bans on diesel-powered vehicles in city centres have been implemented to discourage the use of polluting vehicles. Last but not least, economic and demographic factors influence transport emissions. Population growth, urbanisation and economic expansion are leading to increased demand for the transport of goods and people, which can increase emissions if efficiency measures are not taken. At the same time, in higher-income regions, consumers are more likely to adopt new technologies and use less polluting vehicles, while in developing countries, limited infrastructure and older vehicles contribute to higher levels of pollution. In conclusion, transport emissions are influenced by a combination of technological, economic, behavioural and political factors. An integrated approach, including technological improvements, effective public policies, changes in user behaviour and infrastructure development, is essential to reduce emissions and minimise the impact of transport on the environment and public health.

Indirect emissions from the production of fuels and vehicles

In assessing the environmental impact of the transport sector, it is essential to take into account not only direct emissions from the use of fuels in vehicle engines, but also indirect emissions from the production of fuels and vehicles. These emissions, although less visible, play a significant role in the total carbon footprint of transport, influencing both climate change and environmental degradation. The production of transport fuels is a major source of indirect emissions. In the case of fossil fuels, such as gasoline, diesel and kerosene used in road, sea and air transport, emissions are generated throughout the entire process of extraction, refining, transport and distribution. Crude oil extraction is an energy-intensive process that involves

using large amounts of energy to drill, pump, and transport crude oil to refineries. This leads to the release of emissions of carbon dioxide (CO_2), methane (CH_4) and other pollutants into the atmosphere. Refining oil into final products, such as gasoline or diesel, is another energy-consuming process. Refineries operate on complex technologies that involve heating oil to high temperatures, which requires significant amounts of fossil fuels to generate thermal energy. Depending on the technological efficiency of the refinery, the process can generate considerable emissions of greenhouse gases, nitrogen oxides (NOx) and sulfur oxides (SOx). In addition, the transport of fuels from refineries to refuelling stations or ports contributes to indirect emissions, especially in the case of the use of diesel vehicles or maritime transport by fuel oil-fuelled ships. For alternative fuels, such as biofuels, indirect emissions are influenced by the process of growing the feedstock. Growing plants for biofuels requires the use of fertilizers, pesticides, and other agricultural inputs that generate emissions of nitrogen dioxide (N_2O), a greenhouse gas much more potent than CO_2. Also, the conversion of land for the production of biofuels can lead to the release of carbon stored in soil and vegetation, negating the ecological benefits of their use.

Air transport has a particularity in terms of fuels, as kerosene used for aviation is produced through more intensive processes than those required for gasoline or diesel used on the ground. At the same time, supporting infrastructure, such as airports and distribution networks, adds to indirect emissions. On the other hand, vehicle production contributes significantly to indirect emissions associated with transport, in particular in the case of road and rail transport. The manufacture of a vehicle involves a high consumption of natural resources, energy and materials. The main materials used in vehicle construction – such as steel, aluminium, plastic, copper and electronic components – involve highly polluting extraction and processing processes. For example, the production of steel, an essential material for chassis and vehicle structure, requires coal to be burned for energy, which generates large amounts of CO_2. In the case of electric vehicles, although they do not emit pollutants during use, the manufacture of batteries is an important source of indirect emissions. Lithium-ion batteries used in electric vehicles are produced through complex processes involving the extraction and refining of rare metals, such as lithium, cobalt, and nickel. These processes are not only energy-intensive, but also involve environmental risks related to soil and water contamination. Also, recycling or disposing of used batteries can generate additional emissions and require careful management. In rail transport, indirect emissions mainly come from the production of locomotives, wagons and railway infrastructure, including rails, sleepers and stations. The production of steel rails, for example, is a highly energy-intensive process, and the installation and maintenance of infrastructure requires heavy machinery that runs on fossil fuels. However, compared to other modes of transport, rail transport has a lower impact in terms of indirect emissions per unit of transport, due to the longer lifespan of vehicles and infrastructure. In addition, maritime transport involves indirect emissions from shipbuilding, in particular due to their size and the materials used. A commercial vessel can weigh tens of thousands of tons and requires huge amounts of steel and other materials. Ship maintenance, which includes painting, repair and modernisation, also contributes to indirect emissions. Another important aspect is the life cycle of vehicles and infrastructure. From the extraction of raw materials to recycling or disposal,

each stage involves emissions of pollutants. For example, recycling end-of-life vehicles or demolishing old infrastructure can release pollutants into the air and soil, and the management of the resulting waste is often inadequate in many regions. In conclusion, indirect emissions from fuel and vehicle production are an important component of the carbon footprint of the transport sector. These emissions underline the need for a holistic approach in assessing the environmental impact of different modes of transport. Investing in cleaner technologies, using recyclable materials and optimising production processes are essential solutions to reduce these emissions and transition to a more sustainable transport system.

Life cycle assessment of electric vehicles

Electric vehicles are an essential component of the transition to a sustainable transport system, and are often promoted as a key solution for reducing greenhouse gas emissions and air pollution. However, to fully understand the environmental impact of these vehicles, it is necessary to look at their complete life cycle, from raw material extraction and production to use and disposal. The life cycle of an electric vehicle comprises several distinct stages, each with specific contributions to the total carbon footprint and resource consumption. The production of batteries, for example, is one of the most critical stages, due to the intensive use of rare metals such as lithium, cobalt and nickel, but also the energy required to process them. During use, electric vehicles are significantly more efficient than those with internal combustion engines, having no direct emissions of pollutants, but this benefit depends on the source of electricity used to power them. In the final stage of the life cycle, recycling or disposing of components, especially batteries, presents both technological challenges and opportunities for reducing environmental impact. Thus, the life cycle analysis of electric vehicles not only allows an objective assessment of their benefits and limitations, but also provides a solid basis for the development of more sustainable strategies in the field of electric mobility [106-109]. The production of lithium-ion batteries used in electric vehicles is one of the most complex and critical stages of the life cycle of these vehicles, with a significant impact on the environment. This stage involves extraction, refining and manufacturing processes that require large amounts of natural resources, energy and advanced technologies, contributing to the total ecological footprint of electric vehicles. First of all, the extraction of raw materials, such as lithium, cobalt and nickel, is an environmentally and socially intensive process. Lithium is mainly obtained from salt mattresses (e.g., Salar de Uyuni in Bolivia [110]) or by mining minerals, both of which have environmental implications. In extraction regions, high water consumption is a major problem; For example, to extract one ton of lithium, up to 500,000 liters of water can be needed. This puts pressure on freshwater resources, affecting local communities and ecosystems [111-114]. In addition, cobalt, used to stabilize the chemical structure of batteries, is obtained in significant proportion from the Democratic Republic of Congo, where mining brings ethical challenges, including the use of unskilled labor and exposure to hazardous conditions. Another important factor is the energy required for refining and processing raw materials [115]. These processes involve high temperatures and energy-consuming technologies. For example, nickel, another essential component of batteries, requires complex extraction processes from sulfidic or laterite ores, which generate significant amounts of carbon

dioxide (CO_2) emissions [116]. Estimates show that the production of batteries for an electric vehicle can generate between 61 and 106 kilograms of CO_2 per kWh of battery capacity, depending on the energy source used and the efficiency of industrial processes [117-118]. The actual manufacture of batteries involves the use of advanced equipment and significant electricity consumption, especially for the assembly of battery cells and modules. If the energy used in these processes comes from fossil sources, such as coal or natural gas, the environmental impact increases exponentially. Conversely, integrating renewable energy sources such as solar or wind energy into production processes could significantly reduce associated emissions. Moreover, the size of the batteries directly influences the environmental impact. Larger batteries, used to extend the range of electric vehicles, require larger amounts of raw materials and energy for production. For example, a 100 kWh battery for an electric SUV has a considerably larger carbon footprint than a 40 kWh battery used for a compact vehicle. This underlines the importance of optimising battery design to strike a balance between performance and environmental impact. Another critical aspect of battery production is the management of the resulting waste [118]. Production involves the use of toxic chemicals, which require proper disposal to prevent soil and water contamination. In addition, the lack of efficient recycling infrastructure for lithium-ion batteries poses a significant challenge. Although recycling could reduce the need for raw material extraction and limit pollution, current recycling processes are costly and technologically limited, which prevents the efficient reuse of valuable materials. In conclusion, the production of batteries for electric vehicles is an essential and at the same time challenging stage in their life cycle. The impact of this stage on the environment is influenced by the source of raw materials, the efficiency of industrial processes and the energy sources used. Reducing this impact requires investment in more sustainable technologies, the adoption of renewable energy sources and improved recycling processes. Only through an integrated approach, which takes all these aspects into account, can a real transition to sustainable electric transport be ensured [114]. Unlike vehicles with internal combustion engines, electric vehicles do not emit exhaust gases during use, making them an environmentally friendly alternative in crowded urban areas and helping to improve air quality. However, in order to assess the full environmental impact of these vehicles, it is essential to look at their energy efficiency and consider the energy source used to charge the batteries. This increased efficiency reduces the total energy demand for the same number of kilometers traveled and, implicitly, contributes to the reduction of emissions associated with the energy chain. However, the benefits offered by electric vehicles are closely related to the source of electricity used to charge them. In countries or regions where the energy mix is dominated by fossil fuels such as coal and natural gas, the carbon footprint of electric vehicles can be significantly higher than if the energy comes from renewable sources. For example, in China, where coal makes up a large part of the energy mix, an electric vehicle can generate indirect CO_2 emissions comparable to those of a combustion engine vehicle [119-120]. On the other hand, in countries such as Norway, where electricity is produced almost exclusively from hydropower sources, indirect emissions associated with electric vehicles are almost non-existent. It highlights the importance of decarbonising the energy sector as a complementary element to maximise the benefits of electric vehicles. Another relevant factor is the efficiency of charging infrastructure and its integration into smart

grids. Fast charging stations consume more energy compared to slow charging, which can influence the total energy footprint of the vehicle. At the same time, the use of vehicle-to-grid technologies can help stabilise electricity grids and reduce peak demand, increasing the sustainability of electric vehicle use. During use, electric vehicles also contribute to the reduction of noise pollution, thanks to the silent operation of electric motors, which is particularly beneficial in the urban environment. However, it is important to note that the transition to electric mobility must be accompanied by measures that include the efficient recycling of batteries and the integration of renewable energy sources to reduce the overall environmental impact [121-122]. Recycling and proper management of electric vehicle components, especially lithium-ion batteries, is a key aspect of reducing their impact on the environment. While electric vehicles offer numerous benefits in terms of reducing direct emissions of pollutants, their components pose significant challenges at the end-of-life stage, but also offer important opportunities for the development of sustainable practices. Lithium-ion batteries used in electric vehicles are complex structures, made up of critical metals such as lithium, cobalt, nickel, manganese, and aluminum, etc. The extraction of these materials is an energy-intensive process, and their end-of-life management is crucial to avoid resource losses and negative environmental impacts. Recycling these components provides an opportunity to reduce demand for mining and primary extraction, thereby helping to reduce the environmental footprint of electric vehicles. The technological challenges associated with battery recycling are considerable. First of all, the process of dismantling batteries is complex and requires advanced technologies. Each manufacturer uses a unique battery design, which makes it difficult to standardize the recycling process. Also, the separation of component materials (cathode, anode, electrolytes and other materials) requires high-precision technologies such as hydrometallurgical [123] or pyrometallurgical recycling [124-125]. Although both methods are used on an industrial scale, they are energy-intensive. For example, pyrometallurgical recycling involves extremely high temperatures for metal extraction, resulting in significant CO_2 emissions. Another critical aspect is the lack of a developed global infrastructure for the collection and recycling of lithium-ion batteries. Currently, the worldwide recycling rate is below 10%, which means that most used batteries are stored, disposed of inappropriately, or sent to landfills, where they can release toxic substances into the soil and water. This underlines the urgent need to develop a robust recycling infrastructure, alongside policies that promote efficient battery collection. On the other hand, the opportunities associated with battery recycling are significant. Efficient recycling of critical materials can help reduce reliance on primary mining and ensure a sustainable supply for future generations of batteries. For example, advanced recycling processes can enable the recovery of more than 90% of cobalt and nickel from batteries, two of the most valuable metals used in these devices. In addition, recent research in the field of recycling supports the development of more environmentally friendly methods, such as direct recycling, which allows the reuse of active materials without the need for intensive chemical processing. Another major opportunity lies in the use of end-of-life batteries in secondary applications. Batteries that are no longer suitable for vehicles can be refurbished and used in energy storage systems for buildings or power grids. This practice extends the life of batteries and reduces the demand for the production of new batteries, thus

contributing to the transition to a circular economy. As for other components of electric vehicles, recycling materials such as aluminium, copper and plastics is essential for reducing resource consumption and associated emissions. Aluminum, for example, can be recycled entirely without significant loss of quality, and the recycling process consumes only 5% of the energy required for primary production. In the case of copper, recycling contributes to reducing the environmental impact associated with mining, including greenhouse gas emissions and the destruction of natural habitats. In conclusion, recycling and disposing of electric vehicle components, especially batteries, is both a technological challenge and an important opportunity to reduce environmental impact. The development of advanced recycling technologies, the creation of an efficient global infrastructure and the adoption of supportive policies are essential to ensure the sustainability of this growing industry. In parallel, promoting the circular economy and reusing batteries in secondary applications can significantly contribute to reducing resource consumption and associated emissions.

4.3. Conclusions on climate mitigation and electric vehicles

Electric vehicles are a key element in global climate change mitigation strategies, due to their potential to reduce greenhouse gas emissions and contribute to the transition to a sustainable transport system. The lack of direct emissions of pollutants during use makes electric vehicles a viable solution for combating urban pollution and improving air quality, which has a positive impact on both the environment and public health. However, the benefits of electric vehicles depend significantly on the energy source used to charge them. In a context where the global energy mix is still dominated by fossil fuels, the carbon footprint of electric vehicles may be larger than in scenarios where the energy comes from renewable sources. This highlights the urgent need to accelerate the decarbonisation of the energy sector by expanding the use of wind, solar, hydro and nuclear energy, in parallel with the promotion of sustainable charging infrastructure. At the same time, more attention needs to be paid to the lifecycle stages of electric vehicles that generate indirect emissions, such as battery production. The process of extracting and processing critical metals such as lithium, cobalt and nickel is extremely energy-intensive and has serious environmental implications. Therefore, the development of efficient recycling technologies and the implementation of the circular economy are fundamental to reducing the environmental impact of electric vehicles in the long term. At the same time, the integration of electric vehicles into smart grids and the adoption of vehicle-to-grid technologies can contribute to the stability of electricity grids and the optimal use of energy, which amplifies their environmental advantages. From a climate change perspective, the adoption of electric vehicles on a large scale is a significant step towards achieving the emission reduction targets set by the Paris Agreement. However, the transition to electric mobility must be accompanied by integrated policies that support research and development of advanced technologies, encourage the use of renewable sources and promote public awareness of the benefits of electric vehicles. In this way, electric vehicles can become not only a sustainable means of transport, but also a central pillar of global efforts to mitigate climate change, contributing to the creation of a cleaner and more environmentally resilient future.

Chapter 5: Advanced modeling and simulation techniques for electric and hybrid vehicle powertrains

5.1. Introduction

The complexity of hybrid electric vehicle (HEV) powertrains, arising from the integration of electric components such as energy storage systems, power electronics, and electric machines into traditional mechanical systems, requires a multidisciplinary approach to analysis and design.[126-128] Unlike conventional vehicles, HEVs present a vast design space with numerous interdependent parameters, making prototyping costly and inefficient. Consequently, computer modelling and simulation tools have become essential for exploring system behaviour and optimizing configurations. While conventional vehicle development benefits from extensive prior knowledge and validated models, HEV development often begins with limited information, necessitating flexible, iterative design strategies. Multiple simulation models are typically created for performance, control, and optimization tasks, which introduces challenges in model management and maintenance. As HEV systems grow in complexity, traditional modelling methods struggle to keep pace, highlighting the need for scalable and adaptable modelling frameworks.

5.2. EV and HEV modeling

The complete powertrain model (Figure 5.1) integrates key subsystems such as the driver input, control unit, battery, inverter, electric motor, transmission, and for HEVs/PHEVs, an ICE and fuel tank. Accurate simulation requires a multidisciplinary approach that captures energy flow, control logic, and mechanical interaction. Two main modeling strategies are used: equation-based models for high accuracy, and map-based models for faster computation. An object-oriented, causal modeling framework allows modular development by treating each subsystem independently with equations or lookup tables. These modules exchange data via input-output variables, enabling flexible configuration and scalable system modeling.

Two main system modeling approaches are commonly used: the quasi-static (reverse) approach and the dynamic (forward) approach. As shown in Figure 5.2, the quasi-static method begins with the desired vehicle behavior (e.g., speed and acceleration) and solves backward through each subsystem to determine energy demand, culminating at the battery. It is algebraically simpler, less computationally intensive, and unidirectional in information flow. However, it lacks accuracy in capturing physical constraints and real-time interactions between components.

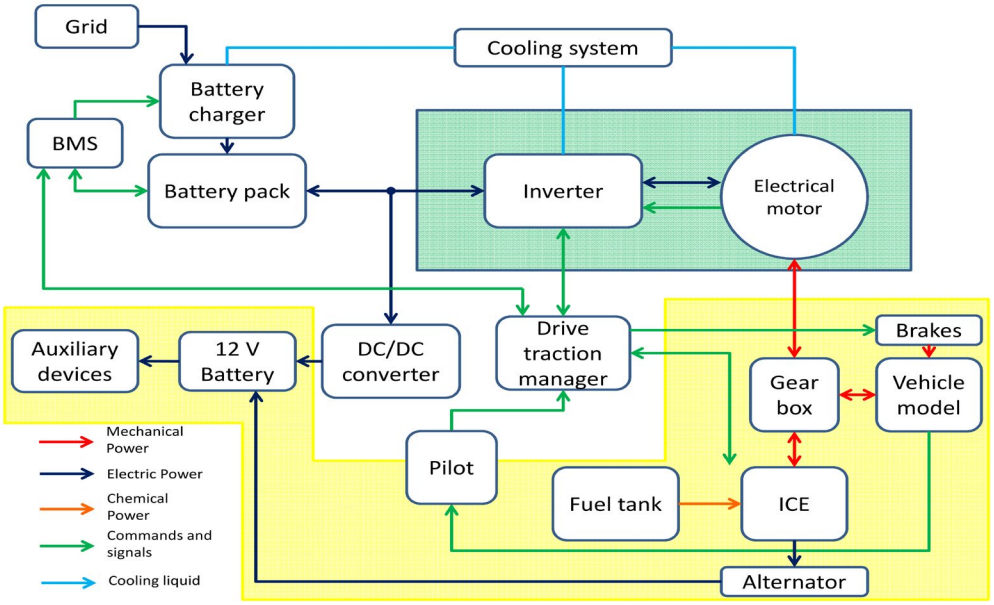

Figure 5.1. Block diagram of a Plug-In HEV [128]

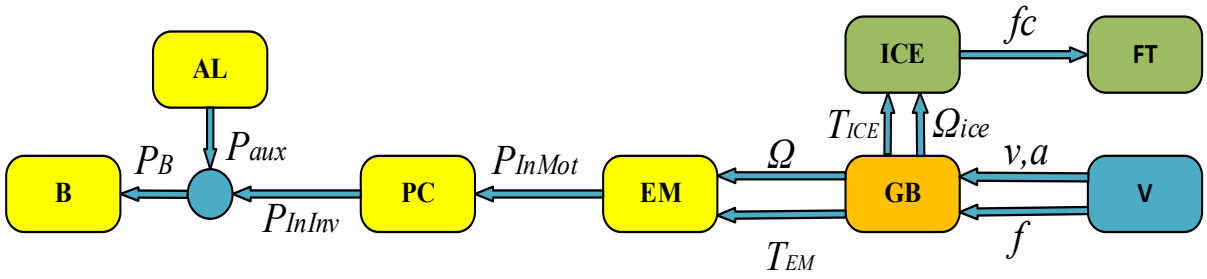

Figure 5.2. Example of HEV quasi-static modeling approach

Where: *V*-is the vehicle model, *GB*-the gear box, *PC*-the power converter, *B*-the battery pack, *FT*-the fuel tank, *AL*-is the auxiliary loads block, ***v*** and ***a***-are respectively the vehicle's speed and acceleration, ***f***-is the vehicle traction force, *W*-is the *EM* angular speed, *TICE* and *TEM* are respectively the *ICE* and the T_{EM} torques, Ω_{ICE} is the *ICE* angular speed, ***fc***-is the fuel consumption, *I* and *Vs* are the electrical motor current and voltage, i_{batt} and V_{batt} are the battery current and voltage, P_{InMot} is the power requested by the EM to the power converter, PB is the total power requested to the battery that is obtained as a sum of the power requested by the power converter P_{InInv} and the auxiliary loads Paux ($PB = PInInv + Paux$) and finally *iaux* is the amount of current requested to the battery for auxiliary electrical loads.

Unlike the static approach, the dynamic method (Figure 5.3) models the system sequentially, offering a more accurate view of energy flow and component behavior. Although more computationally intensive, it better captures operational limits. The next sections expand on this by combining equations and lookup tables to simulate HEV performance.

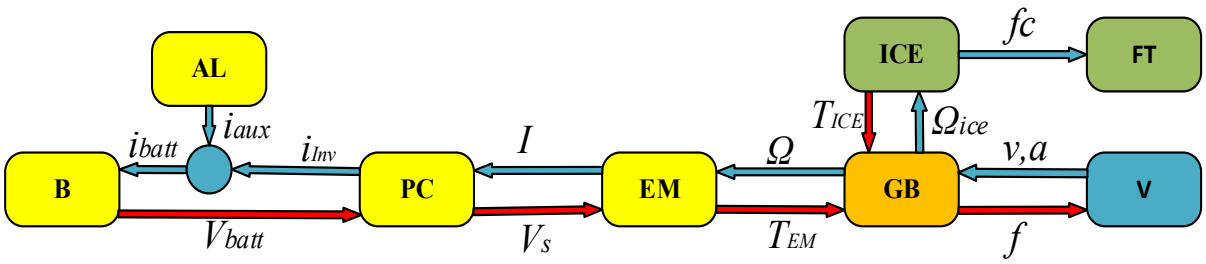

Figure 5.3. Example of HEV-dynamic modeling approach

5.2.1. Battery modeling

In order to correctly simulate the behavior of a EV, HEV or PHEV it is important to set up a battery model that evaluate the output voltage considering the State Of Charge (SOC) of the battery itself. Since a battery pack is obtained by a series connection of many cells (n_{cell}), it is quite usual to construct a numerical model considering one single cell. The total battery voltage V_{batt} is obtained using equation (5.1) assuming that all cells have an uniform behavior and where v_{el} is the voltage of a single cell.

$$V_{batt} = n_{cell} \cdot v_{el} \tag{5.1}$$

The battery model receives as input variables: the current i_{batt} required from the electrical drive model (inverter and electric motor) and the battery temperature ϑ computed by battery thermal model. The model gives as output variables: the battery pack voltage V_{batt}, the SOC and the power losses $P_{LossBatt}$. In order to simulate the battery behavior, instead of a complex electrochemical model, an Equivalent Circuit Model (ECM) can be chosen as a good compromise between accuracy and computational load. For example a first order Randles circuit (represented in Figure 5.4) can be adopted as dynamic model; this model can be easily downgraded imposing R_1=0 in order to obtain a static model. The circuit parameters can be deduced by experimental test or technical literature using the method described in [130].

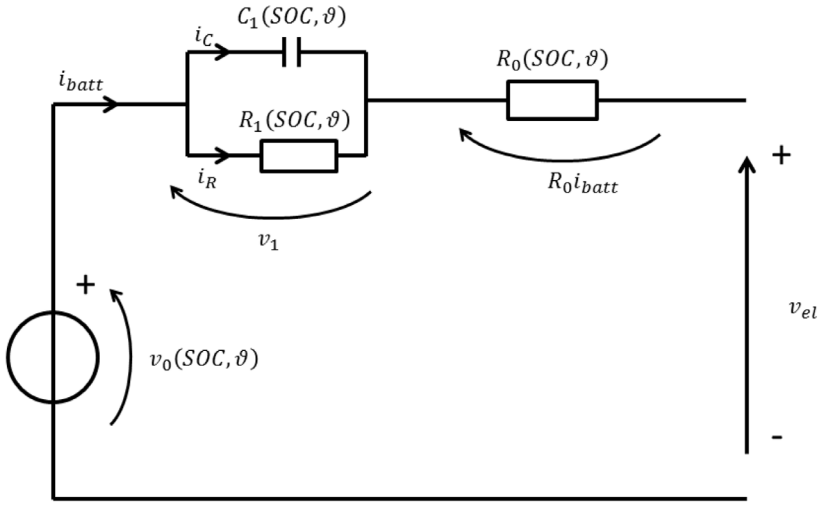

Figure 5.4. Randles electrodynamical model of a cell

Furthermore it is fundamental to calculate the battery SOC using equation (5.2) (where *Cn* is the rated capacity expressed in Ampere-Hours [Ah] and SOC_0 is the initial state of charge) to evaluate the amount of energy stored into the battery pack.

$$SOC(t) = SOC_0 - \int_0^t \frac{i_{batt}(t)}{3600 \cdot C_n} dt \tag{5.2}$$

Static model of battery

Using the manufacturer charge and discharge charts and the data available for different temperature, it is possible to reconstruct the map of *v0*(SOC, *U*) and of R0(SOC, *U*) and consequently to calculate v_{el} (SOC, *U*) as reported in the static equation (5.3).

$$v_{el}(SOC, \vartheta) = v_0(SOC, \vartheta) - R_0(SOC, \vartheta) i_{batt} \tag{5.3}$$

Dynamical model of battery

Due to the highly dynamic load conditions in traction applications, static battery models are insufficient for scenarios requiring accurate transient behavior, such as control analysis. Dynamic models based on Equivalent Circuit Models (ECMs) with RC elements and parasitic branches enable simulation of voltage response and self-discharge. While complex ECMs may involve multiple RC networks, a single RC model, as shown in Figure 5.4, is often sufficient for vehicle-level analysis. Accurate simulation requires fine tuning of ECM parameters. A robust identification procedure, accounting for thermal effects, is detailed in [130].

It possible to solve the circuit considering the cell voltage v_{el}, as reported in equation (5.4), where the splitting of the total current *ibatt* into the capacitor C1 and into the resistor *R1* is considered ad reported in equation (5) and the no load voltage *v0* is SOC dependant.

$$v_{el} = v_0 - R_0 i_{batt} - v_1 \tag{5.4}$$

$$\begin{cases} i_{\text{batt}} = i_c + i_r \\ i_c = C_1 \dfrac{dv_1}{dt} \\ i_r = \dfrac{v_1}{R_1} \end{cases} \tag{5.5}$$

Finally, substituting *ibatt* obtained from equation (5.5) in equation (5.4), is possible to obtain the final dynamic equation of the cell voltage, as reported in equation (5.6).

$$\frac{dv_1}{dt} = \frac{1}{R_0 C_1}\left(v_0(\text{SOC}) - v_{\text{el}} - v_0(\text{SOC})\left(1 + \frac{R_0}{R_1}\right)\right) \tag{5.6}$$

5.3. Inverter modeling

Power converter losses can be estimated using various methods found in the literature [129, 130]. A simplified approach models the converter as an equivalent resistance, with losses proportional to the square of the RMS current. For typical three-phase inverters, losses are expressed as shown in equation (5.7), where R_{Inv} is the inverter equivalent resistance and I is the Root Mean Square (RMS) inverter output phase current (that corresponds to the EM phase input RMS current).

$$P_{\text{LossInv}} = 3 \cdot R_{\text{Inv}} \cdot I^2 \tag{5.7}$$

The inverter input power can be calculated adding the inverter losses $P_{LossInv}$ to the motor input power P_{InMot} that correspond to the inverter output power P_{OutInv} (equation (5.8).

$$P_{InInv} = P_{LossInv} + P_{InMot} = P_{LossInv} + P_{OutInv} \tag{5.8}$$

A more detailed approach can be described if the simulation model adopted includes the control and inverter modulator details: an instant circuit losses model can be also implemented [130]. The losses are computed considering the basic inverter cell composed of an Insulated Gate Bipolar Transistor (IGBT) and a diode. The inverter is formed by six basic cells divided into 3 arms as reported in Figure 5.5.

The instantaneous losses of a basic cell p_{cell} can be evaluated using equation (5.9) where: p_{swT} are transistor switching losses, E_{on} and E_{off} are turn-on and turn off energy, fs is the inverter switching frequency, E_{recD} and p_{recD} are the recovery diode energy and power losses, v_{ce} and v_{ak} are respectively the transistor and diode forward voltage drop, i_c and i_f are the transistor and diode direct current ad p_{fwT} and p_{fwD} are transistor and diode conduction forward losses. The total inverter instantaneous losses are reported in (5.10).

These curves can be simplified as shown in equation (5.11) where all the parameters (A_{fwT}, B_{fwT}, A_{fwD}, B_{fwD}, B_{onT}, C_{onT}, B_{offT}, C_{offT}, B_{recD}, C_{recD}) can be deduced from the semiconductor device technical data sheet. Equation (5.12) can be obtained substituting equation (5.11) into the (5.10). These equations express the instantaneous losses p_{inv} as a function of semiconductor devices current [129].

$$\begin{cases} p_{fwT} = v_{ce}(i_c) \cdot i_c \\ p_{fwD} = v_{ak}(i_f) \cdot i_f \\ p_{swT} = \left[E_{on}(i_c) + E_{off}(i_c) \right] f_s \\ p_{recD} = E_{recD}(i_d) \cdot f_s \\ p_{cell} = p_{swT} + p_{recD} + p_{fwT} + p_{fwD} \end{cases} \tag{5.9}$$

$$p_{\text{inv}} = 6 \cdot p_{\text{cell}} \tag{5.10}$$

$$\begin{cases} v_{ce}(i_c) & = A_{fwT} + B_{fwT} i_c \\ v_{ak}(i_f) & = A_{fwD} + B_{fwD} i_f \\ E_{onT}(i_c) & = B_{onT} i_c + C_{onT} i_c^2 \\ E_{offT}(i_c) & = B_{offT} i_c + C_{offT} i_c^2 \\ E_{recD}(i_f) & = B_{recD} i_f + C_{recD} i_f^2 \end{cases} \tag{5.11}$$

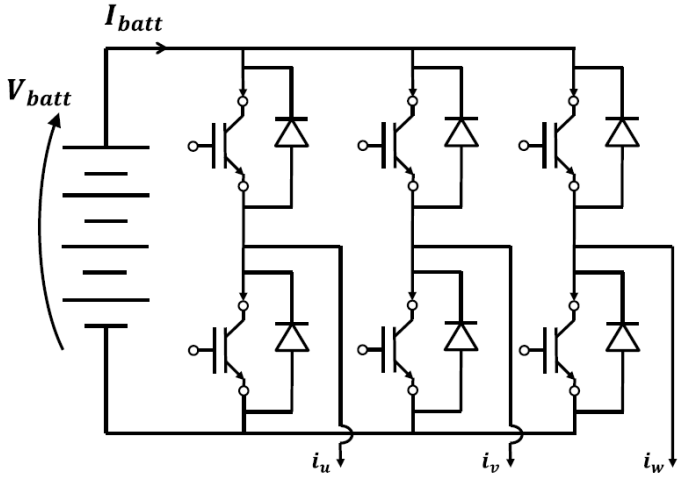

Figure 5.5. Battery fed three phase inverter [127]

$$\begin{cases} p_{fwT}(i_c) & = A_{fwT} i_c + B_{fwT} i_c^2 \\ p_{fwD}(i_f) & = A_{fwD} i_f + B_{fwD} i_f^2 \\ p_{swT}(i_c) & = (B_{onT} i_c + C_{onT} i_c^2) f_s + (B_{offT} i_c + C_{offT} i_c^2) f_s \\ p_{recD}(i_f) & = (B_{recD} i_f + C_{recD} i_f^2) f_s \end{cases} \tag{5.12}$$

Evaluating instantaneous inverter losses, as in equation (5.10), requires high-resolution current data and short simulation time steps, resulting in significant computational effort. However, for EV and HEV powertrain modeling, such precision is unnecessary. Instead, an average-loss approach over one AC period is sufficient. By using RMS values of voltage and current, accurate energy loss estimation can be achieved with longer time steps, reducing simulation time. This method assumes sinusoidal current behavior, as described in equation (5.13), and is suitable for energy and power flow analysis at the vehicle level.

where: I_M is the maximum current value, $w=2\pi/T$ is the current angular frequency and φ is the phase angle between motor voltage and current, substituting the (5.13) into equation (5.12) and assuming that $i=i_c=i_f$, the instantaneous inverter losses with explicit time dependence can be obtained. Averaging the losses on an Alternating Current (AC) variables period T is possible to obtain the losses mean value [127,132]. The average relationships are obtained as reported in equation (5.14) where: Ts is the IGBT switching period, T_{dead} is the dead time between high and low side IGBT switch on operation and $cos\varphi$ is the motor power factor. The total PWM operation cell average losses P_{PWM} are the all terms sum, while the total averaged inverter losses P_{invPWM} are reported in equation (5.15).

$$i(t) = I_M \cos(\omega t - \phi) \tag{5.13}$$

$$\begin{cases} P_{fwT} & = \left(\frac{1}{2} - \frac{T_{dead}}{T_s}\right)\left(\frac{A_{fwT}}{\pi} I_M + \frac{B_{fwT}}{4} I_M^2\right) + m\cos\varphi\left(\frac{A_{fwT}}{8} I_M + \frac{B_{fwT}}{3\pi} I_M^2\right) \\ P_{fwD} & = \left(\frac{1}{2} - \frac{T_{dead}}{T_s}\right)\left(\frac{A_{fwD}}{\pi} I_M + \frac{B_{fwD}}{4} I_M^2\right) - m\cos\varphi\left(\frac{A_{fwD}}{8} I_M + \frac{B_{fwD}}{3\pi} I_M^2\right) \\ P_{onT} & = f_s I_M \left(\frac{B_{onT}}{\pi} + \frac{C_{onT}}{4} I_M\right) \\ P_{offT} & = f_s I_M \left(\frac{B_{offT}}{\pi} + \frac{C_{offT}}{4} I_M\right) \\ P_{recD} & = f_s I_M \left(\frac{B_{recD}}{\pi} + \frac{C_{recD}}{4} I_M\right) \\ P_{PWM} & = P_{onT} + P_{offT} + P_{fwT} + P_{fwD} + P_{recD} \end{cases} \tag{5.14}$$

$$P_{invPWM} = 6 \cdot P_{PWM} \tag{5.15}$$

Since the inverter sub-model receives as input *Vs, I, cosφ* and *w*, previously evaluated by the electric motor model, and V_{batt} (the available battery voltage) it can calculate the current required to the battery i_{inv} and the total inverter losses P_{PWM}. The sequence of equations to be solved is reported as follows:

- total power supplied to the motor calculation: $P_{InMot} = \sqrt{3} Vs\ I\cos\varphi$;
- inverter AC phase current max. value calculation: $I_M = \sqrt{2} I$;
- inverter PWM amplitude modulation index calculation: $m = \sqrt{V_s / V_{batt}}$;
- total inverter averaged losses P_{invPWM} calculation by means of equation (5.14) and (5.15);
- total inverter input power calculation: $P_{InInv} = P_{InMot} + P_{invPWM}$;
- inverter input current calculation: $i_{inv} = P_{InInv} / V_{batt}$.

5.4. Electrical motor modeling

The most adopted motors for FEV and HEV are ***AC induction motors*** and ***AC Permanent Synchronous Magnets Motor*** (PMSM) regulated by means of a field oriented control or direct torque control. In this section the models of both motors will be presented using a phase vector approach [126-128] and considering the motor field oriented controlled. For both motor models it is possible to define the input and output variables as follows:

- **input:** required torque T_{ref}, instantaneous rotating mechanical speed *W*, battery voltage V_{batt};
- **output:** torque T_{EM}, RMS phase current *I*, line to line voltage *Vs*, power factor angle φ, total losses $P_{LossMot}$, Motor input (P_{InMot}) and output power (*Pm*), electrical frequency *f* and angular frequency $w = 2\pi f$.

For FEV and HEV power train modeling and simulation a complete motor model including the detailed electromechanical dynamic is not required; it is better to use a steady state model that consider the controlled motor including all the energetic phenomena (power losses calculation).

The proposed model include also limits and constrains due to the motor power supplier, which is based on batteries and inverter, such as maximum deliverable voltage, power and current.

5.4.1. Induction motor

For the induction motor the steady state equations [126, 127] are reported in equation (5.16) where $\underline{Vs}$, $\underline{Is}$ and $\underline{\Psi}_r$ are respectively stator voltage, stator current and rotor flux phasors, *Rs, Rr, M, Lk* are respectively stator resistance, rotor resistance, mutual inductance and total leakage inductance, *n*-is the pole pairs number, T_{EM}-is the torque, $\underline{Im}$-is the magnetizing current phasor, *Ir*-is rotor or torque current phasor, *ω*-is the mechanical angular speed, *x*-is the relative rotor slip speed, ω-is the AC variable angular frequency and *j*-the imaginary unit.

Equation (5.16) can be represented by means of the equivalent circuit reported in Figure 5.6.

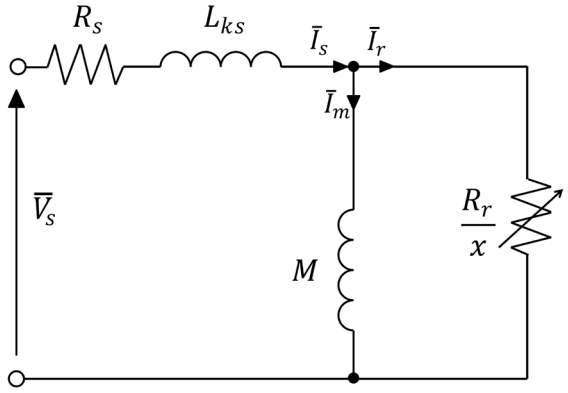

Figure 5.6. Induction motor steady-state equivalent circuit [126]

The three phase motor is modeled using a “rational” approach that correspond to have a “single phase‘equivalent” model also for energetic relations and torque expression. In fact the amplitude of current phasor $\underline{Is}$ and the stator voltage phasor $\underline{Vs}$ are related to the RMS phase current *I* and voltage *V* by means of equation (5.17). The induction motor model includes also equation (5.18) where *Ψrn* is the induction motor rated flux, w_n-is the rated motor angular frequency, P_{Cu} and P_{Fe} represent respectively the copper and iron losses and Q_{InMot} is the motor reactive input power. Equation (5.18) allows to calculate all the power terms and stator quantities to be used as inputs for inverter and battery model.

$$\begin{cases} \bar{V}_s = R_s \bar{I}_s + j\omega L_{ks} \bar{I}_s + j\omega M \bar{I}_m \\ 0 = -\dfrac{R_r}{x} \cdot \bar{I}_r + j\omega M \bar{I}_m \\ \bar{I}_s = \bar{I}_r + \bar{I}_m \\ \bar{\psi}_r = M \bar{I}_m \\ x = \dfrac{\omega - n\Omega}{\omega} \\ T = nMI_m I_r = n\psi_r I_r \end{cases} \tag{5.16}$$

$$\{V_s = V \cdot \sqrt{3} I_s = I \cdot \sqrt{3} \tag{5.17}$$

$$\begin{cases} P_{Cu} = R_s I_s^2 + R_r I_r^2 \\ P_{Fe} = P_{Fen} \dfrac{\omega}{\omega_n} \dfrac{\psi_r^2}{\psi_{r_n}^2} \\ P_{LossMot} = P_{Cu} + P_{Fe} \\ P_m = T\Omega \\ P_{InMot} = P_{LossMot} + P_m \\ Q_{InMot} = \omega M I_m^2 + \omega L_{kS} I_s^2 \\ \varphi = \arctan\left(\dfrac{Q_{InMot}}{P_{InMot}} \right) \end{cases} \tag{5.18}$$

Equations (5.16) and (5.18) have to be solved together with equation (5.19) that define the rotor flux value as function of the rotating speed Ω and of the rated speed Ωn. Equation (5.19) represents the field weakening condition for the induction motor. Furthermore it is also necessary to control that the torque request T_{ref} does not exceed the maximum motor torque T_{refMax} and the consequent power request ($T_{ref} \cdot \Omega$) does not exceed the motor power limit P_{motMax} (see equation (5.20)).

$$\begin{cases} \psi_r = \psi_{rn} & \text{if} \quad \Omega < \Omega_n \\ \psi_r = \psi_{rn} \dfrac{\Omega_n}{\Omega} & \text{if} \quad \Omega > \Omega_n \end{cases} \tag{5.19}$$

$$\begin{cases} T_{ref} = T_{refMax} & \text{if } T_{ref} > T_{refMax} \\ T_{ref} = \dfrac{P_{motMax}}{\Omega} & \text{if } T_{ref} \cdot \Omega > P_{motMax} \end{cases} \tag{5.20}$$

Moreover the global electrical drive limits verification has to be taken into account in order to avoid that the requested operating point do not correspond to an allowed condition. The three conditions to consider are:

– maximum RMS input current I_{max} that is related to the inverter current limit (as reported in equation (5.21));

- maximum motor voltage limit V_{sMax} that correspond to the maximum deliverable inverter voltage for a given battery voltage (as reported in equation (5.22));
- the maximum motor input power limit P_{inMax} that is related to the maximum battery deliverable power (as reported in equation (5.23)).

These conditions have to be verified and imposed after the calculation of equations (5.20), (5.19), (5.16) and (5.18).

$$\begin{cases} I = \frac{I_s}{\sqrt{3}} < I_{max} \end{cases} \tag{5.21}$$

$$V_s < V_{sMax} \text{ then } V_{sMax} = \frac{V_{batt}}{\sqrt{2}} \tag{5.22}$$

$$P_{InMot} < P_{inMax} \tag{5.23}$$

The proposed model can be used for off-line map calculation, that can be included in the simulation model, or calculated directly on-line during the numerical simulation process. The calculus procedure for induction motor can be summarized as follows:

- verify if the torque request *Tref* is compliant with absolute motor torque and power limit otherwise saturate *Tref* using the (5.20);
- solve the field weakening conditions (5.19);
- solve the (5.16), (5.18) using as input variables $T_{EM}=T_{ref}$ and Ω;
- verify the (5.21), (5.22) and (5.23), in order to impose the motor, inverter and battery limitations;
- if the condition (5.21) is not respected reduce *Tref*, go back to step 3 and iterate;
- if the condition (5.22) is not respected reduce Ψr, go back to step 3 and iterate;
- if the condition (5.23) is not respected reduce *Tref* , go back to step 3 and iterate.

5.4.2. Permanent magnets synchronous brushless motor

For the Permanent Synchronous Magnets Motor the steady state equation [126, 127] are reported in equation (5.24) where: *Vd* and *Vq* are the stator voltage phasor $\underline{Vs}$ components ($\underline{Vs} = Vd + jVq$), *Id* and *Iq* are the stator current phasor *Is* components ($\underline{Is}=Id + jIq$), *Rs*-is the stator resistance, *Ls*-is the stator synchronous inductance, Ψm-is the permanent magnet flux phasor. The other symbols, T_{EM}, *W*, ω and *n* assume the same meaning that ones indicated in the induction motor description.

Equation (5.24) has to be solved, also in this case, together with equations (5.25) and (5.26). Similarly to the induction motor a pre-process operation on torque request Tre f has to be implemented in order to impose the respect of torque and power motor limit. Furthermore the

field weakening condition have to be imposed to the motor. It consists in setting the correct value of Id current [126] by means of equation (5.27). In fact the current Id can be maintained equal to zero in the constant torque/flux region and has to be imposed negative in the field weakening zone. Finally also the limit input conditions have to be taken into account using the same equations of the induction motor ((5.21), (5.22) and (5.23)).

$$\begin{cases} V_d = R_s I_d - \omega L_s I_q \\ V_q = R_s I_q + \omega L_s I_d + \psi_m \omega \\ T_{EM} = n \psi_m I_q \\ \Omega = \dfrac{\omega}{n} \end{cases} \tag{5.24}$$

$$\begin{cases} P_{Cu} = R_s I_d^2 + R_s I_q^2 \\ P_{Fe} = P_{Fen} \dfrac{\omega}{\omega_n} \\ P_m = T_{EM} \Omega \\ P_{LossMot} = P_{Cu} + P_{Fe} \\ P_{InMot} = P_m + P_{LossMot} \end{cases} \tag{5.25}$$

$$\begin{cases} I_s = \sqrt{I_d^2 + I_q^2} \\ V_s = \sqrt{V_d^2 + V_q^2} \\ Q_{InMot} = V_q I_d - V_d I_q \\ \varphi = \operatorname{atan}\left(\dfrac{Q_{InMot}}{P_{InMot}} \right) \end{cases} \tag{5.26}$$

$$\begin{cases} \psi_r = \psi_m & \text{if} \quad \Omega < \Omega_n \\ \psi_r = \psi_m \dfrac{\Omega_n}{\Omega} & \text{if} \quad \Omega > \Omega_n \\ I_d = \dfrac{\psi_r - \psi_m}{L_s} \end{cases} \tag{5.27}$$

Also in this case the model can be used both for off-line map calculation and on-line numerical simulation process. The calculus procedure for PMSM can be summarized as follows:

- verify if the torque request *Tref* is compliant with absolute motor torque and power limit otherwise saturate *Tref* using equation (5.20);
- solve the field weakening conditions (equation (5.27));
- solve equations (5.24), (5.25) and (5.26) using as input $T_{EM} = T_{ref}$ and Ω;

- verify equations (5.21),(5.22) and (5.23), in order to impose the motor, inverter and battery limitation;
- if the condition (5.21) is not respected reduce T_{ref}, go back to step 3 and iterate;
- if the condition (5.22) is not respected reduce Ψs, go back to step 2 and iterate;
- if the condition (5.23) is not respected reduce T_{ref}, go back to step 3 and iterate.

The per unit efficiency η_{EM} can be calculated using equation (5.28).

$$\eta_{EM} = \frac{P_m}{P_{InMot}} \tag{5.28}$$

5.5. Vehicle dynamic modeling

In order to reconstruct the energetic power flow between FEV and HEV components a simple vehicle longitudinal dynamic model has to be considered. In this paragraph the model will be described considering the most general case constituted by an HEV; the model of a FEV can be simply deducted neglecting all the ICE contributions. This model receives as input the torque given by the ICE T_{ICE} and by the EM T_{EM} coming from the respective simulation models and the gear ratio of the mechanical gearbox coming from the pilot model and calculate the vehicle speed $v(t)$ and distance covered $s(t)$.

As first it is necessary to evaluate the total torque at the wheels Tw as sum of the EM torque reported at the wheel TEMw with the ICE torque reported at the wheel T_{ICEw}. For this all the reduction ratios and the efficiencies of the transmission chain have to be considered, as reported in equations (5.29) and (5.30), which are specialized for traction condition (5.29) and for braking condition (5.30). In these equations τ_{EM} and $\eta_{\tau EM}$ are respectively the reduction ratio of the EM and its efficiency, τ_{ICE} and $\eta_{\tau ICE}$ are respectively the reduction ratio of the ICE and its efficiency, τ_{diff} and η_{diff} are respectively the differential reduction ratio and its efficiency.

$$\begin{cases} T_{EMw} = T_{EM} \cdot \tau_{EM} \cdot \tau_{diff} \cdot \eta_{\tau EM} \cdot \eta_{diff} \\ T_{ICEw} = T_{ICE} \cdot \tau_{ICE} \cdot \tau_{diff} \cdot \eta_{\tau ICE} \cdot \eta_{diff} \end{cases} \tag{5.29}$$

$$\begin{cases} T_{EMw} = \dfrac{T_{EM} \cdot \tau_{EM} \cdot \tau_{diff}}{\eta_{\tau EM} \cdot \eta_{diff}} \\ T_{ICEw} = \dfrac{T_{ICE} \cdot \tau_{ICE} \cdot \tau_{diff}}{\eta_{\tau ICE} \cdot \eta_{diff}} \end{cases} \tag{5.30}$$

Usually for an HEV the ICE has a mechanical gearbox with 5 ÷ 7 fixed reduction ratios and the EM has an unique fixed reduction ration. For this reason the longitudinal dynamic model receive as input from the driver model the correct gear that has to be considered. In order to define the longitudinal equivalent dynamic equation it is also necessary to introduce all the resistance forces acting on the vehicle, as reported in equation (5.31), where:

- m-is the total mass of the vehicle,
- g-is the gravitational acceleration,
- f_v-is the rolling resistancecoefficient,
- ρ-is the air density,
- Cx-is the aerodynamic penetration coefficient,
- S-is the total frontal area of the vehicle ,
- a-is the slope of the road.

$$F_{res} = m \cdot g \cdot f_v + \frac{1}{2}\rho C_x S v(t)^2 + m \cdot g \cdot \sin\alpha \tag{5.31}$$

Finally it is possible to evaluate the vehicle acceleration a, as reported in equation (5.32), where rw-is the radius of the vehicle wheels, m*-represents the equivalent mass of the rotating part of the vehicle (wheels, rotor, shaft)[2].

$$\begin{cases} f = \dfrac{T_w}{r_w} \\ a = \dfrac{\dfrac{T_w}{r_w} - F_{res}}{(m + m^*)} \end{cases} \tag{5.32}$$

Using vehicle longitudinal acceleration a from equation (5.32), it is possible to obtain vehicle speed and position.

$$\begin{cases} v(t) = \int_0^t a(t)dt \\ s(t) = \int_0^t v(t)dt \end{cases} \tag{5.33}$$

Finally the EM and the ICE speed are obtained as described in equation (5.34).

$$\begin{cases} \Omega = \dfrac{v(t)\tau_{EM}\tau_{diff}}{r_w} \\ \Omega_{ICE} = \dfrac{v(t)\tau_{ICE}\tau_{diff}}{r_w} \end{cases} \tag{5.34}$$

As example the equivalent mass representing the EM inertia referred to the vehicle can be evaluated considering the following equation.

$$m^*_{EM} = \frac{J_{EM}\tau^2_{EM}\tau^2_{diff}}{r^2_w} \tag{5.35}$$

5.6. Auxiliary loads model

5.6.1. Auxiliary electrical loads

In order to correctly estimate the energy consumption on a FEV it is important to consider all the auxiliary electrical loads that the traction battery has to fed.

Particularly the low voltage loads (12V or 24V dc), represented for example by light, circulating pump, fan and control units, have to be estimated considering an adequate average value of power consumption during the trip. The energy for these loads is usually delivered by the traction battery through a DC/DC converter. The battery current i_{aux} can be calculated with equation (5.36) using the power consumption P_{aux} of electrical auxiliary loads, the battery voltage V_{batt} from the battery model and the efficiency of the DC/DC converter $\eta_{DC/DC}$.

$$i_{\text{aux}} = \frac{P_{\text{aux}}}{V_{\text{batt}}\eta_{\text{DC/DC}}} \tag{5.36}$$

5.6.2. Pumps

On HEVs and FEVs are usually installed liquid cooled electrical traction devices, in particular motor and inverter. For this reason auxiliary circulation pumps are needed in order to guarantee an adequate heat exchange between the components and the cooling fluid.

It is possible to estimate the hydraulic power P_{hy} required for the pump using equation (5.37), where ρ-is the fluid density, Q-the volumetric flow rate, g-the gravity constant, h-is the total head of the hydraulic circuit and h_l-is an equivalent of hydraulic losses expressed in meter of water column. Usually the term h_l , that is responsible of a pressure drop Δ_{pl} , is preponderant with respect to h and strictly depends from the design of the cooling circuit into the component.

$$P_{hy} = \rho Q_g \left(h + h_1\right) = \rho Q_g \left(h + \frac{\Delta p_l}{\rho g}\right) \tag{5.37}$$

At last, using a pump efficiency (η_{pump}) given by the manufacturer, it is possible to evaluate the electrical power requirement on the auxiliary load using equation (5.38).

$$P_{el} = \frac{P_{hy}}{\eta_{pump}} \tag{5.38}$$

5.7. Internal combustion engine modeling

Due to the complexity of accurately modeling the thermal combustion process, a **map-based ICE model** is used to estimate fuel consumption and efficiency over typical drive cycles. The model takes as input the torque request from the energy management system and the ICE speed

from the longitudinal dynamics. Outputs include the effective torque T_{ICE}, fuel consumption (**fc**), and CO_2 emissions. This simplified yet effective structure is well-suited for system-level simulations. The overall model layout is shown in Figure 5.7**.**

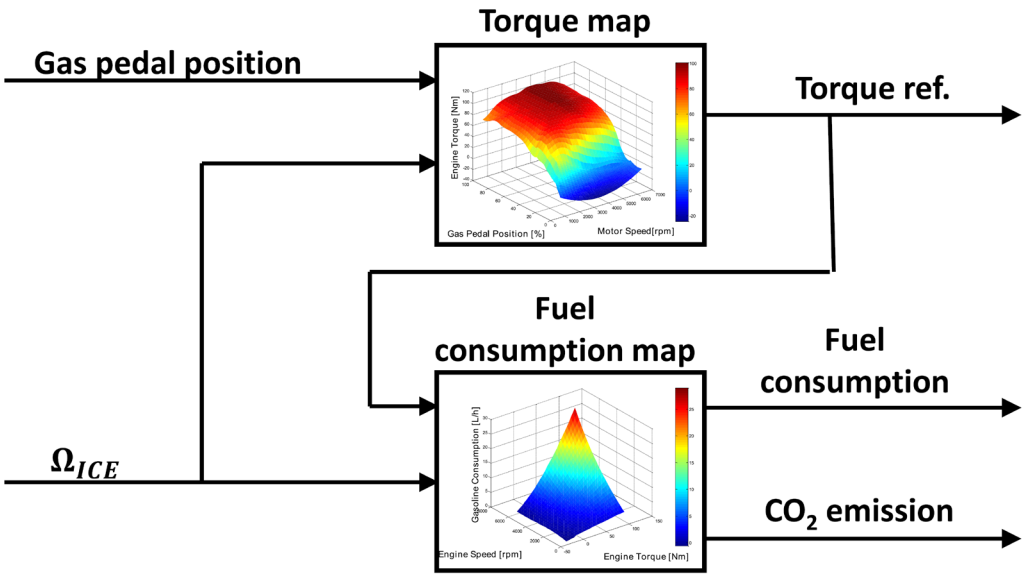

Figure 5.7. ICE model [128]

The maps inserted into the ICE block can be obtained directly from the engine manufacturer; otherwise they can be obtained through experimentally tests using an engine test bench or directly on the vehicle using the Controller Area Network (CAN) information.

For the volume L of fuel present in the tank equation (5.39) can be used, where *L0* represents the initial volume condition.

$$L = L_0 - \int_0^t f_c \, dt \tag{5.39}$$

Other approach for ICE modeling can be settled up using theoretical approaches as reported in [130-132].

Finally a rough estimation of the CO_2 emission can be established using equation (5.40), in which ρ_C is the average content of carbon in gasoline, M_{mCO2} is the molar mass of CO_2, M_{mC} is the carbon molar mass and φ is a coefficient for incomplete combustion.

$$CO_2 = f_c \cdot \rho_C \cdot \frac{M_{mCO_2}}{M_{mC}} \cdot \varphi \tag{5.40}$$

Chapter 6: ELECTRIC TRANSPORT POWER SOURCES

6.1. Introduction

Modern off-grid electric transport predominantly uses batteries as the energy storage. Alternatively, fuel cells can be used but nevertheless batteries will be used as energy buffer. In engineering, one time use batteries are in primary battery group while secondary batteries are rechargeable ones. Electric vehicles (EV) use secondary batteries hence in this chapter the term battery means secondary battery unless noted otherwise. From economic perspective, batteries are a serious business approaching 100-billion-euro market size. About a third of all batteries are used as automotive traction batteries (EV, HEV), other third is used in industrial applications and portable applications (consumer electronics) while the last third is used in other applications like power tools and conventional car batteries [133-140].

In electrical engineering a battery is recognized as a voltage source. A major difference is that the voltage of this source will gradually decrease when a load is applied (discharge) while connecting a battery to a higher voltage source will cause its voltage to gradually increase (charge up). A more precise definition claims that a battery is in fact an electrochemical device which can provide voltage and release electrical energy stored inside of it in the form of chemical bonds.

This electrochemical device has four main parts: two electrodes, electrolyte and separator. Both electrodes typically are solid materials made to store charge and conduct current. One of the electrodes is cathode while other is anode. From the basics of electronics, current flows out of the cathode and into the anode. This holds true for the battery as well – however only if the battery is being discharged. When the battery is being charged, the current flows in other direction, hence cathode and anode switches places. This can cause some confusion. To avoid it, in electronics battery electrodes are typically denoted by their polarity: electrode with higher polarity is the positive electrode (positive terminal, positive pole or just +) and electrode with lower polarity is the negative electrode (negative terminal, negative pole or just -). The switching of anode and cathode can cause confusion even in the field of battery chemistry. Probably due to the fact that batteries are most useful when they are being discharged (and on stand-by) battery chemists have fixed anode and cathode to this position: anode is negative and cathode is positive. The next essential part of the battery is the electrolyte which typically is a liquid although a major research is performed to develop and introduce solid-state materials. Electrolyte connects both electrodes to provide ion transfer between them during charging and discharging while inhibiting internal flow of electrical current. The electrical current, in the form of electrons, flows through an external circuit. If both electrodes inside the battery would come into direct contact, a short circuit would form which would lead to a failure of the battery. A separator layer is introduced to provide electrical and mechanical isolation between the electrodes. The separator typically is a solid-state material with micro pores to allow ion

transfer. Some of modern batteries are made of three distinct layers: anode, electrolyte-soaked separator and cathode. Other parts of the battery include the case with markings, external isolation materials like plastic coating, current collectors and external terminals or connectors.

6.2. Technical parameters

Batteries have a wide array of different technical parameters: electrical, physical, chemical and sustainability. The most critical parameter is the battery chemistry. It defines all other parameters of the battery. Chemistry in regard to batteries describes composition of both electrodes and the electrolyte. Some examples are lead-acid battery, nickel-metal hydride (NiMH) battery and many types of lithium-ion (Li-ion) batteries which can be further classified by cathode and anode materials.

6.2.1 Voltage

The chemical composition of electrodes defines the voltage of a single cell. All types of battery cells have a certain nominal voltage Unom. As previously noted, the nominal voltage of different chemistries is in the range of 1.2 V to 3.9V. The nominal voltage is somewhere between maximal voltage Umax (charging voltage) and minimal voltage Umin (discharge cut-off voltage, end-of-discharge) and it is defined by the manufacturer of the cell. The nominal voltage is used for calculations to determine the voltage of the battery pack if cells are series connected. It is also used to calculate the watt-hour (Wh) capacity of cell or whole battery pack. Nominal voltage of a single lead-acid cell is 2.1V, of NiMH cell it is 1.2V and for majority of Li-ion cells it is 3.6V. Charging voltage is the maximal voltage which can used to charge the cell. Higher voltage leads to overcharging and often to harmful effects which degrade the battery. Discharge cut-off voltage is the voltage beyond which discharge should be terminated to prevent damage to the cell. At this point it should be clear that battery voltage is not a fixed value – it changes depending on the depth-of-discharge (*DoD*). The fuller the cell/battery the higher the voltage and vice versa. A battery discharge voltage curve is given in Figure 6.1. It can be seen that for most part the voltage is changing little as the cell is being discharged. This is regarded as the flatness of the voltage curve. For primary batteries it is desirable to have a flat curve which translates to stable supply voltage.

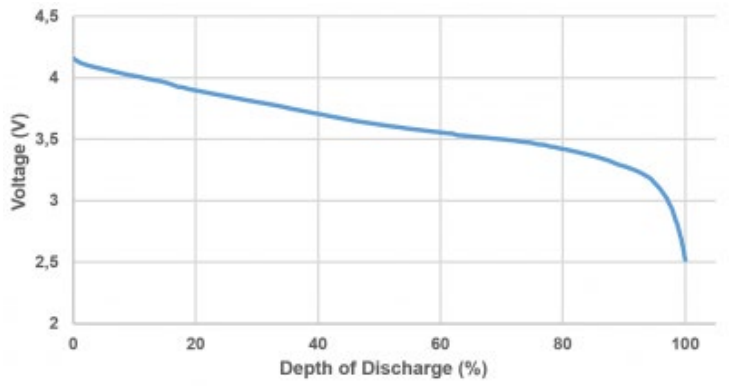

Figure 6.1. Discharge voltage curve of a single Li-ion cell: voltage decreases as the *DoD* increases

6.2.2 Capacity and energy

The second most important quantitative battery parameter is capacity Qbat. Capacity determines how much charge a battery can store. It is measured in amp hours (Ah). Higher Ah rating means the battery will be able to run longer before requiring a recharge. If the load current Iload is known then the runtime t can be calculated as follows:

$$t = \frac{Q_{bat}}{I_{load}}. \tag{6.1}$$

For example, a battery rated at 3Ah will be able to deliver 1A for three hours or run for one hour while delivering current of 3A. It can be seen that change in current results in inversely proportional change in discharge time. If one wants to compare two batteries with identical nominal voltages then Ah capacity rating can be used to determine which battery can store more charge. For example, when selecting a lead-acid battery for car, the voltage of the battery is determined by the car: it has to be 12V battery. A higher capacity battery can be used to improve performance. However, if an engineer has to select a battery for an application which can use different nominal voltages then energy rating Ebat (measured in watt hours Wh) should be used instead of capacity. While nominal voltage and capacity is typically printed on the battery label, the energy rating is only occasionally given on some Li-ion cells. The energy rating can be obtained by multiplying capacity and nominal voltage:

$$E_{bat} = Q_{bat} \cdot U_{nom}. \tag{6.2}$$

For example, a 10Ah lithium-ion cell with 3.6V nominal voltage will be able to store 36Wh of energy. A 3Ah lead-acid battery with 12V nominal voltage will also store 36Wh which means that both batteries have the same energy rating albeit at different nominal voltages. Both capacity Qbat and energy Ebat ratings have time (expressed in hours h) in their definitions. This can be used to calculate battery runtime if the load power Pload is known:

$$t = \frac{E_{bat}}{P_{load}}. \tag{6.3}$$

For example, if a battery has 200Wh of energy and it is connected to a constant 50W load then the battery will be fully discharged after 4h. If an engineer needs to select a battery to supply 100W load for at least a full day (24h) then she should select at least 2400Wh (2.4kWh) battery. However, for these equations one has to remember that rarely the load is constant power or constant current. Moreover, as the battery discharges, its voltage will decrease which will lead to changes in load current and power in most cases.

6.2.3 Current and C-rate

The next electrical parameter is current. A good battery datasheet will provide at least a few current values at different conditions. Common parameters are standard charge current, rapid charge current, max. continuous discharge current and standard discharge current. Often the charging current ratings are significantly lower than discharge ratings. Battery lifetime will be

improved if it is used at standard ratings. Standard ratings are often used to determine nominal capacity – at increased currents the battery will not be able to deliver its nominal capacity. The rapid charge current and max. continuous current typically depends on the thermal performance of the battery cells, especially in the case of Li-ion. A high rate discharge/charging will lead to heating of the cell – once temperature gets too high the current has to be stopped to prevent damage to the cell.

In engineering and battery datasheets there is another battery-specific parameter which is directly related to Ah rating: the C-rate. The value of 1C is a number same as the nominal capacity of the battery. The C-rate itself has no unit of measurement but when it is converted to current it is expressed in amps A. C-rate is used to determine current for both charge and discharge. It comes handy when comparing current capabilities of different batteries and simply estimating how large the current is in respect to capacity of the battery. For example 2C discharge rate of a 10Ah battery is 20A while 0.5C charge rate of the same battery is 5A. From previous paragraphs one should notice that capacity and current of a battery is closely related to time: if a battery is discharged at 2C it will be empty after 0.5h. A 0.1C discharge rate will empty the battery in 10h. And of course 1C discharge results in 1h operation. As one can see the C-rate can be used to determine battery runtime without revealing the actual current or capacity of the battery. Table 8.1. shows some examples of C-rate and related current and charge/discharge time. Additionally C-rate shows how intense the current is in respect to battery capacity. For lead-acid batteries high C-rate discharge will lead to decreased available capacity while very low C-rate discharge will be able to deliver even more charge than the nominal capacity. Often 1C rate does not even correspond to 1h operation.

Table 6.1. C-rate table for a 100Ah battery

Capacity	C-rate	Equation	Current	Time
100Ah	10C	10·100A	1000A	6 minutes
100Ah	5C	5·100A	500A	12 minutes
100Ah	3C	3·100A	300A	20 minutes
100Ah	2C	2·100A	200A	30 minutes
100Ah	1C	1·100A	100A	1 hour
100Ah	0.5C	0.5·100A	50A	2 hours
100Ah	0.33C	0.33·100A	33A	3 hours
100Ah	0.2C	0.2·100A	20A	5 hours
100Ah	0.1C	0.1·100A	10A	10 hours

6.2.4. Cycle life and ageing

Battery lifetime is a critical parameter of secondary batteries. Depending on the chemistry battery lifetime is affected by to ageing mechanisms: cyclic ageing and calendar ageing. As the name suggests calendar ageing is related to the absolute age of the battery: as battery ages, its

performance will deteriorate – capacity will decrease and internal impedance will increase leading to decreased current capability. The rate of calendar ageing is related to the temperature of the battery. As Arrhenius' equation suggests, the rate of chemical reactions is proportional to the temperature: if battery is operated/stored at elevated temperature, it will deteriorate faster. Additionally the rate of calendar ageing for some battery chemistries is related to the depth-of-discharge. Being fully charged or discharged can increase or decrease battery ageing rate, however it depends on battery chemistry. For example in stand-by applications lead-acid batteries should be fully charged to extend lifetime, while most Li-ion batteries (LIBs) will degrade faster if left fully charged.

The other ageing mechanism – cyclic ageing, is related to the intensity of battery usage. A full battery cycle is a full charge followed by a full discharge. Battery manufacturers in battery datasheets give an estimated cycle life – typically few to several hundreds of cycles. For this cycle number to be true it is of importance to follow a specific charge and discharge test pattern: the manufacturer will specify exact charging and discharging current, exact charging and discharging cut-off criterions and exact rest periods between each charge and discharge as well as the ambient temperature (typically 25°C) at which the battery should be cycled. These cycle life testing parameters are different for each battery model. The estimated cycle life has been reached when the battery capacity has decreased by a certain amount. Unfortunately for different manufacturers and different battery models this end-of-cycle life criterion is different and can be in the range of 85% to 60% from initial nominal capacity – this complicates comparison of different battery models. A key fact is that batteries degrade with each cycle even if the cycle is not full. However this degradation rate and linearity is not the same for all models. For battery with perfect linear degradation each next cycle would be a bit smaller until the capacity eventually decrease from initial 100% to 0%. However, in real life batteries the degradation is nonlinear, especially in the end-of-life (EoL) region. While initial capacity drop per cycle might be linear after reaching the rated cycle life there might be a knee in the cycle life graph after which the degradation happens much faster. This knee point is after the datasheet's 85% to 60% end-of-cycle life point. Typical battery datasheets does not provide full cycle life graphs from 100% to 0% capacity but only from 100% to the rated end-of-life point which is those 85% to 60%. A key point to note is that the datasheet cycle life number can be easily exceeded if certain actions are taken to decrease degradation. The degradation rate is strongly affected by the temperature, discharge depth (Depth-of-Discharge *DoD*) and charging level. Deep discharge and overcharging can quickly decrease cycle life. In worst case situations a single full over discharge (well below absolute minimum battery voltage) can lead to immediate battery failure. The same is true for overcharging, especially in the case of LIBs, which can catch fire or explode if overcharged. Even small deep discharges and overcharging will lead to decreased cycle life. High rate discharging and charging can also decrease cycle life if battery temperature is not limited to optimal range. For Li-ion and lead-acid batteries the key action to increase battery lifetime is to limit *DoD*. For lead-acid batteries it should be as small as possible while fully charged (0% *DoD*) and fully discharged (100% *DoD*) regions should be avoided for LIBs.

6.2.5. State-of-Charge/Depth-of-Discharge

During battery operation there are two similar but opposite variables which indicate how much charge is left in the battery: depth-of-discharge (*DoD*) and state-of-charge (*SoC*). Both of variables are relative indicators and are expresses in percent. As the name suggests *DoD* indicates how much charge is left in battery in respect to a fully charged battery. A 0% *DoD* level means that the battery is fully charged while 100% *DoD* level means that a battery has been fully discharged. *DoD* can be calculated using (8.4) where Cdis is discharged capacity and Cnom is the nominal capacity. The *SoC* is an inverse of *DoD*: it indicates how much charge is remaining in the battery. A fully charged battery is at 100% *SoC* while 0% *SoC* means that the battery is completely discharged. *DoD* indicator has the benefit to go over 100% - it can happen in situations when a low discharge rate is used and thus battery can deliver more charge than nominal. The *SoC* indicator in this case would go negative which can cause confusion. In practical use, the *SoC* is mostly used as indicator to describe the remaining charge of a battery in operation, in essence, it is a fuel gauge indicator. Rarely *DoD* is expressed not in percentage points but in discharged amp hours (Ah) as shown in expression (6.5). In this case the user must know the nominal capacity to make sense of the *DoD* reading.

$$DoD = \frac{C_{dis}}{C_{nom}} \cdot 100\%. \tag{6.4}$$

$$DoD = C_{dis}. \tag{6.5}$$

6.2.6. Performance parameters

When selecting a battery for a particular application certain comparison of available models has to be done to make an optimal choice from price and performance perspective. For portable applications gravimetric energy density (also specific energy, gravimetric density) and volumetric energy density (occasionally energy density) are common indicators of battery performance. The gravimetric energy density DEm can be calculated using (6.6) where Ebat is the nominal energy and mbat is the mass of the battery. It is traditionally expressed in Wh/kg units. It shows how much energy can be stored in one kilogram of battery mass. For example, a 300Wh battery weighting 2kg has 150Wh/kg gravimetric energy density. A high-performance LIB has approximately 200Wh/kg specific energy density.

$$DE_m = \frac{E_{bat}}{m}. \tag{6.6}$$

While specific energy describes the relative weight of the battery, volumetric energy density is used to describe the relative volume or size of the battery. A battery with higher volumetric energy density will be smaller at the same rated energy. The volumetric energy density DEv can be calculated using (6.7) where Ebat is the nominal energy and Vol. is the volume measured in liters l. The result is expressed in Wh/l units. A battery datasheet most likely will provide the mass however the volume will have to be calculated using provided dimensions. High-performance LIBs can have volumetric energy density of 400Wh/l or even more.

$$DE_v = \frac{E_{bat}}{Vol}. \tag{6.7}$$

When using both volumetric and gravimetric energy densities one must remember that in most cases these values are for cell-level parts. A fully designed battery pack has more components (interconnections, electronics, thermal management, structural case) which will add to both mass and volume and as a result both energy density performance indicators will be decreased. In most applications the costs of the solution are of great importance. The same is true for battery powered devices. It is occasionally estimated that an EV battery can cost as much as one third of the whole vehicle. The costs of battery can be divided into two parts: cost of cells and cost of auxiliary components. The cost of cells is straightforward – one can use the price set by manufacturer or dealer to compare different cell models. It is more complicated with auxiliary components which are required to make the battery pack/battery energy storage system. These components include battery management electronics, safety devices, contactors, connectors, interconnections, thermal management and the case. In case of EV LIB packs, cell costs make approximately 70% and remaining 30% are the costs of auxiliary components.

One more interesting battery comparison indicator is the lifetime energy throughput. In its simplest version it can be obtained by multiplying nominal capacity with cycle life. The result is an amount of energy which will be delivered by the battery during its lifetime. It must be noted that this calculation does not take into consideration the capacity fading and it assumes that battery will be used only with full cycles. As previously described, the cycle life can be significantly increased if certain operational modes are employed – it would result in much larger total lifetime energy throughput.

$$E_{lifetime} = E_{nom} \cdot cyclelife. \tag{6.8}$$

For economical perspective, Elifetime can be divided by the price of the battery to estimate how much energy will be delivered per unit of currency as shown in equation:

$$E_{1EUR} = \frac{E_{lifetime}}{Cost_{battery}}. \tag{6.9}$$

For example, a small 300Wh battery costs 150€. Its nominal cycle life is 500 cycles which results in 150000Wh or 150kWh of total discharged energy throughout its lifetime. If this number is divided by the price, then a 1kWh/1€ figure is obtained. It shows that each single euro was converted to 1kWh of discharged energy throughout batteries lifetime. This performance indicator can be used to compare different battery technologies and individual cells which have different cycle life parameters.

6.3. Battery pack

As previously described, a battery pack consists of cells and a set of auxiliary components. Both in literature and practice the word “pack” is often omitted as is here as well. For stationary applications there is a term “battery energy storage system” which basically is a battery pack

with additional interface converter which takes care of voltage conversion, charging and SoC control. If the interface converter is not integrated in the battery energy storage system, then one could say that it basically is the equivalent of a typical battery pack. Cells of small battery packs (electric scooters, bicycles, drones) are arranged in one group and equipped with basic auxiliary components – bus bars, electromechanical contractors, safety disconnect devices and thermal management. The main reason for less complexity is low cell count relatively small voltage. The voltage of larger battery packs (light- and heavy-duty electric vehicles) are in the range of 300V to 800V. While some sources claim that DC voltage below 120V are low risk, it is safer to assume 48V limit. Such large battery packs are typically composed of several low voltage battery modules which are series connected to produce higher voltage.

Each battery module or a small battery pack consists individual cells. All cells are of the same model and are preferably parameter-matched to provide maximum performance utilization. There are two types of connections which can be used to combine individual cells: series connection and parallel connection. In a series connection cells are connected in a string so that positive pole of one cell is connected to the negative pole of the next cell. The correct polarity is critical. Series connection is used to increase voltage of the pack. A single cell has nominal voltage of 1.2V to 3.8V. Higher voltages can be obtained by series connecting cells. Voltage of a string is the sum of individual cells. n is the number of series connected cells.

$$V_{string} = V_{cell1} + V_{cell2} + ... + V_{celln} = n \cdot V_{cell}. \tag{6.10}$$

In series connection the capacity rating (Ah rating) stays the same as for a single cell – all cells will experience the same current during charging/discharging. However, the total energy of the string will be the sum of individual cells energies. The total energy can be calculated if total voltage and capacity of individual cells is known.

$$E_{string} = E_{cell1} + E_{cell2} + ... + E_{celln} = n \cdot E_{cell}. \tag{6.11}$$

$$E_{string} = V_{string} \cdot C_{cell}. \tag{6.12}$$

In a parallel connection all positive poles of all cells are connected together, and all negative poles are connected together as well. The correct polarity is of utmost importance as incorrect polarity of a single cell will cause immediate short circuit which in worst case can result in fire and/or explosion. The total voltage of a parallel connection is equal to that of a single cell. Parallel connection affects the total capacity which can be calculated as the sum of combined cells.

$$V_{parallel} = V_{cell}. \tag{6.13}$$

$$C_{parallel} = C_{cell1} + C_{cell2} + ... + C_{celln}. \tag{6.14}$$

$$C_{parallel} = n \cdot C_{cell}. \tag{6.15}$$

As the capacity rating is increased, the C-rate is increased proportionally as well, resulting in higher permissible charge/discharge current levels. Similarly, as in series connection, the total energy of a parallel connection is equal to the sum of individual cells.

$$E_{parallel} = E_{cell1} + E_{cell2} + ... + E_{celln}. \tag{6.16}$$

$$E_{parallel} = n \cdot E_{cell}. \tag{6.17}$$

$$E_{parallel} = C_{parallel} + V_{parallel} = C_{parallel} \cdot V_{cell}. \tag{6.18}$$

One of a battery pack's description parameters is the cell configuration: how much cells are connected in series and how much in parallel. A thirty-cell series connection is described as 30S while ten cell parallel combination is described as 10P. Both parts are typically combined: 30S10P – the battery pack consists of 30 series connected cells and each "cell" is made of 10 actual cells in parallel. This pack contains 300 cells in total. Given cell configuration tells that cells are connected in parallel first (making a larger cell or cell group) and then connected is series to form a single string. An alternative would be 10P30S. In this configuration there would be 10 series strings composed of 30 cells in the first step (series first configuration). In the second step these strings would be connected in parallel to achieve required capacity and C-rate performance.

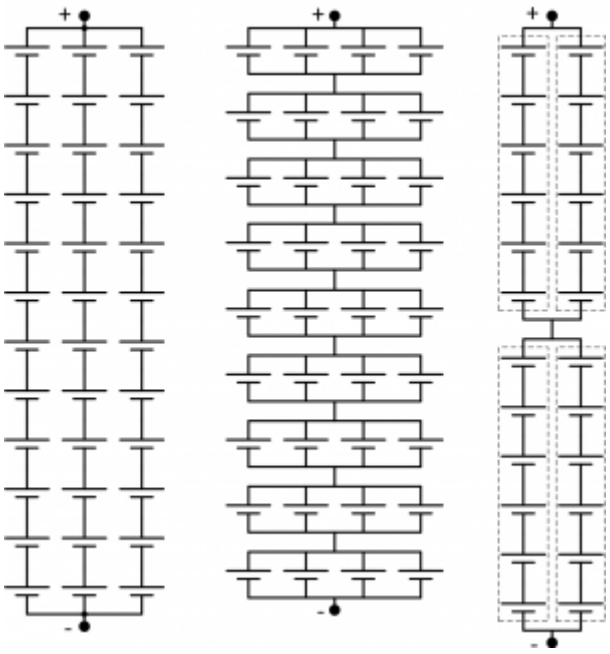

a b c

a - series first 3P12S battery; b - parallel first 9S4P battery, c - a mixed connection battery pack where each dashed box could be an 6S1P (12V) lead-acid battery hence total configuration could be labeled as 2S2P

Figure 6.2. Battery pack

There exists a mixed cell configuration where in first step smaller series strings are connected in parallel to make a sort of battery module. In second step modules are connected in series to

produce finished battery pack. Common 12V lead acid battery has 6 series connected cells (6S1P). One could connect 2 batteries in parallel to double capacity and 2 in series to double voltage: a total of 4 batteries would be used to make a 2S2P configuration – in this case the configuration regards batteries not cells. See Figure 8.2.c for clarification.

When designing LIB packs it is a rule of thumb to connect individual cells in parallel first, series second. Such configuration assures that the cells connected in parallel have identical voltage. It is beneficial to parameter-match cells before connecting them in parallel to achieve optimal resulting capacity. During second step, paralleled cell groups are connected in series to build the whole battery pack. A battery management system (mandatory in case of Li-ion) can then be connected to each parallel cell group. If cells were first series connected, then each series string would require individual battery management system due to monitor cell voltages and perform balancing. In parallel-first configuration all parallel cells share the same voltage hence it is simpler to perform monitoring and balancing.

Typical EV LIBs have voltage in the range of 300V to 800V and energy in the range of dozen kWh to 100kWh. It is obvious that such battery packs require a multitude of cells which need to be series and parallel connected to achieve desired performance. Due to reliability, safety and handling issues, such battery packs are composed of smaller parts – battery modules. Modules are connected in series to make a battery pack. The size of the module can depend on several aspects: mechanical integrity – modules are made to be mechanically robust; safety – modules often have voltage (much less than the total battery pack voltage) which can be considered safe, handling – the relatively small size and weight of a module allows easier handling during manufacturing, assembly and repair. While a battery pack consists of series connected modules, the modules themselves can consist of individual cells or cell groups. If individual cells are sufficiently large (tens of Ah) then a module can be made of series connected cells. If cells are smaller (few tens of Ah) then they can be separately connected in parallel to make a cell group or cell pack – several such groups can be connected in series to make a module. However, in some EVs (example: Tesla) the battery pack is composed of modules which are directly made of a large number of small cells (few Ah).

6.4. Lithium-ion battery

The lithium-based rechargeable batteries were last to enter the market, yet they have evolved quickly, overtaken significant part of the market and the total worth of related technologies is expected to grow in the future. As the name implies, the chemical element lithium (Li) is a key component of every lithium-based battery: primary or secondary, metal or ion variety. Lithium is the lightest metal (lighter than water) with one of the lowest electrode potentials hence it fulfills requirements for a performance battery. However, lithium is highly reactive: it aggressively reacts with water and oxygen from air – both lead-acid and NiMH chemistries uses electrolyte with water hence lithium-based batteries needs a new type of electrolyte. Studies in lithium electrochemistry was already done as early as in the second decade of 20th century. However, the research and development of lithium batteries took off only in 1970s - the first rechargeable lithium battery prototype was demonstrated in 1976. The first

commercially available non-rechargeable (primary) lithium battery was already sold in the same decade. It took a couple of decades for the rechargeable battery – it was commercialized in 1991. Initial models used metallic lithium anode (negative electrode) with titanium disulfide cathode (positive electrode) but it was noticed that this construction under certain circumstances and cycling can grow so called dendrites – treelike structures which extend from anode, pierce separator layer and cause an internal short circuit which causes venting with flame, fire or explosion. It was found to be difficult to prevent dendrite growth in lithium metal batteries hence research was shifted to another lithium battery type: lithium-ion battery (LIB) in which there is no metallic lithium and only lithium ions are used transfer and store charge.

Rechargeable LIBs became available in year 1991 with key advantage: higher specific energy density than other available battery chemistries. Gradual development of new cathode materials adjusted LIB technology for most requirements of portable applications from highest energy density smartwatches and cell phones to high current hand tools and long life EV batteries. Additionally, less expensive LIB chemistries were developed for stationary applications. It is estimated that total LIB market is in the 30-billion-euro range and it is expected to increase fourfold in this decade. LIBs constitute approximately 60% of all automotive batteries. Over the 30-year period of commercialization, LIBs have become a dominant battery technology with room for improvement. This technology has changed our lives by enabling personal portable devices and now it is a key-enabler for EVs. In 2019 three researchers were awarded Nobel prize in chemistry for the development of lithium-ion batteries.

6.4.1. Construction

Li-ion cell construction is fairly complex if compared to simplistic lead-acid cell. The basic essential components are the same: two electrodes, electrolyte and separator. For basic functionality, electrolyte has to be able to transfer lithium ions at the same time it should not react with those highly reactive ions. While the electrolyte of lead-acid and NiMH cells is rather simplistic inorganic water-based liquid, the electrolyte of li-ion cells is a non-aqueous organic carbonate-based liquid which contains some sort of lithium salt or mixture of salts to provide some free lithium ions for energy transfer. The electrolyte is flammable which adds to the overall safety issues of the LIB technology.

The separator layer has the same basic function – prevent contact of electrodes (internal short circuit) while providing free path for the ion flow. In general, it is made of porous polymer material which can be internally composed of different layers of plastic (polypropylene, polyethylene and others) with additives to provide additional safety by blocking short circuit currents and decreasing flammability. From the cell performance perspective, separator layer is an unwanted element of the cell as it does not contribute to the actual electrochemical reaction. It adds dead weight and volume which in turn decreases volumetric and gravimetric energy density. For this reason, it is desirable to make this layer as thin as possible – some cells can have separator thickness of around a dozen micrometers and constitute just a few percent of the total mass of the cell.

A li-ion cell is made as an ion transfer cell in which both electrodes can accept and store Li ions. During charging/discharging these ions are transferred from one electrode to the other. This operational principle is known as the rocking chair. At this point it must be emphasized that a Li-ion cell can be made using a variety of different electrode materials. There are six most prevalent material combinations which result in six types of Li-ion cells. For description of cell construction, the most popular construction will be used: the negative electrode (anode) is made of graphite (an allotrope of carbon); the positive electrode (cathode) is made of lithium and some other metal/s oxide. Both anode and cathode active materials are selected to provide the required capacity, current and life. Electrodes can have some additives to improve current carrying capability. Additionally, both electrodes are bonded to current collectors (passive material) – high conductivity metal conductors used collect electrons from active material and provide path to the external connection of the cell. In some cell constructions the current collector metal is actually a part of the external connector. Aluminum for positive electrode and copper for negative electrode is a common current collector material choice as both metals have high conductivity, adequate electrochemical stability and are easily available.

The case of a cell is another contributor of passive material. Li-ion cells are being manufactured in all shapes according to the application requirements. In most situations, the internal structure of a cell is made as a jelly roll. First each electrode-current collector combination is made as a sheet roll then both electrodes and separator layer are combined by rolling all layers into one roll. Finally, the electrolyte is filled. Naturally, the resulting roll is of cylindrical shape hence the most effective (from manufacturing perspective) cell shape is cylindrical. In case of pouch/flat and prismatic cell shapes, the jelly roll is pressed and processed into required shape and then encapsulated in casing. Alternatively, a cell can be made of individual material sheets which are stacked together to produce flat cells – this process is more expensive and time consuming than jelly roll process.

6.4.2. Operation

The basic operation of li-ion cell is simple: positively charged lithium ions flow from negative electrode to positive during discharge and vice versa during charging. At the same time, during discharge electrons travel through the external circuit from negative electrode to positive and from positive to negative during charging. At fully discharged state the porous structure of negative graphite electrode is empty (without Li ions) and oxidized (without electrons) while the positive electrode is fully reduced to metal (lithium and others) oxide. The situation is reversed when cell is fully charged: negative electrode structure is filled with lithium ions taken from the positive electrode. Corresponding chemical reactions are given below in Figure 8.3.

6.4.3. Types of Li-ion chemistries

As previously noted, there are six common Li-ion chemistries. They differ according to the materials used in both electrodes. The widest variety is for the positive electrode (cathode) which can have five compositions: LCO, LMO, NMC, NCA and LFP. These three letters are

abbreviations of the main chemical components of the active material. LCO and LMO are among the first commercially available Li-ion chemistries. Their composition is straightforward: L stands for lithium, C stands for cobalt, M stands for manganese and O stands for oxide/oxigen. Therefore, LCO Li ion cell has lithium cobalt oxide (LiCoO2) cathode (positive electrode) and LMO cell has lithium manganese oxide (LiMn2O4 or Li2MnO3). cathode. It gets a little bit complicated with NMC and NCA where N is nickel, C is cobalt, M is manganese and A is aluminum. In the names of these two materials lithium (L) and oxide (O) parts are omitted to maintain three-letter format. Therefore, NMC is lithium nickel manganese cobalt oxide (LiNiMnCo2) and NCA is lithium nickel cobalt aluminum oxide (LiNiCoAlO2).

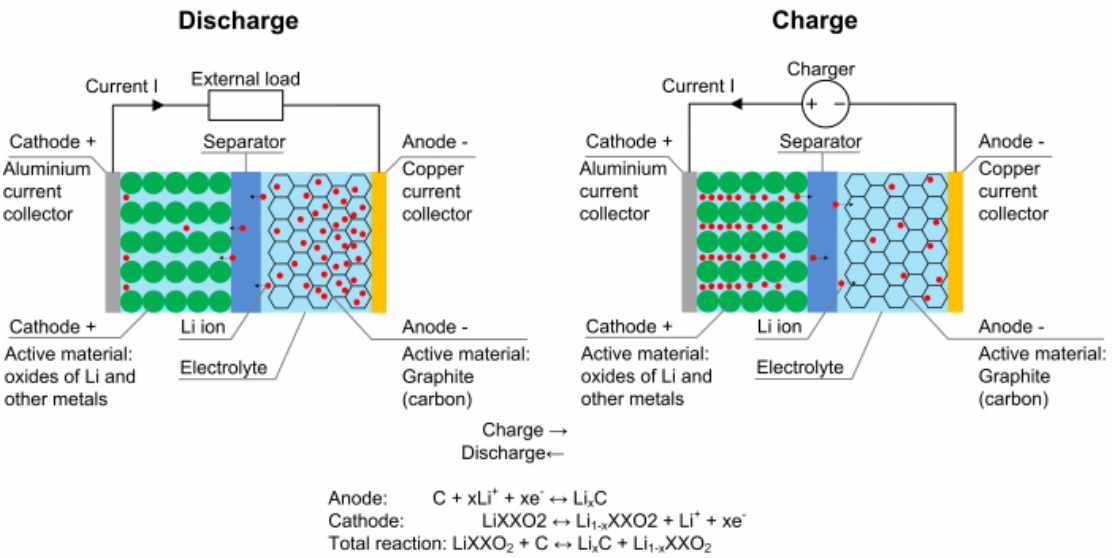

Figure 6.3. Generic chemical reactions of a Li-ion cell

Finally, in LFP L stands for lithium, F for iron (from Latin: ferrum) and P for phosphate. Therefore, the cathode of LFP chemistry is made of lithium iron phosphate (LiFePO4). In all these five chemistries only the cathode (positive electrode) was the variable. The anode material in all five types remained the same: graphite. The remaining type is LTO where L is for lithium, T is for titanium and O is for oxide/oxygen. Due to some chemical nomenclature rules this material is called lithium titanate (Li2TiO3). LTO is used to replace the graphite anode. For some confusion, the cathode of an LTO cell can be made of LMO or NMC material. Additionally, the performance of these types is changing as battery technology is advancing. For example, NMC is a popular type for EVs. It used to have 1:1:1 ratio between nickel, manganese and cobalt hence an extended name was NMC111. Then chemistry was improved to reduce cobalt content (an expensive conflict mineral) and new NMC622 type modification was introduced. It is expected that NMC811 material will be available and become mainstream in near future. The key difference between these variations is the increase in gravimetric energy density.

To summarize, each of six basic types have their specific characteristics: cost, energy density, specific power, safety, life span, temperature range even the voltage. A graphical representation of some different features is given in figure 6.4. From this, one significant conclusion can be

drawn: the name “Li-ion battery” is quite generic – the true performance is revealed when the exact type of chemistry is known. To continue the confusion, a term lithium polymer (Li-poly, LiPo) battery exists. Despite the rumors that Li-poly is some special battery type, it is a type of Li-ion battery which has a sort-of solid electrolyte. In a Li-poly battery, the common liquid electrolyte of a traditional Li-ion battery is replaced with a gel-like electrolyte. In practice, majority of Li-ion cells have some additives and improved separator structure to confine liquid electrolyte thus essentially making Li-poly cells. These cells are mainly made in pouch format. A different variation is the solid-state Li-ion – as the name implies, the electrolyte is made fully solid thus making it possible to produce cells thinner than 1mm. Fully solid-state Li-ion technology is still in research and development stage, however it promises higher charge/discharge rates, longer lifecycles, higher energy density while being safer and less expensive. Most likely all promises will not be carried out but announcements from developer companies indicate that solid-state batteries will become commercially available during this decade. Progress in solid-state technology is intertwined with development of lithium-sulfur (Li-S) battery. Li-S battery could be the next breakthrough in energy density however it heavily relies on functional solid-state technology. A closer future is improved anode materials for existing chemistries. The common graphite anode can be replaced by silicon material which can store significantly more Li ions resulting higher energy density. However, silicon anode cannot provide required cycle life. Both materials are being combined to achieve both features. Advances in carbon materials promise improvements in battery chemistry. One novel carbon allotrope is graphene which excels in high electrical and thermal conductivity – both features can be used to improve performance of traditional graphite-based anodes.

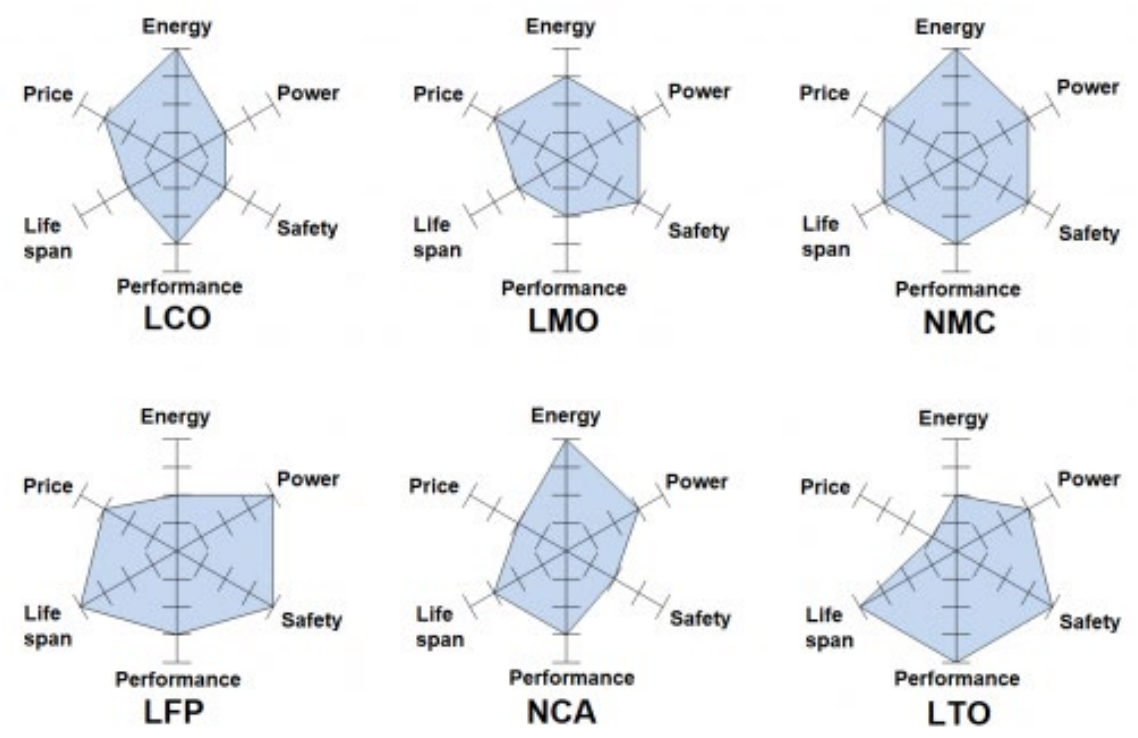

Figure 6.4. Characteristics of common Li-ion types

6.4.4. Discharging

All LIBs are characterized by relatively low self-discharge and no memory effect as opposed to the NiMH chemistry which requires occasional full discharge. In case of LIBs, full discharge is to be avoided to maximize battery lifespan. As for most batteries, the discharge rate affects the voltage of the cell – at high rates the voltage will drop more, in some cases it is beneficial to decrease the cut-off voltage to achieve desired end *DoD*. In most LIBs the discharge curve (vertical axis represents battery voltage while horizontal axis represents *SoC* or *DoD*) is linear with a drop at the final stage of discharge (90-100% *DoD*) when discharged at low rate. However, as the rate is increased, the drop at high *DoD* becomes flatter while the voltage drops faster at the opposite end of the curve, at low *DoD* (Fig. 10). The discharge performance is heavily affected by the temperature of the cell - in figure 8.5., the 6.6C rate curve does not reach 2.0V cut-off voltage because temperature of the cell has risen to the max limit. The nominal curve is given at 20, 23 or 25°C. At 45°C ambient temperature, the voltage curve of the cell is increased by less than 100mV, hence increased temperature minimally affect voltage under discharge. The situation is different if ambient temperature is decreased. At 0°C the voltage of a cell can a couple hundred mV lower (fig. 11). At negative temperatures the voltage decreases further limiting the discharge rate – if rate is too high the voltage drops below cut-off voltage and discharge should be terminated. This effect is somewhat mitigated if cell is operated at moderate discharge rate – due to internal losses the cell can self-heat and thus improve its performance. For most Li-ion types the available capacity rapidly decreases at low temperature (below -15°C). However, there exists a wide variety of different types and special purpose battery models which are designed to operate at high rates or low temperatures.

It can be said that the type of chemistry plays a critical role in the discharge performance. The most obvious initial difference is the nominal voltage (figure 12). It is commonly assumed that a single Li-ion cell has 3.6V nominal voltage although 3.7V are prevalent as well – these values are for the dominant group of LCO, LMO, NMC and NCA. On top of these two numbers, values around them can exist as well, for example, LG Chem produces 18650-size INR18650MJ1 cell (NMC type) whose datasheet's nominal voltage is 3.635V. However, 3.6 and 3.7 values are close together and difference is not critically important in most cases.

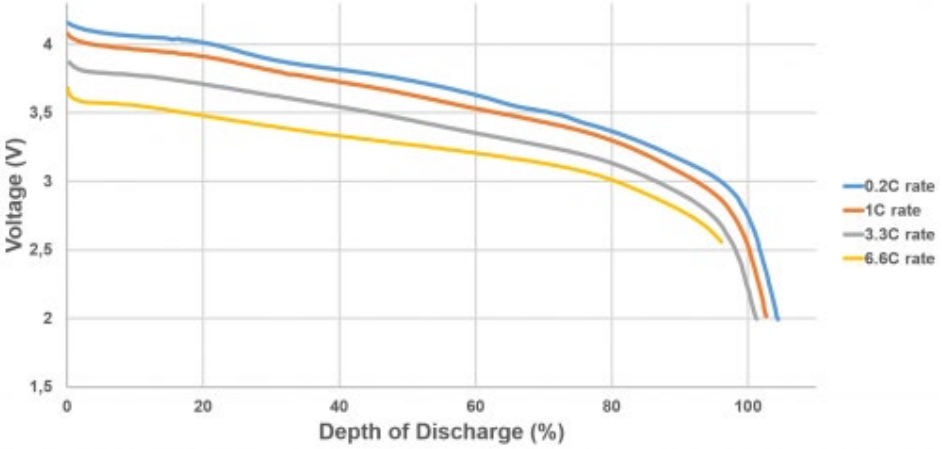

Figure 6.5. Voltage curves of a single NMC Li-ion cell at different discharge rates.

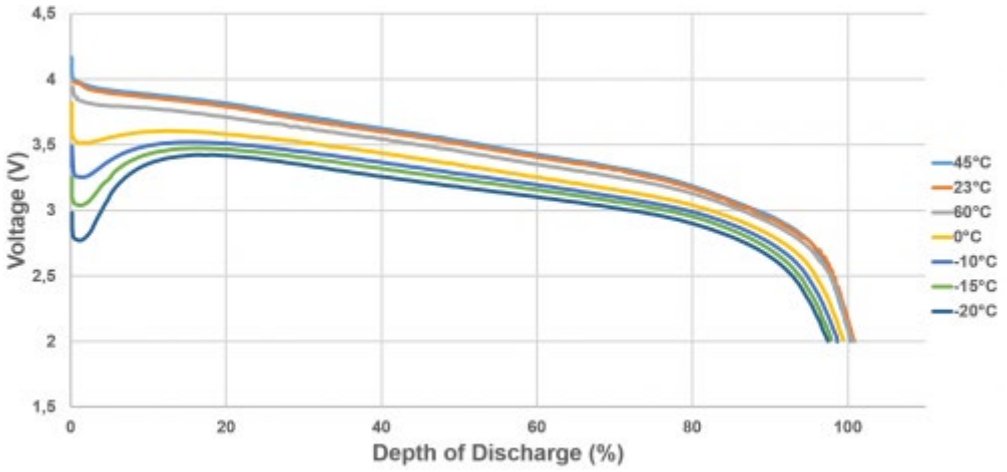

Figure 6.6. Voltage curves of a single NMC Li-ion cell at different ambient temperatures

LCO is rated at 3.6V with 3.0V optimal discharge cut-off. This type is known for its high gravimetric energy density and hence used in space/weight critical applications like mobile phones and laptops. The specific power is poor: discharge rate should not exceed 1C. LCO can be considered as an energy cell – used in applications where high energy is more important than high power. High rates and overcharging can lead to thermal runaway. LCO was one of the initially successful chemistries, but now the high price of cobalt and low safety has made this older type obsolete, putting more focus on NCA and NMC chemistries.

LMO is rated at 3.7V with the same 3.0V optimal discharge cut-off although the minimal voltage can go as low as 2.5V. The energy density is considerably lower than LCO however this type is capable of much larger discharge rates. The recommended discharge rate remains the same – 1C (for max life) but max rate can go as high as 10C or even 30C for brief periods. This high specific power density makes LMO a good choice for power tools and other high rate devices. High current can be achieved due to more stable manganese-based cathode structure – this type is safer than LCO. Thermal runaway would occur at much higher temperature Unfortunately, lower energy density is not the only drawback – cycle rate is lower than that of LCO. Drawbacks have been minimized in NMC chemistry which combines features of both cobalt and manganese, making LMO less relevant.

NMC can be rated at 3.6 to 3.7V depending on the exact materials and proportions of the cathode. The discharge cut-off varies from 2.7 to 3V with 2.5V as the absolute minimum. NMC is considered to be the leading LIB chemistry with ability to produce cells with both high energy and power at good cycle life. Gravimetric energy density is more than 200Wh/kg and discharge rates up to 2C are achievable. For example, the US18650VTC6 cell made by Sony has 3.6V nominal voltage and 3Ah rated capacity at weighting 46.6g. This translates to 10.8Wh energy storage and 231Wh/kg gravimetric energy density. At the same time this cell has 5C (15A) continuous discharge rate. Depending on various additives and construction, NMC is used in power tools, hobby electronics, EVs and industrial applications. More than 60% of all LIBs are NMC and adoption in EVs is more than 50%. The use of manganese improves safety at higher discharge rates however NMC is not considered to be the safest and highest power chemistry.

NCA has 3.6V nominal voltage and cut-off at 2.5V if max discharged capacity is required (100% *DoD*). It was introduced at the end of 20th century as a replacement for unsafe LCO chemistry. This type is regarded as high energy with good power capability and long life, additionally EV manufacturer Tesla together with battery manufacturer Panasonic has proven that battery packs with price less than 200€ per kWh can be manufactured using cylindrical NCA cells. NCA chemistry does not provide as discharge rate as NMC, the limit is in 2C to 3C range. Additional drawback is the inherently lower safety and easier thermal runaway. These negative effects can be controlled if proper battery and thermal management system is used.

LTO and LFP chemistries significantly differ from the previous two cobalt and manganese chemistries. The nominal voltage of an LFP cell is 3.2V while the cut-off varies from 2.0 to 2.5V depending on the model and mode of operation. If longer life is desired, then cut-off voltage should be increased to 2.8V. The discharge curve is very flat at rapid voltage curves at both ends, hence making it harder to estimate SoC. Despite the low cost of materials, LFP cells are rather expensive because of low gravimetric energy density. The advantages are high power, high safety and long life under specific discharge conditions. Safety includes chemical and thermal stability as well as some tolerance to overcharge and short circuit. For example, A123 Systems manufactures AMP20M1HD-A flat pouch cell which has 19.6Ah at 3.3V nominal voltage (higher than usual 3.2V) at gravimetric energy density of 131Wh/kg which is low if compared to NMC or NCA types. However, this cell can be discharged 363A current which translates to 18C rate. Additionally, the manufacturer claims that this cell model will retain 90% capacity after 3000 cycles at 100% *DoD*. LFP chemistry is popular in China for EVs, industrial applications and utility level energy storage.

LTO is characterized by even lower nominal voltage ranging from 2.2 to 2.4V. The minimum discharge cut-off is at 1.5V while in some models it is recommended to stop discharging when voltage decreases to 1.85V. The relatively low nominal voltage is the greatest disadvantage of this chemistry. As previously described, energy of a cell can be calculated by multiplying capacity (Ah) with nominal voltage (V). At same capacity and significantly lower voltage the resulting energy and volumetric/gravimetric energy density will be low. This further translates to high initial cost per kWh of the battery pack – the highest among all LIBs. Otherwise, LTO has some significant advantages. Both charging and discharging rates are high: typically quoted discharge rates are up to 10C with 30C pulses. Pulse (10 seconds) current capability of actual high-power optimized models can be as high as 75C. The cycle life is measured in several thousands and if reduced DoD range is used then cycle life can extend to tens of thousands of cycles. Additionally, the operational temperature range is wide and thermal stability is high making LTO the safest Li-ion chemistry. For a practical example, Leclanche manufactures LT34 LTO cell with 34Ah capacity at 2.2V weighting 1080g. Simple calculation yields that gravimetric energy density is just 70Wh/kg – less than high performance NiMH chemistry can provide. However, this cell can be discharged at 6C and 10C in pulses at temperature range from -20 to +55°C. Additionally, at 100% DoD cycling it is rated for 15000 cycles while 80% DoD cycling will extend cycle life to 20000 cycles. Given parameters make LTO suitable for

large EVs (bus, tram, train) and stationary energy storage which requires high charge and discharge rates.

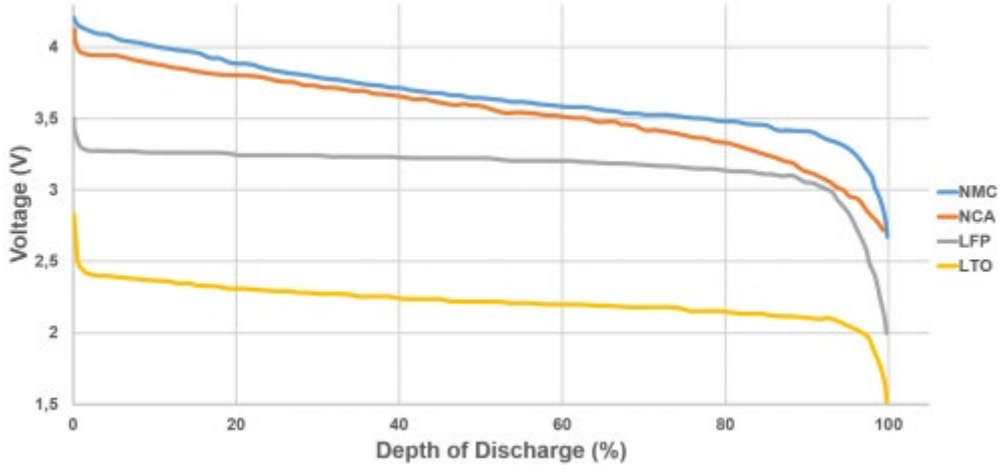

Figure 6.7. Generalized voltage curves of single Li-ion cells of various chemistries

6.4.5. Charging

In general, the CCCV charging method is used to charge LIBs similarly to lead-acid chemistry. Hence, there are two main charging phases: the faster constant-current phase and the slower constant-voltage phase as shown in figure 8.8. If a battery is deeply discharged (below minimum voltage) then a pre-charge phase should be introduced before full current CC phase. The pre-charge current should be 10% or less than the nominal charging current (given in the datasheet) of the battery. Once the voltage of the battery is higher than minimal discharge voltage, charger can switch to full current charging in CC phase. In normal operation, pre-charge phase should be omitted as BMS (battery management system) has to prevent deep discharge and associated damage to the LIB. However, if the battery voltage is indicating deep discharge then pre-charge should be carried out to pre-condition both electrodes for effective lithium ion transport. Immediately applying full current (or even worse fast-charge current) to a deeply discharged LIB can result in additional heating (risk of thermal runaway and associated danger) and permanent damage to the electrodes.

Most of the charge to the battery is delivered during the CC charging phase. The controllable parameter is current. The standard charging rate commonly is 0.5C which results in approximately 2-hour 0-100% battery charging (including CV phase). Older Li-ion chemistries were quite sensitive to charging current – higher rates would result in metallic lithium plating on electrodes, electrode expansion (package deformation) and overall performance deterioration. In worst case it would result in thermal runaway and venting with flame. Progress of technology and development of new types (NMC, NCA) have resulted in more robust cells with higher allowable charging rates. Now, faster charging can be achieved by using 1C or even 2C rates. However, fast charging has its limits. In standard charging, most time of charging is spent in CC phase, when battery is charged to 80-90% *SoC*. CC phase is terminated when charging voltage level is reached and charging transitions to CV phase during which the

remaining charge is delivered to the battery. Charging during CV phase happens much slower due to ever decreasing current. When high rate is used in CC phase, the charging voltage limit is reached much faster due to cell heating and resistive drop (seen as voltage increase) similar to that of discharge curve (at high discharge current battery voltage drops, at high charge current voltage steps up). As a result, less charge is transferred to the cell, for example just 60 – 80% or even less. The remaining charge must be delivered in the slower CV phase. The other issue with fast charging is temperature rise. Both resistive losses and ionic conductivity losses produce heat which increase temperature of the battery. When max temperature threshold has been reached, charging current must be decreased hence fast charging transitions to standard charging. This problem can be alleviated if proper thermal management is used for the battery pack. A quality cooling system can keep temperature low (well below max limit, preferably not more that around 30°C) to allow fast charging while avoiding performance degradation. For some battery models, active cooling can allow to increase charging current even higher to achieve faster charging time. In general, it is commonly assumed that EV fast charging (CC phase) can charge battery only to 80% *SoC* level.

Both LFP and LTO chemistries have some charging advantages. As LFP is thermally more stable it can be charged with 3C rate if proper temperature monitoring is used. The charging performance of some LTO cell models is dramatically different. While typical charging rates can be as high as 6C, cells with 10C and 60C pulse charging capability are available on the market. Some of such cells can be charged to 80% SoC in just 6 minutes.

The CC phase ends and transition to CV phase happens once the voltage of the cell reaches charging voltage limit. For LCO, LMO, NMC and NCA chemistries, the charging voltage is 4.2V. Charging to a higher voltage will result in small addition to the capacity however the cell will degrade faster and the safety risks increase dramatically. Some high-energy optimized cells can be charged to 4.3V however in automotive applications the charging voltage is lowered to improve battery lifespan. Lower charging voltage naturally results in lower max SoC hence it is an easy method to decrease used capacity range. As previously noted, decreased used capacity (never fully charged, never fully discharged) increases cycle life. Additionally, keeping a Li-ion cell at its maximum voltage (same as charging voltage) stresses the internal structure which leads to overall degradation. Lowering max voltage reduces this internal chemical stress and promotes longer calendar life. Again, LFP and LTO max charging voltage is significantly different, same as nominal voltage. Depending on the exact chemistry LFP max charging voltage can be in 3.65 - 4V range. 3.65V is the dominating voltage level while 4V in some datasheets will be given as the absolute maximum level after which damage is imminent. LTO cells can be charged to 2.8 – 3V level – significantly less than other graphite anode-based LIBs.

The charging (*SoC* increase) speed gradually decreases during CV phase as the current rate declines. In standard charging, CC phase lasts less than 1 hour while CV phase can be in the range of 1 to 2 hours. As previously noted, majority of charge is delivered to the battery during the short CC phase while the long CV phase delivers remaining fraction. If it is required to fully charge a battery the additional step of cell balancing can increase charging time. The charging is terminated when charging current decreases below cut-off limit. This limit traditionally is

10-3% of the 1C rate. Charging cut-off conditions are not always provided by the battery manufacturer, hence there is some engineering freedom. Additionally, charging timeout can be introduced as well. For example, the datasheet of US18650VTC6 cell (manufactured by Sony) states CCCV charging to 4.2V at 2.5A (0.5C) with 2.5h cut-off - a current cut-off limit is not specified. The timeout criterion can be helpful when the battery reaches its end of life. In some cases, the self-discharge/leakage current increases as the battery ages. If the leakage current is higher than current cut-off level, then battery charging current will never decrease below set cut-off and charger will indefinitely continue charging the battery. A timeout can prevent this situation.

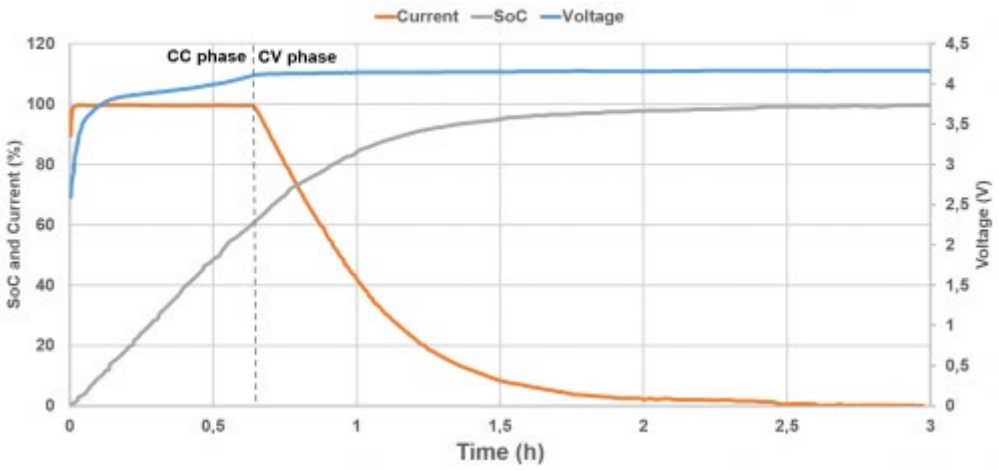

Figure 6.8. Charging curves of an NMC Li-ion cell. Current is expressed in percent where 100% represents 1C rate

Charging is affected by temperature. Cell/battery datasheets provide information about ambient temperature for three situations: discharge, charge and storage. Traditionally one would expect that storage temperature range is the broadest. It is not so in case of LIBs. For short term storage (less than a month) it is the same as discharge operating temperature whose range can be -20°C to +60°C. As the storage time increases, ambient temperature should be kept within -20°C to 25°C range to maintain calendar life. Temperature during charging must be in 0 to 45°C range, preferably below 30°C. Already under 10°C standard charging rate should be decreased to 0.25C. It is generally assumed that LIBs should not be charged if temperature is below 0°C – if temperature is lower, ion mobility is restricted and charging will cause deformation of electrodes, which in turn will degrade performance and safety due to plating of metallic lithium. Both the LIB and the charger should be equipped with temperature monitoring to perform charging only if temperature is within safe operation range. If a battery will be required to be charged at freezing temperatures (an EV in northern countries where the winter temperatures are well below 0°C), then battery pack has to be equipped with thermal management which can provide heating. Of course, the temperature of the LIB will rise on its own during charging due to internal losses – BMS has to prevent temperature rise above operating point. Temperature can be controlled by controlling current or by using active thermal management. It can be noted that charging temperature can vary from model to model and from chemistry to chemistry. Again, LTO excels in operation at low temperatures. An LTO LT34 pouch cell made

by Leclanche can be both discharged and charged at temperatures ranging from -20°C to +55°C. Research laboratories are working on improvements for all Li-ion chemistries to allow charging at temperatures below freezing point. There are reports that some LIBs (non-LTO) can be charged at freezing temperatures albeit at very low rates.

6.4.6. Battery management system

LIBs and even single cells require an obligatory BMS which can have a variety of functions. The main task of a BMS is to maintain a safe operation of the battery – the safety of LIBs has always been an issue which requires special care. The functions can be divided in four groups: protection, monitoring, estimation and balancing. Safety essentially is protection. Some cells have some inherent safety features, such as overpressure, short circuit and thermal protection. Overpressure is implemented as a valve which will open when the internal pressure of a cell reaches critical level. Short circuit protection can be made as an internal fuse or a PTC resistive element whose resistance increases if its temperature gets too high – this acts as thermal protection as well. As these three mechanisms are parts of a cell, they do not constitute a BMS which is made using a set of external elements.

In simplest single cell batteries, the BMS (sometimes called cell/battery protection circuit) can be realized as a single printed circuit board which is equipped with a control logic (microcontroller, ASIC or analog), some measurement circuitry and switch elements. The control element uses measurement circuit to measure cell voltage, current and temperature. The measured voltage is processed to provide undervoltage (UV) and overvoltage (OV) protection. UV condition happens when the cell is being deep discharged. OV condition happens when the cell is overcharged. To prevent both of these damaging conditions, the control logic opens switch elements to stop further discharge or charging. Switches can be implemented as integrated elements of an ASIC, as discrete semiconductors (MOSFETs for example) or as electromechanical switches like relays or contactors. The same switches can be used to stop short circuit current (SC) and over current (OC). The SC condition happens when cell current is higher than absolute maximum rating. The OC condition happens when cell current is higher than rated nominal level for prolonged period. For example, some cell can have a pulse/peak current rating of 20A at 10 seconds. If the current is 20A for longer period than 10 seconds, then OC protection should be activated. In some cases, cell manufacturer limits pulse current depending on the cell temperature hence OC protection is often implemented together with thermal protection – high current naturally causes cell's temperature to rise. When temperature hits some set threshold (over temperature condition (OT)), current must be terminated. Both charging and discharging can be prohibited if temperature is out of safe operation area. This adds under temperature (UT) condition which is particularly important to prevent charging if temperature is below 0°C. When implemented on cell level, these basic protection functions can be realized using small printed circuit boards. For example, the abundant 18650 size cell can be purchased in two variants: unprotected and protected. The unprotected variant is the basic cell with built-in PTC and vent features. The protected variant is equipped with an additional cell protection PCB (18mm in diameter) which is attached to one side of the cell and

the whole package is covered with plastic insulation. The resultant cell is a few millimeters longer as opposed to the unprotected one which is 65mm long. A small protection board is incorporated in even the smallest pouch cells to provide at least minimal protection. In simplest form, the protection board can lack logic circuits and switches. A resettable fuse (for example PPTC) could be used instead.

The same protection features are implemented on battery pack level as well. Naturally, the complexity of the BMS increases with number of cells. In a multi-cell pack, parameter monitoring can be separated as a distinctive function. Designated front-end integrated circuits are being manufactured to fit most battery pack requirements. These ICs perform individual cell voltage measurements, pack voltage measurements, pack current measurements and temperature measurements. Some safety actions can be implemented in the monitoring ICs while others are performed by central controller. Front-end monitoring ICs are equipped with some sort of communication protocols to transfer obtained values to higher level controllers. In large battery packs (such as EVs) the battery is split in modules and each module can have its own module management board which transfers individual cell data to the central BMS board where it is processed, and appropriate actions are taken. Some new variables are generated at the pack level: max and min cell voltage, pack voltage, max and min temperature. These values can be further used not only for basic protection functions but for estimation of various performance indicators and cell balancing. Current monitoring can have its own board or at least IC. Shunt or Hall-effect sensors are used to measure instant values which can be used locally for fast short circuit protection or sent to central controller for advanced processing. For large high-performance packs, thermal management becomes and important issue as proper temperature conditions can greatly expand life span of LIBs. Thermal management system can be a part of overall BMS. Battery packs can be actively cooled (or heated) – temperature of coolant medium and its flow must be monitored as well. BMS monitoring functions might include data logging of all mentioned measured parameters and additional ones like total cycles, max and min discharge levels, total delivered energy and other time and charge related variables.

The central BMS controller uses data from monitoring circuits to implement safety and protection functions. Additionally, data is used to calculate and estimate various performance indicators which can be further used to govern the pack or sent to higher level controllers and user interface. From overall vehicle system perspective, SoC estimation is one of the most important functions as it provides information about the remaining available proportion of charge. There are various SoC estimation algorithms depending on battery chemistry and application. Traditional input parameters are current which is being integrated over time (known as coulomb counting) and voltage of the pack which in turn depends on the instantaneous current value and temperature. As the battery ages, the inner parameter values change and SoC estimator must adapt to those changes. Additional information can be obtained from battery electrochemical impedance spectroscopy (EIS), which in some cases can provide direct information about SoC and in others it can aid to determine other parameters. It must be noted that SoC provides estimate in percent of nominal capacity and not the actual available

energy. When the battery is new, 100% SoC indicates that full rated energy is available, however as the battery ages, the capacity decreases thus after some years of operation the SoC of a fully charged battery will be 100% but the actual energy might be just 80% of what it was when the battery was new. This brings to another battery performance indicator: the state-of-health (SoH). In simplest form, SoH indicates how much the capacity of the battery has degraded. It can be estimated by dividing actual capacity by nominal rated capacity. The result is expressed in percent. A 100% SoH indicates that battery is new – this number will gradually decrease as the battery ages. SoH can be defined differently: it can represent the remaining useful life (RUL) of the battery. In this case the estimation becomes a lot more complex as it takes into consideration the impedance change (using EIS), the cycle life (in form of cycle counter) and other parameters like self-discharge. The result can be expressed in percent, remaining total storable energy or even remaining days before failure. Another parameter to estimate is the state-of-power (SoP) or simply available power. The available power depends on the ambient temperature, temperature of pack and SoC. It indicates how much power for how long time can be discharged. This parameter is important is systems where future activity (high discharge rates) can be and has to planned.

These previously described BMS function groups (protection, monitoring, estimation) to some extent are common for all high-performance/high-cost/high-reliability applications and battery chemistries. The last function – balancing, is not obligatory for most chemistries (although it can be used in all), however it is essential for LIBs. Lead-acid and NiMH chemistry cells can be balanced by trickle charging; however, it is not allowed for Li-ion chemistries, hence external circuits must be introduced to provide balancing. The balancing function is used to keep all cells of a battery at the same charge level although typically, balancing keeps cells at the same voltage level. There are two reasons for cell mismatch. The first one is that all cells are not created equal – manufacturing differences affect capacities, leakage and other parameters of individual cells. The other cause of misbalance stems from usage and ageing – temperature gradient, interconnection structure and just plain ageing can cause cells to develop different capacities, OCV curves and leakage over time. When all cells of a battery pack are perfectly balanced, the available capacity is maximal. However, if one cell is at lower SoC, it decreases the SoC of the whole pack – it will be the first cell to reach discharge cut-off threshold and hence the battery is rendered empty although other cells still have usable charge. This is the case where the weakest link determines the strength of the chain. Additionally, when a misbalanced pack is charged and a single cell is misbalanced at higher SoC, it will reach full voltage faster. If charging is continued, this cell will be overcharged with all damaging consequences. Hence charging must be stopped when any of the cells of a battery pack reach full voltage.

A variety of balancing topologies can be used to equalize cell voltages/SoC levels to maintain optimal battery performance. The simplest and most widespread is the passive balancing. The topology consists of a switch (for example MOSFET) which connects a resistor across a cell whose voltage is too high (more than other cells). The resistor is referenced to as shunt or bleeder resistor as its removes excessive charge. The operation of the switch is controlled by

BMS balancing controller. Commonly, this passive balancing (also know as resistor balancing, shunting balancing) is done only during the end phase of the charging. When first cell reaches full voltage, the charging current is decreased to prevent overcharging the full voltage cell while still charging remaining cells. The balancing process can take a long time as shunting resistor usually provide just a few mA of discharging current. Hence it can be continued after the charger is disconnected from the pack. Balancing at the full SoC is known as top balancing. Alternatively, balancing can be done at discharge: all cells are fully discharged using balancing resistors to achieve equal SoC. Passive balancing while being simple, easy to implement and cost effective, has its drawbacks: the balancing rate is low and can take hours to achieve good balance (depending on the level of misbalance); it wastes energy – all excessive charge is dissipated as heat in the shunting resistors. An alternative is to use active balancing. A variety of topologies have been developed which can transfer charge from full cells to ones with less charge thus preserving valuable energy. Active balancing can be used at all times as opposed to passive which usually is used only during charging. It can be designed to provide high balancing current to deal with high mismatch. However, the main drawback is complexity which adds to cost and reliability issues. Passive balancing is sufficient in most situations, especially if cells of a battery pack are sorted and matched prior to pack assembly – only miniscule balancing is required during charging for most of battery life. Furthermore, battery chemistries and manufacturing process is being continuously improved to minimize cell parameter dispersion (both of fresh and aged cells) and increase overcharge tolerance thus reducing requirements of balancing circuits.

BMS and its functions can extend further. As mentioned, thermal management can be a part of BMS, especially if active temperature control is used: forced air or liquid cooling/heating. In EVs charging is controlled by the BMS as it has information about charging voltage, current and can provide temperature and safety control. BMS has communication interface to the main vehicle control system. Some sort of charger is usually implemented in an EV and in some cases the charger is a part of the battery pack. EV batteries are equipped with fuses and set of contactors: for work current and precharge. Smaller batteries can have some human machine interface (HMI), for example a set of LEDs, to indicate remaining charge. All of these features are controlled by the BMS.

6.5. Fuel cell technology

Fuel cells (FC) are devices somewhat like batteries. Their purpose is to provide electrical energy by converting chemical energy. Same as batteries they are electrochemical devices. The main difference is that fuel cells uses some sort of chemical compound (fuel) which is supplied to the cell to produce electricity by controlled electrochemical redox reaction. The fuel and oxidizing material (oxygen from air) is consumed during the process. On the other hand, battery already had all components embedded in a closed package and no material was consumed during charging/discharging. Fuel cell technology has a long history as it was invented in 19th century. Since then various configurations have been developed and implemented in stationary or portable applications ranging from few Watts of power to mega-watt systems. The most

notable fuel cell technology is the proton exchange membrane fuel cell (PEM FC). The basic elements of a fuel cell are anode, cathode and electrolyte. A PEM layer contains electrolyte and separates anode from cathode. Fuel is delivered to the anode side while oxygen is delivered to the cathode side. Popular fuels are hydrogen and methanol. As an electrochemical reaction takes place, protons from fuel are transferred through the PEM to the cathode side where waste is produced: water in case of hydrogen fuel and CO_2 if methanol FC is used. As usual, electrical load is connected to anode and cathode to deliver electrical energy. The reaction is unidirectional – PEM FC delivers energy and it cannot be charged.

Several FC cells are stacked together to increase current and/or voltage thus making a FC stack similarly as in the case of battery packs. The nominal voltage of a single PEM FC cell is approximately 1V and it is load dependent. A hydrogen PEM FC is considered compact power source (high specific energy and energy density) and it can be refueled quickly – one just needs to fill the hydrogen container – a process which takes just a couple minutes. These features make hydrogen FCs a good candidate for powering EVs and other mobile applications. However, widespread adaptation has not been successful so far due to some disadvantages. PEM FCs have high initial costs, in part due to expensive catalyst materials, additionally as FCs age, their voltage and power output decreases hence they have a limited life span (operating hours). FCs are not as efficient as LIBs. Common efficiencies are in 50 to 60% range which means that significant amount of heat will be generated during power production – a cooling system like the one of common ICE vehicles is required as the temperature operational range of FCs is limited. The high cost and limited power density results in requirement of additional energy storage element – a battery or supercapacitor. FCs have an optimal power output level which usually is lower than the power required to accelerate a vehicle. During constant speed driving there is supplementary power which can be used to charge a battery which in turn can be used to provide the required power boost during acceleration. A battery is beneficial for regenerative braking – FC cannot be used to store braking energy. A key issue for hydrogen FC adoption is the lack of refueling infrastructure. Hydrogen gas is extremely flammable, it can diffuse in and through metals and it can cause metal embrittlement hence manufacturing, handling and storing hydrogen requires additional care. The final problem is the source of hydrogen. The amount of hydrogen in atmosphere is negligible hence it must be manufactured. It can be produced by electrolysis of water however this process is inefficient even further decreasing the total FC technology full-cycle efficiency. Currently, majority of hydrogen is produced by reforming fossil fuel – not a sustainable solution. Despite these drawbacks, hydrogen FC technology has been and is used in some commercial EV products. There are a few available automobile models and several public transport buses. The later has shown good performance as buses have stable cyclic usage and plenty of space for FC and hydrogen storage tank installation.

6.6. Supercapacitors

In simplistic terms, supercapacitors (SC) are capacitors with extremely high capacity. In fact, they use special physical effects (electrochemical pseudocapacitance and/or electrostatic double-layer capacitance) to provide capacity. Depending on brand-names and physical effects, supercapacitors are also called boost capacitors, ultracapacitors, pseudocapacitors and electrostatic double-layer

capacitors (EDLC). One must not confuse SCs with common high-capacity aluminum electrolytic capacitors which are made with rated voltages from few to hundreds of volts. The rated voltage of a single SC cell is in the range of 2.1 to 3V. While majority of SCs are available as single cells, commercial SC batteries (series/parallel) with voltages higher than 100V are available on the market. The capacity of single SCs ranges from hundreds of millifarads to a few kilofarads – they extend capacitor capacity range as the largest electrolytic capacitors are just around 1F in capacity. If compared to LIBs, SC main advantage is the high specific power density (up to 14kW/kg) and vast cycle life (1000000 cycles). However, they have not replaced LIBs or other batteries due to relatively minuscule specific energy (7.4Wh/kg for 3400F capacitor) which makes them inappropriate for bulk energy storage. SCs can be used to improve the power capability of battery systems, especially in applications where the bulk energy storage is a relatively low capacity battery (with low power) as in hybrid vehicles and fuel cell vehicles. SCs can be successfully implemented in applications requiring regenerative braking: the power handling capability of SCs is perfect for absorbing high power pulses of braking while the stored energy can be used for the following acceleration also requiring high power.

SC technology is evolving to improve the overall performance. Hybrid capacitors have been developed – they use both SC and Li-ion technology. The result is so called lithium ion capacitor – as name suggests, it is more like a capacitor with some features of the Li-ion battery. The main advantage is elevated voltage: 3.8V rated voltage increases the specific energy narrowing the gap between SCs and LIBs. Future improvements using graphene materials could increase performance of SC, the same is true for LIBs.

To conclude this chapter see Figure 6.9. - a Ragone plot which is an effective tool to graphically compare gravimetric energy density (specific energy) and gravimetric power density (specific power) of various energy storage elements. The lowest performance is at the bottom left corner while the highest performance is at the top right corner - a spot to be taken by future technologies. Given figure represents generalized performance - higher performing application specific technologies exist and are under continuous development. As can be seen fuel cell technology can provide the highest specific energy while capacitors can provide the highest specific power. However, Li-ion technology with its high specific energy and good specific power is the right choice for most mobile/portable applications.

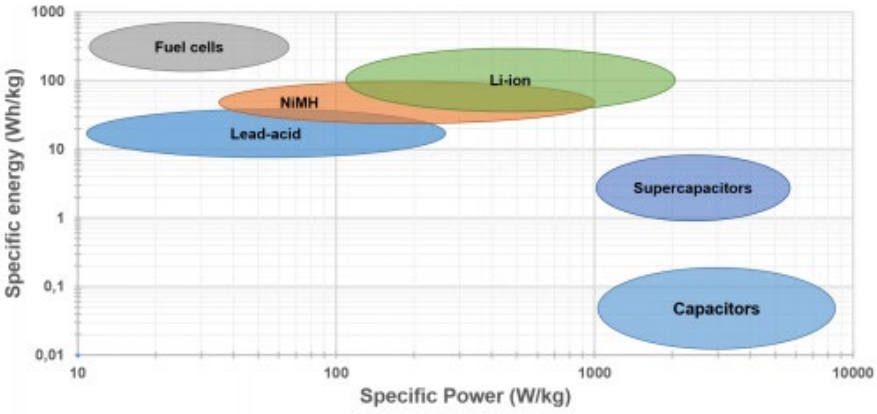

Figure 6.9. General Ragone plot of energy storage elements

References

1. Hnatov, Andrii. Field of study - electrical engineering : Synopsis of lectures on the discipline "Electrical systems of environmentally friendly motor vehicles" [Electronic resourse] / Andrii Hnatov, Olha Ulianets ; Kharkiv National Automobile And Highway University. – Kharkiv, 2025. – 101 p. ftp://194.44.189.147/libfulltxt/UCHLIB/ER/2025/KL_ElectricalSystems_HnatovUlianets_2025.pdf
2. Hnatov, Andrii. Field of study - electrical engineering : Synopsis of lectures on the discipline "Electric drive theory" [Electronic resourse] / Andrii Hnatov, Olha Ulianets ; Kharkiv National Automobile and Highway University. – Kharkiv, 2025. – P. 1 : Mechanical characteristics of DC and AC electric drives. – 114 p. ftp://194.44.189.147/libfulltxt/UCHLIB/ER/2025/KL_HnatovUlianets_EDT_P1_2025.pdf
3. Zabasta, A., Kunicina, N., Nikiforovab, O., Peuteman, J., Fedotovd, A. K., Fedotovd, A. S., & Hnatove, A. Development of industry oriented cross-domain study programs in cyber-physical systems for Belarusian and Ukrainian universities. Multi-Paradigm Modelling Approaches for Cyber-Physical Systems, 2021, Pages 271-292. ISBN 978-0-12-819105-7, DOI: https://doi.org/10.1016/B978-0-12-819105-7.00016-7
4. Kuņicina, N., Zabašta, A., Romānovs, A., Pečerska, J., Ribickis, L., Hnatov, A., Shchasiana, A., Dziubenko, O., Rudenko, N., Borodenko, Y., Danylenko, K., Morkun, N., Zavsiehdashnia, I., Sistuk, V., Monastyrskyi, Y., Ruban, S., Tron, V., Peuteman, J.: підручник/ Cyber-Physical Systems for Clean Transportation. Rīga: RTU Izdevniecība, 2022. 391 p. ISBN 978-9934-22-676-2. (DOI 10.7250/9789934226762) https://ebooks.rtu.lv/product/cyber-physical-systems-for-clean-transportation/?lang=en
5. Теорія електроприводу транспортних засобів: підручник / [А.В. Гнатов, Щ.В. Аргун, І.С. Трунова]. – Х.: ХНАДУ, 2016 – 292 с.
6. Hnatov A. Energy saving technologies for urban bus transport / A. Hnatov, Shch. Arhun, S. Ponikarovska // International Journal of Automotive and Mechanical Engineering. 2017. – №14(4). – P. 4649-4664. doi: https://doi.org/10.15282/ijame.14.4.2017.5.0366.
7. Hnatov A. ESTET – New innovative specialty for master students / A. Hnatov, Shch. Arhun, O. Ulyanets // Автомобільний транспорт. – Х. : ХНАДУ. – 2018. – Вып. 42. – С. 103-110.
8. Hnatov, A., Arhun, S., Dziubenko, O., & Ponikarovska, S. (2018). Choice of Electric Engines Connection Circuits in Electric Machine Unit of Electric Power Generation Device. Majlesi Journal of Electrical Engineering, 12(4), 87-95. Retrieved from http://mjee.iaumajlesi.ac.ir/index/index.php/ee/article/view/2760
9. S. Arhun, A. Hnatov, O. Dziubenko, S. Ponikarovska. A Device for Converting Kinetic Energy of Press into Electric Power as a Means of Energy Saving. J. Korean Soc. Precis. Eng., Vol. 36, No. 1, pp. 105-110. January 2019. Doi:http://doi.org/10.7736/KSPE.2019.36.1.105.

10. Migal, V., Arhun, S., Hnatov, A., Dvadnenko, V., & Ponikarovska, S. Substantiating the Criteria for Assessing the Quality of Asynchronous Traction Electric Motors in Electric Vehicles and Hybrid Cars //한국정밀공학회지. – 2019. – Т. 36. – №. 10. – С. 989-999.

11. Arhun S., Migal V., Hnatov A., Hnatova H., & Ulyanets O. (2020). System Approach to the Evaluation of the Traction Electric Motor Quality. EAI Endorsed Transactions on Energy Web, 7(26). DOI:10.4108/eai.13-7-2018.162733

12. Гнатов А. В., Аргун Щ. В., Гнатова Г. А. Тягові характеристики силової установки електробуса //Науковий вісник Херсонської державної морської академії. – 2019. – Т. 2. – №. 21. – С. 36-43.

13. Mygal, V., Arhun, S., Shuliak, M., Hnatov, A., Kalinin, E., & Mysiura, M. (2021). Functional and Engineering Methods of Upgrading the Quality of Induction Traction Electric Motors. EAI Endorsed Transactions on Energy Web, e20. http://eprints.eudl.eu/id/eprint/4901/

14. Hnatov, A., & Arhun, S. (2022). Electric vehicles and energy-saving technologies – master's degree program under the Erasmus project Cybphys. Automobile Transport, (51), 85–95. https://doi.org/10.30977/AT.2219-8342.2022.51.0.09

15. Borodenko Y. M., Hnatov A. V., Arhun S. V., Sokhin P. A. (2023)Energy aspects of automobile transport development. Automobile Transport, (53). P.37-50. DOI: 10.30977/AT.2219-8342.2023.53.0.05

16. Hnatov A., Arhun Shch., Ponikarovska S., Ulyanets O. Ultracapacitors electrobus for urban transport. IEEE 38th International Conference on Electronics and Nanotechnology (ELNANO-2018) – April 24 –26, 2018. – Kyiv, Ukraine. – P. 539–543. doi: 10.1109/ELNANO.2018.8477449.

17. Patlins A., Hnatov A., Kunicina N., Arhun S., Zabasta A., Ribickis L. Sustainable pavement enable to produce electricity for road lighting using green energy. 2018 Energy and Sustainability for Small Developing Economies (ES2DE). 9-12 July, 2018. – Funchal, Portugal. – P.1–2. doi: 10.1109/ES2DE.2018.8494236.

18. Patlins, A., Hnatov, A., Arhun, S., & Dzyubenko, O. (2019). Design and research of constructive features of paving slabs for power generation by pedestrians. Transportation Research Procedia, 40, 434-441. Doi: https://doi.org/10.1016/j.trpro.2019.07.063.

19. Patļins, A., Hnatov, A., Arhun, S., Bogdan, D., Dziubenko, O. Development of an Energy Generating Platform for Converting Kinetic Energy into Electrical Energy Using the Kinematic Synthesis of a Three-Stage Multiplier. In: TRANSPORT MEANS 2019. Sustainability: Research and Solutions. PROCEEDINGS OF THE 23rd INTERNATIONALSCIENTIFIC CONFERENCE PART I., Lithuania, Palanga, 2-4 October, 2019. Kaunas: Kaunas University of Technology, 2019, pp.403-408. ISSN 1822-296X. e-ISSN 2351-7034.

20. Hnatov, A., Arhun, S., Tarasov, K., Hnatova, H., Mygal, V., Patļins, A. Researching the model of electric propulsion system for bus using Matlab Simulink //2019 IEEE 60th

International Scientific Conference on Power and Electrical Engineering of Riga Technical University (RTUCON). – IEEE, 2019. – C. 1-6.
DOI: 10.1109 / RTUCON48111.2019.8982352

21. Arhun Shch., Hnatov A., Mygal V., Khodyriev S., Popova A., Hnatova H. An integrated system of alternative sources of electricity generation for charging urban electric buses. 2020 IEEE 40th International Conference on Electronics and Nanotechnology (ELNANO) – April 24-26, 2020. –
Kyiv, Ukraine – P. 619-624 10.1109 / ELNANO50318.2020.9088911

22. Hnatov, A., Ribickis, L., Hnatova, H., Zabasta, A., Kunicins, K. Study of the Operation of the Energy Generating Platform on the Basis of a Multiplier with Spur Gears //2020 6th IEEE International Energy Conference (ENERGYCon). – IEEE. – pp. 231-237. DOI: 10.1109 / ENERGYCon48941.2020.9236460. https://ieeexplore.ieee.org/document/9236460

23. Hnatov, A., Patlins, A., Arhun, S., Ulianets, O., Romanovs, A. Development of an unified energy-efficient system for urban transport //2020 6th IEEE International Energy Conference (ENERGYCon). – IEEE. – pp. 248–253.
DOI: 10.1109/ENERGYCon48941.2020.9236606. https://ieeexplore.ieee.org/document/9236606

24. Hnatov, A., Arhun, S., Hnatova, H., Bagach, R., Patlins, A., & Zabasta, A. (2021, November). Implementation of the double degree master's program on the example of the Erasmus project CybPhys. In 2021 IEEE 62nd International Scientific Conference on Power and Electrical Engineering of Riga Technical University (RTUCON) (pp. 1-6). IEEE. DOI: 10.1109/RTUCON53541.2021.9711716.

25. Zabasta, A., Peuteman, J., Kunicina, N., Kazymyr, V., Hnatov, A., Sistuk, V., & Bisenieks, M. (2023, February). Implementing the Practically-Oriented Curricular in the Field of Cyber-Physical Systems: A Case Study of the School for Ukrainian Students. In Learning in the Age of Digital and Green Transition: Proceedings of the 25th International Conference on Interactive Collaborative Learning (ICL2022), Volume 2 (pp. 861-872). Cham: Springer International Publishing. https://doi.org/10.1007/978-3-031-26190-9_88

26. Patlins, A., Hnatov, A., & Arhun, S. (2018). Safety of pedestrian crossings and additional lighting using green energy. In Transport Means-Proceedings of the International Conference (pp. 527-531).

27. Hnatov, A., Arhun, S., Mygal, V., Bisenieks, M., Grants, R., & Ulianets, O. (2023, October). Prospects for the Use of Electric Drives in Urban Passenger Vehicle Transport in Ukraine. In 2023 IEEE 64th International Scientific Conference on Power and Electrical Engineering of Riga Technical University (RTUCON) (pp. 1-6). IEEE. https://ieeexplore.ieee.org/abstract/document/10413061

28. Arhun, S., Hnatov, A, Kunicina, N., Trunova, I., Ulianets, O., Daleka, V. Integrating Sustainability in Engineering with a Double Degree Program Case Study. In: 2024 IEEE 65th International Scientific Conference on Power and Electrical Engineering of Riga Technical University (RTUCON), Latvia, Riga, 10-12 October, 2024. Riga, Latvia: Riga Technical University, 2024. P. 1-6. DOI: 10.1109/RTUCON62997.2024.10830879 https://www.scopus.com/record/display.uri?eid=2-s2.0-85217217162&origin=recordpage

29. Arhun, S., Hnatov, A, Kunicina, N., Research on the “Electric Vehicles and Automotive Electronics” Curriculum Aimed at Modernization within the DIGITRANS Project. In: 2024 IEEE 65th International Scientific Conference on Power and Electrical Engineering of Riga Technical University (RTUCON), Latvia, Riga, 10-12 October, 2024. Riga, Latvia: Riga Technical University, 2024. P. 1-4. DOI: 10.1109/RTUCON62997.2024.10830865 https://www.scopus.com/record/display.uri?eid=2-s2.0-85217210603&origin=recordpage

30. Arhun, S., Dvadnenko, V., Hnatov, (2024). Optimization of Battery Management Systems to Enhance Efficiency and Reliability of Lithium Iron Phosphate Batteries. Transport Means - Proceedings of the International Conference. 2024-October, 2024 28th International Scientific Conference Transport Means 2024. Kaunas, (2 - 4 October 2024). P. 116 – 121. DOI 10.5755/e01.2351-7034.2024.P247-252

31. Arhun, S., Migal, V., Hnatov, A., Ponikarovska, S., Hnatova, H., & Novichonok, S. (2020). Determining the Quality of Electric Motors by Vibro-Diagnostic Characteristics. EAI Endorsed Trans. Energy Web, 7(29), e6.

32. Arhun, S., Hnatov, A., Hnatova, H., Patlins, A., & Kunicina, N. (2020, November). Problems that have arisen in universities in connection with COVID-19 on the example of the Double Degree Master's Program “Electric Vehicles and Energy-Saving Technologies”. In 2020 IEEE 61th international scientific conference on power and electrical engineering of Riga Technical university (RTUCON) (pp. 1-6). IEEE.

33. Zabasta, A., Peuteman, J., Kunicina, N., Kazymyr, V., Hvesenya, S., Hnatov, A., ... & Ribickis, L. (2020). Research on cross-domain study curricula in cyber-physical systems: A case study of Belarusian and Ukrainian Universities. Education Sciences, 10(10), 282.

34. Аргун, Щ. В., Гнатов, А. В., & Ульянець, О. А. (2016). Екологічний та енергоефективний атомобільний транспорт та його інфраструктура. ВІСНИК ЖДТУ. 2016. № 2 (77), 18-26.

35. Borodenko, Y., Ribickis, L., Zabasta, A., Arhun, S., Kunicina, N., Zhiravetska, A., ... & Kunicins, K. (2020). Using the method of the spectral analysis in diagnostics of electrical process of propulsion systems power supply in electric car. Przeglad Elektrotechniczny, 96(10), 47-50.

36. Гнатов, А. В. Електромобілі – майбутнє, яке вже настало / А. В. Гнатов, Щ. В. Аргун, О. А. Ул'янець // Автомобіль і електроніка. Сучасні технології : зб. наук. пр. [Електронний ресурс] / М-во освіти і науки України, ХНАДУ. - Харків, 2017. - Вип. 11.

37. BIRKE, K.P. Modern Battery Engineering: A Comprehensive Introduction. World Scientific Publishing Co Pte Ltd, 2019, 304 p. ISBN: 9811215987.

38. EHSANI, M., GAO, Y., LONGO, S., EBRAHIMI, K., Modern Electric, Hybrid Electric, and Fuel Cell Vehicles, 3rd Edition, CRC Press, 2018.

39. IQBAL, H. Electric and Hybrid Vehicles Design Fundamentals, 3rd Edition, CRC Press, 2021.

40. INCI, M., BÜYÜK, M., DEMIR, M.H., ILBEY G. A review and research on fuel cell electric vehicles: Topologies, power electronic converters, energy management methods, technical challenges, marketing and future aspects, Renewable and Sustainable Energy Reviews 137 (2021) 110648.
41. WINTER, M., BRODD, R. J. What Are Batteries, Fuel Cells, and Supercapacitors?, Chemical Review Journal, (2004) 104, 4245, https://www.matsusada.com/column/edlc.html
42. VIVEKCHAND, S.R.C., ROUT, Ch.S., SUBRAHMANYAM, K.S., GOVINDARAJ, A., RAO, C.N.R. Graphene-based electrochemical supercapacitors. J. Chem. Sci., Indian Academy of Sciences, no. 120, January, 2008, p. 9−13.
43. CHAU, K.T. Electric Vehicle Machines and Drives. John Wiley & Sons Inc, 2015, 424 p. ISBN: 111875252X.
44. DENTON, T., PELLS, H. Electric and Hybrid Vehicles. Taylor & Francis Ltd, 2023, 296 p. ISBN: 9781032556796.
45. NIKOWITZ, M. Advanced Hybrid and Electric Vehicles. Springer International Publishing AG, 2018, 211 p. ISBN: 9783319799261.
46. PAWAR, S.R. Electrical Vehicle Technology. Notion Press, 2021, 132 p. ISBN: 1685545610.
47. ENGE, P., ENGE, N., ZOEPF, S. Electric Vehicle Engineering (Pb). MCGRAW HILL BOOK CO, 2020, 210 p. ISBN: 1265900523.
48. IQBAL, H. Electric and Hybrid Vehicles. Taylor & Francis Ltd, 2021, 498 p. ISBN: 0367693933.
49. BHOI, A.K., PADMANABAN, S. Electric Vehicles. Springer Verlag, Singapore, 2020, 300 p. ISBN: 9811592500.
50. New passenger cars by type of motor energy, Available online: https://ec.europa.eu /eurostat/databrowser/view/road_eqr_carpda/default/table?lang=en&category=road.road_eqr (accessed on 20 October 2024).
51. EAFO Analysis: Trends in EV Charging Infrastructure Across Europe, Available online: https://alternative-fuels-observatory.ec.europa.eu/general-information/news/eafo-analysis-trends-ev-charging-infrastructure-across-europe (accessed on 15 October 2024).
52. New Study on Accelerating EU Electric Vehicle Charging Infrastructure Roll-out, Available online: https://alternative-fuels-observatory.ec.europa.eu/general-information/news/new-study-accelerating-eu-electric-vehicle-charging-infrastructure-roll (accessed on 15 October 2024).
53. Sanguesa, J.A.; Torres-Sanz, V.; Garrido, P.; Martinez, F.J.; Marquez-Barja, J.M. A Review on Electric Vehicles: Technologies and Challenges. Smart Cities 2021, 4, 372–404
54. Different types of EV Charging Connectors Available online: ttps://bestchargers.eu/blog/ different-types-of-ev-charging-connectors/ (accessed on 29 October 2024).

55. SAE International. Vehicle Architecture for Data Communications Standards—Class B Data Communications Network Interface; Standard; SAE International: Warrendale, PA, USA, 2009.

56. International Electrotechnical Commission. Plugs, Socket-Outlets, Vehicle Couplers and Vehicle Inlets—Conductive Charging of Electric Vehicles—Part 1: General Requirements; Standard; IEC: Geneva, Switzerland, 2014.

57. EV plug of GB20234 and recommended size of their charging cable.

58. EV Industry Blog, Available online: https://evchargingsummit.com/blog/everything-about-vehicle-to-grid-v2g/ (accessed on 1 October 2024).

59. The Solution To Sustainable Urban Mobility And Energy Available online: https://www.amsterdamvehicle2grid.nl/ (accessed on 3 December 2024

60. G. C. Carmen Angelina, H. Rosales Manuel, and F. De la Mota Idalia, "Pilot simulation for public passenger transport energy consumption," Comput Into Eng, vol. 197, p. 110535, Nov. 2024, doi: 10.1016/J.CIE.2024.110535.

61. "Eclipse SUMO - Simulation of Urban MObility." Accessed: Jan. 23, 2025. [Online]. Available: https://eclipse.dev/sumo/

62. J. Fu, H. Lin, Y. Niu, and S. He, "Share Ratio Change of Public Transport in Airport Landside under the Background of Car Population Rapid Increase—A Case of Shanghai Pudong International Airport," Transportation Research Procedia, vol. 25, p. 92-102, 2017, doi: 10.1016/j.trpro.2017.05.384.

63. Shanghai-Hangzhou Maglev. Accessed: Jan. 24, 2025. [Online]. Available: https://www.railway-technology.com/projects/shanghai-maglev/

64. "Everything about Shanghai Maglev Train: Speed, Station, Map, Ticket & Price, Facts...," www.chinadiscovery.com, Accessed: Jan. 24, 2025. [Online]. Available: https://www.chinadiscovery.com/shanghai/shanghai-maglev.html

65. D. Ding and X. Y. Wu, "Hydrogen fuel cell electric trains: Technologies, current status, and future," Applications in Energy and Combustion Science, vol. 17, p. 100255, Mar. 2024, doi: 10.1016/J.JAECS.2024.100255.

66. Y. Peng et al., "Energy consumption analysis and multiple-criteria evaluation of high-speed trains with different marshaled forms in China," Science of The Total Environment, vol. 759, p. 143678, Mar. 2021, doi: 10.1016/J.SCITOTENV.2020.143678.

67. I. González–Franco and A. García–Álvarez, "Can High–Speed Trains Run Faster and Reduce Energy Consumption?," Procedia Soc Behav SciPhys., Vol. 48, pp. 827–837, Jan. 2012, doi:10.1016/j.SBSPRO.2012.06.1060.

68. B. Igliński et al., "Renewable energy transition in Europe in the context of renewable energy transition processes in the world. A review," Heliyon, vol. 10, no. 24, p. 40997, Dec. 2024, doi: 10.1016/J.HELIYON.2024.E40997.

69. R. Damián and C. I. Zamorano, “Life cycle greenhouse gases emissions from high-speed rail in Spain: The case of the Madrid – Toledo line,” Science of The Total Environment, vol. 901, p. 166543, Nov. 2023, doi: 10.1016/J.SCITOTENV.2023.166543.

70. D. Liu, J. Wang, L. Xu, H. Zhang, and X. Tan, “Comparison of energy consumption and carbon emissions of high-speed rail with other transportation modes from life cycle perspective: A case of Beijing-Shanghai,” Research in Transportation Business & Management, vol. 59, p. 101278, Mar. 2025, doi: 10.1016/J.RTBM.2024.101278.

71. G. Ling, C. Han, Z. Yang, and J. He, “Energy consumption and emission analysis for electric container ships,” Ocean Coast Manag, vol. 261, p. 107505, Feb. 2025, doi: 10.1016/J.OCECOAMAN.2024.107505.

72. K. Wang et al., “A comprehensive review on the prediction of ship energy consumption and pollution gas emissions,” Ocean Engineering, vol. 266, p. 112826, Dec. 2022, doi: 10.1016/J.OCEANENG.2022.112826.

73. J. Yuan and V. Nian, “Ship Energy Consumption Prediction with Gaussian Process Metamodel,” Energy Procedia, vol. 152, pp. 655–660, Oct. 2018, doi: 10.1016/J.EGYPRO.2018.09.226.

74. Y. Shu et al., “Investigation of ship energy consumption based on neural network,” Ocean Coast Manag, vol. 254, p. 107167,
Aug. 2024, doi: 10.1016/J.OCECOAMAN.2024.107167.

75. C. Wang, Y. Ju, T. Wang, and S. Zou, “Transient performance study of high pressure fuel gas supply system for LNG fueled ships,” Cryogenics (Guildf), vol. 125, p. 103510, Jul. 2022, doi: 10.1016/J.CRYOGENICS.2022.103510.

76. Z. Wang, B. Dong, M. Li, Y. Ji, and F. Han, “Configuration of Low-Carbon fuels green marine power systems in diverse ship types and Applications,” Energy Convers Manag, vol. 302, p. 118139, Feb. 2024, doi: 10.1016/J.ENCONMAN.2024.118139.

77. Y. Chen, B. Sun, X. Xie, X. Li, Y. Li, and Y. Zhao, “Short-term forecasting for ship fuel consumption based on deep learning,” Ocean Engineering, vol. 301, p. 117398, Jun. 2024, doi: 10.1016/J.OCEANENG.2024.117398.

78. Y. Yuan, J. Wang, X. Yan, Q. Li, and T. Long, “A design and experimental investigation of a large-scale solar energy/diesel generator powered hybrid ship,” Energy, vol. 165, pp. 965–978, Dec. 2018, doi: 10.1016/J.ENERGY.2018.09.085.

79. M. Maaruf and M. Khalid, “Power management and control of an all-electric ship powered by solar photovoltaic and hydrogen energy system,” Performance Enhancement and Control of Photovoltaic Systems, pp. 285–296, Jan. 2024, doi: 10.1016/B978-0-443-13392-3.00015-3.

80. T. Jayson, A. S. M. Bakibillah, C. P. Tan, M. A. S. Kamal, V. Monn, and J. ichi Imura, “Electric vehicle eco-driving strategy at signalized intersections based on optimal energy consumption,” J Environ Manage, vol. 368, p. 122245, Sep. 2024, doi: 10.1016/J.GENVMAN.2024.122245.

81. H. Huang, B. Li, Y. Wang, Z. Zhang, and H. He, “Analysis of factors influencing energy consumption of electric vehicles: Statistical, predictive, and causal perspectives,” Appl Energy, vol. 375, p. 124110, Dec. 2024, doi: 10.1016/J.APENERGY.2024.124110.

82. A. Urooj and A. Nasir, “Review of intelligent energy management techniques for hybrid electric vehicles,” J Energy Storage, vol. 92, p. 112132, Jul. 2024, doi: 10.1016/J.EST.2024.112132.

83. F. Jiang et al., “A comprehensive review of energy storage technology development and application for pure electric vehicles,” J Energy Storage, vol. 86, p. 111159, May 2024, doi: 10.1016/J.EST.2024.111159.

84. F. Earrings et al., “Energy consumption of a last generation full hybrid vehicle compared with a conventional vehicle in real drive conditions,” Energy Procedia, vol. 148, pp. 289–296, Aug. 2018, doi: 10.1016/J.EGYPRO.2018.08.080.

85. X. Zeng, J. Li, C. Duan, Y. Huang, and D. Song, “An optimal energy consumption calculation method of hybrid electric vehicles with frequency distribution characteristics of driving conditions,” Sustainable Energy Technologies and Assessments, Vol. 72, P. 104083, DEC. 2024, Doi: 10.1016/j.Ceta.2024.104083.

86. H. Tang, A. Rauf, Q. Lin, G. Dou, and C. Qin, “Hybrid mutual authentication for vehicle-to-infrastructure communication without the coverage of roadside units,” Vehicular Communications, vol. 50, p. 100850, Dec. 2024, doi: 10.1016/J.VEHCOM.2024.100850.

87. H. Mehrjerdi and R. Hemmati, “Electric vehicle charging station with multilevel charging infrastructure and hybrid solar-battery-diesel generation incorporating comfort of drivers,” J Energy Storage, vol. 26, p. 100924, Dec. 2019, doi: 10.1016/J.EST.2019.100924.

88. E. C. Jones and B. D. Leibowicz, “Contributions of shared autonomous vehicles to climate change mitigation,” Transp Res D Transp Environ, vol. 72, pp. 279–298, Jul. 2019, doi: 10.1016/J.TRD.2019.05.005.

89. E. A. Nanaki and C. J. Koroneos, “Climate change mitigation and deployment of electric vehicles in urban areas,” Renew Energy, vol. 99, pp. 1153–1160, Dec. 2016, doi: 10.1016/J.RENENE.2016.08.006.

90. F. W. Mohd Hasan Wong, D. Al Kez, D. F. Del Rio, A. Foley, D. Rooney, and M. Abai, “Decarbonizing and offsetting emissions in the airline industry: Current perspectives and strategies,” Energy, vol. 313, p. 133809, Dec. 2024, doi: 10.1016/J.ENERGY.2024.133809.

91. D. Wu, Y. Zhang, and Q. Xiang, “Could improving public transport accessibility reduce road traffic carbon dioxide emissions? A simulation-based counterfactual analysis,” J Transp Geogr119, P. 103970, Jul. 2024, Yogurt: 10.1016/J.Jetrange.2024.103970.

92. S. Cui, X. Zhou, Z. Zhang, F. Liu, and C. Kou, “A comprehensive review of chemical reaction mechanisms and soot generation mechanisms for hydrogen and diesel additions to ammonia fuel and their emission characterization,” Process Safety and Environmental Protection, vol. 190, pp. 413–442, Oct. 2024, doi: 10.1016/J.PSEP.2024.07.059.

93. P. Halder et al., “Performance, emissions and economic analyses of hydrogen fuel cell vehicles,” Renewable and Sustainable Energy Reviews, vol. 199, p. 114543, Jul. 2024, doi: 10.1016/J.RSER.2024.114543.

94. M. Karimi, H. Simsek, and K. Kheiralipour, “Advanced biofuel production: A comprehensive techno-economic review of pathways and costs,” Energy Conversion and Management: X, vol. 25, p. 100863, Jan. 2025, doi: 10.1016/J.ECMX.2024.100863.

95. R. Hu, X. Chen, L. Li, F. Kong, and Y. Liu, “Exhaust emissions and energy conversion of hybrid and conventional CNG buses,” Transp Res D Transp Environ, vol. 135, p. 104405, Oct. 2024, doi: 10.1016/J.TRD.2024.104405.

96. “IEA – International Energy Agency - IEA.” Accessed: Jan. 27, 2025. [Online]. Available: https://www.iea.org/data-and-statistics/data-sets

97. “World Health Organization (WHO).” Accessed: Jan. 27, 2025. [Online]. Available: https://www.who.int/

98. S. R. K. Velho, A. S. G. Vanderlinde, A. H. A. Almeida, and S. C. M. Barbalho, “Electromobility strategy on emerging economies: Beyond selling electric vehicles,” Cleaner Energy Systems, vol. 9, p. 100166, Dec. 2024, doi: 10.1016/J.CLES.2024.100166.

99. N. Lin, “CO2 emissions mitigation potential of buyer consolidation and rail-based intermodal transport in the China-Europe container supply chains,” J Clean Prod, vol. 240, p. 118121, Dec. 2019, doi: 10.1016/J.JCLEPRO.2019.118121.

100. E. Y. C. Wong, K. K. T. Ling, A. H. Tai, and A. Yuen, “Two-stage multilateral trade-based prediction model for freight transport carbon emission of Belt and Road countries along Eurasian Landbridges,” Int J Sustain Transp, vol. 18, no. 8, pp. 633–650, Aug. 2024, doi: 10.1080/15568318.2024.2392190.

101. X. Chen and J. Yang, “Analysis of the uncertainty of the AIS-based bottom-up approach for estimating ship emissions,” Mar Pollut Bull, vol. 199, p. 115968, Feb. 2024, doi: 10.1016/J.MARPOLBUL.2023.115968.

102. R. Fisher et al., “Innovative waste heat valorisation technologies for zero-carbon ships − A review,” Appl Therm Eng, vol. 253, p. 123740, Sep. 2024, doi: 10.1016/J.APPLTHERMALENG.2024.123740.

103. M. Emami Javanmard, Y. Tang, and J. A. Martínez-Hernández, “Forecasting air transportation demand and its impacts on energy consumption and emission,” Appl Energy, vol. 364, p. 123031, Jun. 2024, doi: 10.1016/J.APENERGY.2024.123031.

104. X. Li and X. Yan, “Fast penetration of electric vehicles in China cannot achieve steep cuts in air emissions from road transport without synchronized renewable electricity expansion,” Energy, vol. 301, p. 131737, Aug. 2024, doi: 10.1016/J.ENERGY.2024.131737.

105. Y. Wang, X. Jiang, and J. Ma, “Emissions reduction of air transport and high-speed rail with policy intervention considering the modal competition in a network market: Environment and welfare implications,” Transp Policy (Oxf)162, pp. 379–395, Mar. 2025, Doi: 10.1016/j.Tranpaul.2024.10.037.

106. S. H. Kim, S. H. Park, and S. R. Lim, “Identification of principal factors for low-carbon electric vehicle batteries by using a life cycle assessment model-based sensitivity analysis,” Sustainable Energy Technologies and Assessments, Vol. 64, P. 103683, APR. 2024, Doi: 10.1016/j.Ceta.2024.103683.

107. D. Khanna, E. Gemechu, N. Mahbub, J. Joy, and A. Kumar, “Assessment of life cycle environmental impacts of materials, driving pattern, and climatic conditions on battery electric and hydrogen fuel cell vehicles in a cold region,” Environ Impact Assess Rev110, P. 107680, Jan. 2025, Doi: 10.1016/J.AER.2024.107680.

108. H. Liu, D. Hu, L. Kelleher, and L. Wang, “Life cycle assessment: Driving strategies for promoting electric vehicles in China,” Int J Sustain Transp, vol. 18, no. 10, pp. 843–857, Oct. 2024, doi: 10.1080/15568318.2024.2410362.

109. Y. Liu, Q. Liu, L. Gao, Y. Xing, Y. Chen, and S. Zhang, “The life cycle assessment and scenario simulation prediction of intelligent electric vehicles,” Energy Reports, vol. 12, pp. 6046–6071, Dec. 2024, doi: 10.1016/J.EGYR.2024.11.056.

110. “La Paz to Uyuni: How to Get to Salar de Uyuni From Bolivia | Salar De Uyuni.” Accessed: Jan. 28, 2025. [Online]. Available: https://www.salardeuyuni.com/la-paz-to-uyuni/

111. M. Romare and L. Dahllöf, “The Life Cycle Energy Consumption and Greenhouse Gas Emissions from Lithium-Ion Batteries A Study with Focus on Current Technology and Batteries for light-duty vehicles,” 2017, Accessed: Jan. 28, 2025. [Online]. Available: www.ivl.se

112. J. Farahbakhsh et al., “Direct lithium extraction: A new paradigm for lithium production and resource utilization,” Desalination, vol. 575, p. 117249, Apr. 2024, doi: 10.1016/J.DESAL.2023.117249.

113. V. Roy, M. P. Paranthaman, and F. Zhao, “Lithium from clay: Assessing the environmental impacts of extraction,” Sustain Prod Consum, vol. 52, pp. 324–332, Dec. 2024, doi: 10.1016/J.SPC.2024.11.008.

114. L. Gaines, “The future of automotive lithium-ion battery recycling: Charting a sustainable course,” Sustainable Materials and Technologies, vol. 1–2, pp. 2–7, Dec. 2014, doi: 10.1016/J.SUSMAT.2014.10.001.

115. X. Cao, M. Sharmina, and R. M. Cuéllar-Franca, “Sourcing cobalt in the Democratic Republic of the Congo for a responsible net-zero transition: Incentives, risks and stakeholders,” Resources Policy, vol. 95, p. 105149, Aug. 2024, doi: 10.1016/J.RESOURPOL.2024.105149.

116. J. Sun, H. Zhou, and Z. Huang, “The future nickel metal supply for lithium-ion batteries,” Green Chemistry, vol. 26, no. 12, pp. 6926–6943, Jun. 2024, doi: 10.1039/D4GC01980F.

117. C. Scheller, K. Schmidt, and T. S. Spengler, “Effects of CO2-Penalty Costs on the Production and Recycling Planning of Lithium-Ion Batteries,” Procedia CIRP2021, Vol. 98, pp. 643–647, Jan. 2021, Doi: 10.1016/j.Prasir.2021.01.168.

118. Y. Bai, N. Muralidharan, Y. K. Sun, S. Passerini, M. Stanley Whittingham, and I. Belharouak, “Energy and environmental aspects in recycling lithium-ion batteries: Concept of Battery Identity Global Passport,” Materials Today, vol. 41, pp. 304–315, Dec. 2020, doi: 10.1016/J.MATTOD.2020.09.001.

119. Z. Wang, S. Zeng, and Z. Khan, “Impact of sustainable energy, fossil fuels and green finance on ecosystem: Evidence from China,” Heliyon, vol. 10, no. 18, p. e36712, Sep. 2024, doi: 10.1016/J.HELIYON.2024.E36712.

120. F. Muhire, D. Turyareeba, M. S. Adaramola, M. Nantongo, R. Atukunda, and A. M. Olyanga, “Drivers of green energy transition: A review,” Green Energy and Resources, vol. 2, no. 4, p. 100105, Dec. 2024, doi: 10.1016/J.GERR.2024.100105.

121. N. Tilly, T. Yigitcanlar, K. Degirmenci, and A. Paz, “How sustainable is electric vehicle adoption? Insights from a PRISMA review,” Sustain Cities Soc, vol. 117, p. 105950, Dec. 2024, doi: 10.1016/J.SCS.2024.105950.

122. S. R. Golroudbary, D. Calisaya-Azpilcueta, and A. Kraslawski, “The Life Cycle of Energy Consumption and Greenhouse Gas Emissions from Critical Minerals Recycling: Case of Lithium-ion Batteries,” Procedia CIRP20, Vol. 80, pp. 316–321, Jan. 2019, Doi: 10.1016/j. Prasir.2019.01.003.

123. H. Li et al., “One-step green hydrometallurgical recycling of spent lithium-ion batteries’ cathode,” J Hazard Mater, Vol. 484, P. 136769, Fab. 2025,
Doi: 10.1016/j.Jhajmat.2024.136769.

124. L. Wiszniewski, I. Marschall, T. Hochsteiner, T. McFarlane Hoad, K. Doschek-Held, and H. Raupenstrauch, “Evaluating refractory material performance in pyrometallurgical recycling of lithium-ion batteries under a reducing atmosphere,” Ceram Int, vol. 50, no. 21, pp. 43683–43698, Nov. 2024, doi: 10.1016/J.CERAAS.2024.08.220.

125. X. He et al., “A comprehensive review on the distribution behaviors of precious metals through pyrometallurgical processes and implications for recycling,” Miner Eng, vol. 219, p. 108998, Dec. 2024, doi: 10.1016/J.MINENG.2024.108998.

126. Ilie NUCA, Vadim CAZAC. Modelarea mathematică a sistemelor electromecanice. Indicații metodice privind efectuarea lucrărilor de laborator. Editura „Tehnică-UTM” Chișinău 2022. ISBN 978-9975-45-781-1

127. Doru Adrian NICOLA, Daniel Cristian CISMARU Tracțiunea electrică. Fenomene Modele soluții Vol.1 Editura SITECH. Craiova 2006. Romania, ISBN 973-746-291-6

128. F. L. Mapelli, D. Tarsitano. Modeling of Full Electric and Hybrid Electric Vehicles. Chapter 7 Published: 19 December 2012 DOI: 10.5772/53570

129. F. L. Mapelli, D. Tarsitano, and M. Mauri. Plug-in hybrid electric vehicle: Modeling, prototype realization, and inverter losses reduction analysis. IEEE Transactions on Industrial Electronics, 57:598–607, 2010.

130. F.L. Mapelli, D. Tarsitano, and A. Stefano. Plug-in hybrid electrical commercial vehicle: Modeling and prototype realization. In 2012 IEEE International Electric Vehicle Conference, IEVC 2012, Greenville, SC, 2012.

131. A. Fratta and F. Scapino. Modeling inverter losses for circuit simulation. In Conference of E 35th Annual Power Electronics Specialists Conference, PESC04;, volume 6, pages 4479–4485, Aachen, 2004.

132. R. Manigrasso and F.L. Mapelli. Design and modelling of asynchronous traction drives fed by limited power source. In Conference of 2005 IEEE Vehicle Power and Propulsion Conference, VPPC, volume 2005, pages 522–529, Chicago, IL, 2005.

133. Гнатов, А. В. Енергозберігаючі технології на транспорті : конспект лекцій [Електронний ресурс] / А. В. Гнатов, Щ. В. Аргун ; М-во освіти і науки України, Харків. нац. автомоб.-дор. ун-т. - Харків, 2021. - 142 с. https://dspace.khadi.kharkov.ua/dspace/bitstream/123456789/4809/1/KL_energozber_gnatov_21.pdf

134. Гнатов А. В., Аргун Щ. В., Гнатова Г. А., Сохін П. А. Переобладнання автомобіля з ДВЗ в електромобіль. Автомобіль і електроніка. Сучасні технології. – 2022. – № 21. – С. 22-30. DOI: https://doi.org/10.30977/VEIT.2022.21.0.1.

135. Arhun, S., Borodenko, Y., Hnatov, A., Popova, A., Hnatova, H., Kunicina, N., ... & Ribickis, L. (2020). Choice of parameters for the electrodrive diagnostic system of hybrid vehicle traction. Latvian Journal of Physics and Technical Sciences, 57(4), 3-11.

136. Аргун Щ.В. Екологічний та енергоефективний атомобільний транспорті його інфраструктура / Щ. В. Аргун, А. В. Гнатов, О.А. Ульянец // Вісник Житомирського державного технологічного університету. – 2016. – № 2 (77). – С. 18–27.

137. Patlins, A., Hnatov, A., Arhun, S., Hnatova, H., & Saraiev, O. (2022, May). Features of converting a car with an internal combustion engine into an electric car. In 2022 IEEE 7th International Energy Conference (ENERGYCON) (pp. 1-6). IEEE.

138. Trunova, I., Arhun, S., Hnatov, A., Apse-Apsitis, P., Kunicina, N., & Myhal, V. (2023). Sustainable approach development for education of electrical engineers in Long-Term online education conditions. Sustainability, 15(18), 13289.

139. Patļins, A., Hnatov, A., Arhun, S. Using of Green Energy from Sustainable Pavement Plates for Lighting Bikeways. In: Transport Means 2018: Proceedings of 22nd International Scientific Conference, Lithuania, Trakai, 3-5 October, 2018. Kaunas: Kaunas University of Technology, 2018, pp.574-579.

140. Technical and economic calculation of a solar-powered charging station for electric vehicles. Автомобільний транспорт, Вип. 49, 2021, С. 71-78. DOI: https://doi.org/10.30977/AT.2019-8342.2021.49.0.05.